UNITED STATES

DEPARTMENT OF THE INTERIOR

GEOLOGICAL SURVEY

SEDIMENTOLOGY AND GEOCHEMISTRY OF SURFACE SEDIMENTS AND THE DISTRIBUTION OF FAULTS AND POTENTIALLY UNSTABLE SEDIMENTS, ST. GEORGE BASIN REGION OF THE OUTER CONTINENTAL SHELF, SOUTHERN BERING SEA

BY

James V. Gardner[1.], Tracy L. Vallier[1.], Walter E. Dean[2.], Keith A. Kvenvolden[1.], and George D. Redden[1.].

1. U. S. Geological Survey, Menlo Park, California
2. U. S. Geological Survey, Denver, Colorado

U. S. Geological Survey

OPEN FILE REPORT

79-1562

TABLE OF CONTENTS

INTRODUCTION

Purpose and Organization

This final report summarizes data and interpretations from studies of surface sediments, faults, and areas of potentially unstable sediment masses in the St. George Basin region of the outer continental shelf, southern Bering Sea (Fig. 1). We have divided the report into four major parts: Part 1 is an introduction which reviews methods used and the quantity of data collected during the contract period; Part 2 deals with the sedimentology and geochemistry of surface sediments; Part 3 discusses distributions of faults and areas of potentially unstable sediment; and Part 4 is a review of the major conclusions. Information on other aspects of our studies can be found in our 1977 and 1978 annual reports to OCSEAP and in the various publications and reports tabulated in Appendix A.

Ship-board Data Collection

Most data used in this report (Table 1) were collected onboard the U. S. Geological Survey research vessels SEA SOUNDER and SAMUEL P. LEE. A small part of the single channel seismic reflection data was collected onboard the R/V STORIS. Navigation of R/V SEA SOUNDER and R/V LEE was by integrated satellite and Loran C which has a nominal position accuracy of ±200m or better. In addition, the R/V LEE used doppler sonar integrated into the navigation system. Navigation on the R/V STORIS was by satellite with a position accuracy of ±500m or better.

Acoustic data used to interpret distributions of reflectors, faults, and areas of potentially unstable sediments were collected by the following seismic-reflection equipment: 1) 3.5 kHz; 2) 2.5 kHz (Uniboom source); 3) single-channel seismic reflection (60KJ to 160KJ sparker and up to 1300 in^3 air gun sources); and 4) 24-channel multichannel equipment using a 1300 in^3 airgun array. The various types of seismic-reflection data and the cruises are shown in Table 2. Tracklines for cruises S4-76 and S6-77 of the R/V SEA SOUNDER are given in Figs. 2 and 3. In addition to seismic-reflection data, both gravity and magnetics were collected routinely while underway.

In general, the quality of the 3.5 kHz data is only fair, but the 2.5 kHz data are fair to good and the low-resolution seismic-reflection data are fair to excellent. The 3.5 kHz system generally penetrated only to the first subbottom reflector (0.005 sec; approximately 4 m), but in a few places it penetrated to 0.05 sec (approximately 35 m). The 2.5 kHz system typically penetrated to 0.05 sec or less. The single-channel seismic-

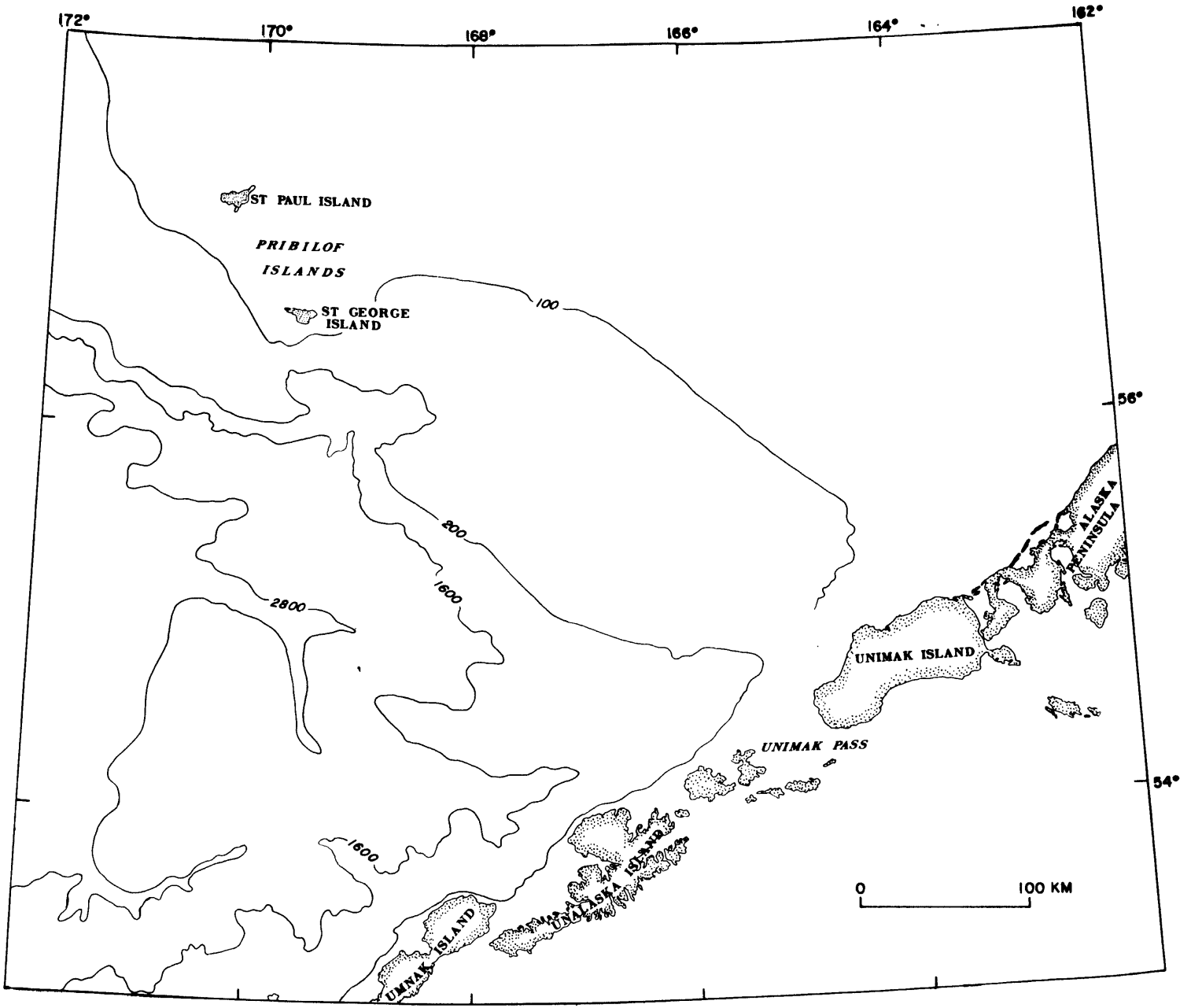

Figure 1. Index map of the southern Bering Sea.

Table 1. Summary of data collected on cruises S4-76 and S6-77 of the R/V SEA SOUNDER and multichannel data collected on the R/V LEE in St. George basin region, southern Bering Sea.

Data Type	Approximate Number of Kilometers	Number of Samples or Stations
12 kHz Profiles	6,500	
3.5 kHz Profiles	14,800	
2.5 kHz Profiles	5,900	
80-160 KJ Profiles	11,500	
Magnetometer Records	7,500	
Gravity Data	16,500	
Sea Surface T & S Profiles	13,000	
Side Scan Sonar Profiles	150	
Multichannel Reflection Profiles	2,800	
Gravity Cores		124
Piston Cores		8
Van Veen Samples		31
Dredge Hauls		5
XBT Stations		79
Current Meter Stations		27
Water Bottle Casts		143
CTD Profiles		41
Sea Floor TV (Hours)		6
Bottom Camera Stations		11

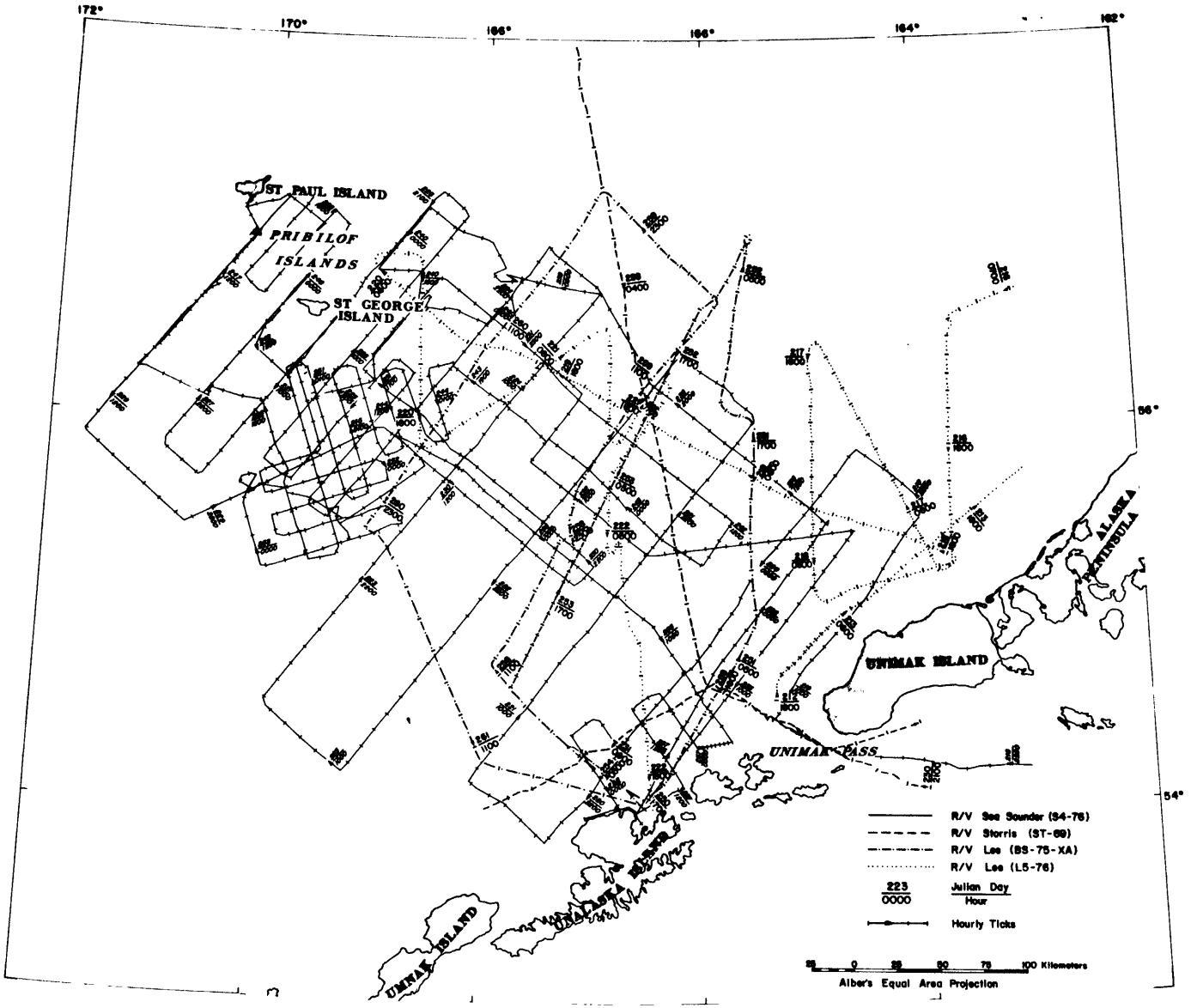

TRACK CHART

Figure 2. Track chart for cruises S4-76, L5-76, ST-69, and BS-75-XA.

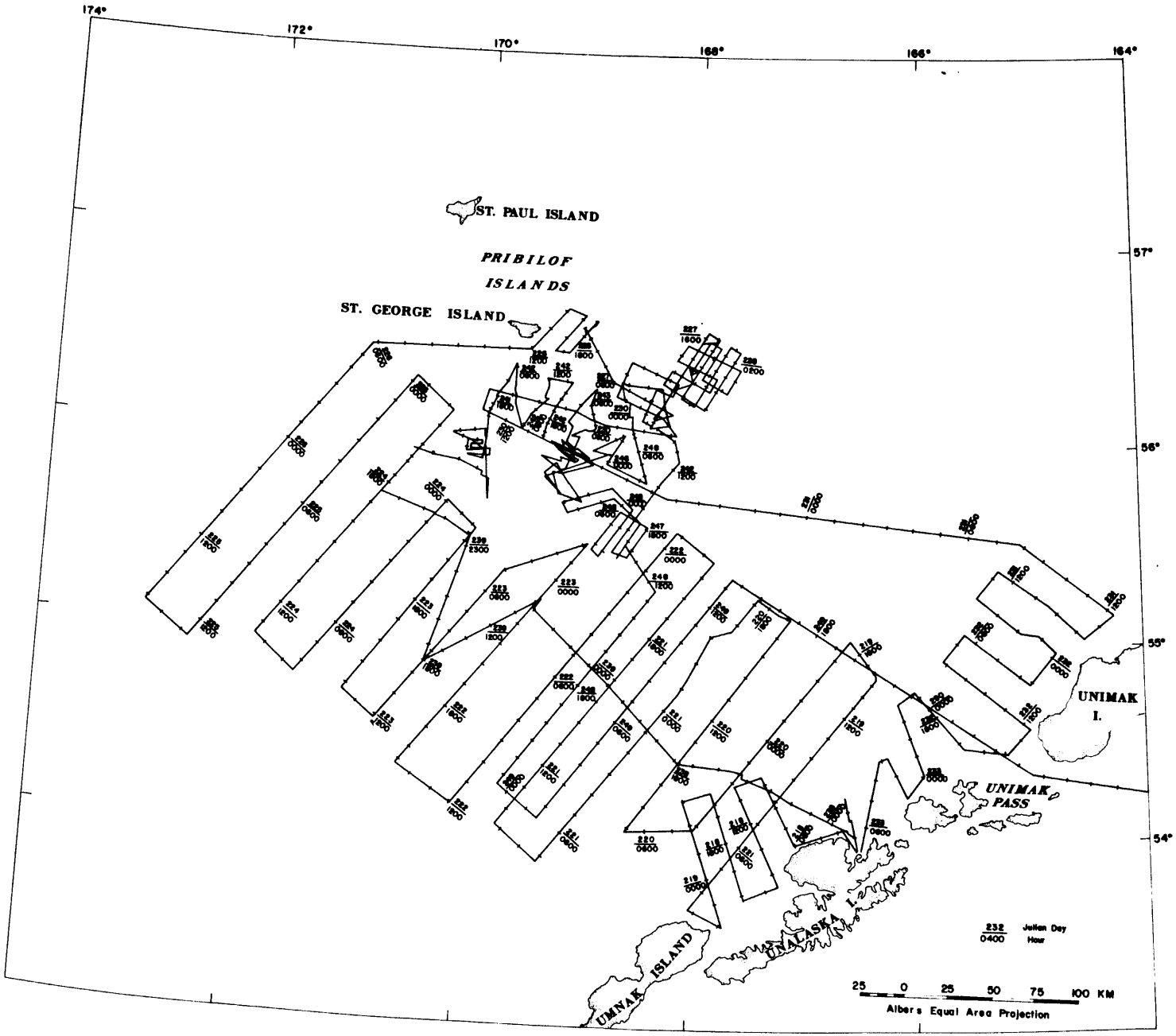

Figure 3. TRACK CHART FOR U.S.G.S. CRUISE S 6-77

reflection profiling systems penetrated to a maximum of about 2.0 sec in deep water and multichannel system was able to penetrate as much as 5.5 sec over the St. George basin (Marlow et al.,1976; 1977).

Table 2. Cruises and types of Seismic-Reflection Data

Ship	Cruise	Data Type: High Resolution 3.5 kHz	High Resolution 2.5 kHz	Low Resolution single channel airgun	Low Resolution single channel sparker	Low Resolution multi-channel
R/V SEA SOUNDER						
	S4-76	X	X		X	
	S6-77	X	X		X	
R/V LEE						
BERS-	75-XA	X	X			X
	LS-76	X	X	X		X
R/V STORIS						
	ST-69				X	

Factors which affect the quality of the seismic data can be grouped in two broad categories: (1) the types of seismic systems used and their environments, and (2) the surface andsubsurface geology. The environment of the seismic system includes the sea-state at the time of recording, ambient acoustic interference generated by the vessel, depth of water, and the watchstander overseeing the system. The first two factors affect the high-resolution systems much more than the low-resolution systems. Sea-state conditions during which most data were collected ranged between calm and Force 8, but were typically between Forces 1 and 4. Rough sea-states result in the decoupling of hydrophones and/or transducers from the water column, thus seriously reducing the quality of high-resolution records. Ambient acoustic interference generated by the vessel adds further to the noise level on all the data. The depth of water affects the high- and low-resolution systems in opposite ways. On the low-resolution single-channel systems, shallow water depths influence the records by producing a first harmonic (multiple) that on many records obliterates the signals beneath it. As the water depth increases, the interference by the first multiple is at deeper levels on the records, thus allowing more signals to be recorded. The high-resolution systems, however, performed well in shallow water because of the high repetition rates of the outgoing signals (generally 1/4 to 1 sec), but they did not perform well in deep water because of their relatively low power output. Reverberations create a "ringing" that also tends to mask out some signals.

Despite the weaknesses of the various systems and because of the coverage of the area and the large amount of good quality data collected, we feel that the data are more than adequate to interpret the regional surface and near-surface geology.

The resolution of the seismic systems (Table 3) were calculated using the velocity of sound in water and by following the procedure of Moore (1972) who showed that the resolution of seismic-reflection systems is between 0.25 and 0.75 the wavelength of the source. However, as we noted above, the actual resolution of a feature is not only a function of the outgoing frequencies but also is affected by the environments of the systems (e.g., sea-state, depth of water, acoustic interference, watchstander) and the surface and subsurface geology. There is a gap in the resolving range of our systems between about 0.5 m and 4 m which suggests that features with thicknesses or offsets in that range would not necessarily be resolved.

Table 3. Ranges of resolution for seismic systems.

Approximate Peak Frequency	Range of Minimum Resolution (m)
40 Hz (multichannel)	9.4 to 28.1
100 Hz (single channel)	3.2 to 11.2
2.5 kHz	0.15 to 0.5
3.5 kHz	0.1 to 0.3

Sampling stations are given in Figs. 4 and 5 and the data collected are given in Table 1. Sampling equipment included piston and gravity corers, van Veen samplers and dredge hauls. We photographed the sea floor using television, 35 mm, and 70 mm cameras. Physical oceanographic measurements were made by CTD profilers, water bottle casts, current meters, and expendable bathythermographs. We cut the cores onboard the R/V SEA SOUNDER into 1.5 m sections, sliced them in half, retaining one half for archiving and the other for sampling, and described the cores using megascopic and microscopic techniques. The archive halves were photographed, using an 8 x 10 camera, and X-rayed. Sampling of the cores for subsequent shore-based studies was done on the ship.

Shore-Based Data Collection

The upper 30 cm or more of piston and gravity cores were homogenized by mixing with sea water as a result of coring operations; consequently, analyses of surface samples represent average values for the upper 30 cm of the sediments. Samples collected using the van Veen sampler were undisturbed, and are representative of surface sediment to within a few centimeters below the sediment-water interface. Subsamples for analyses of

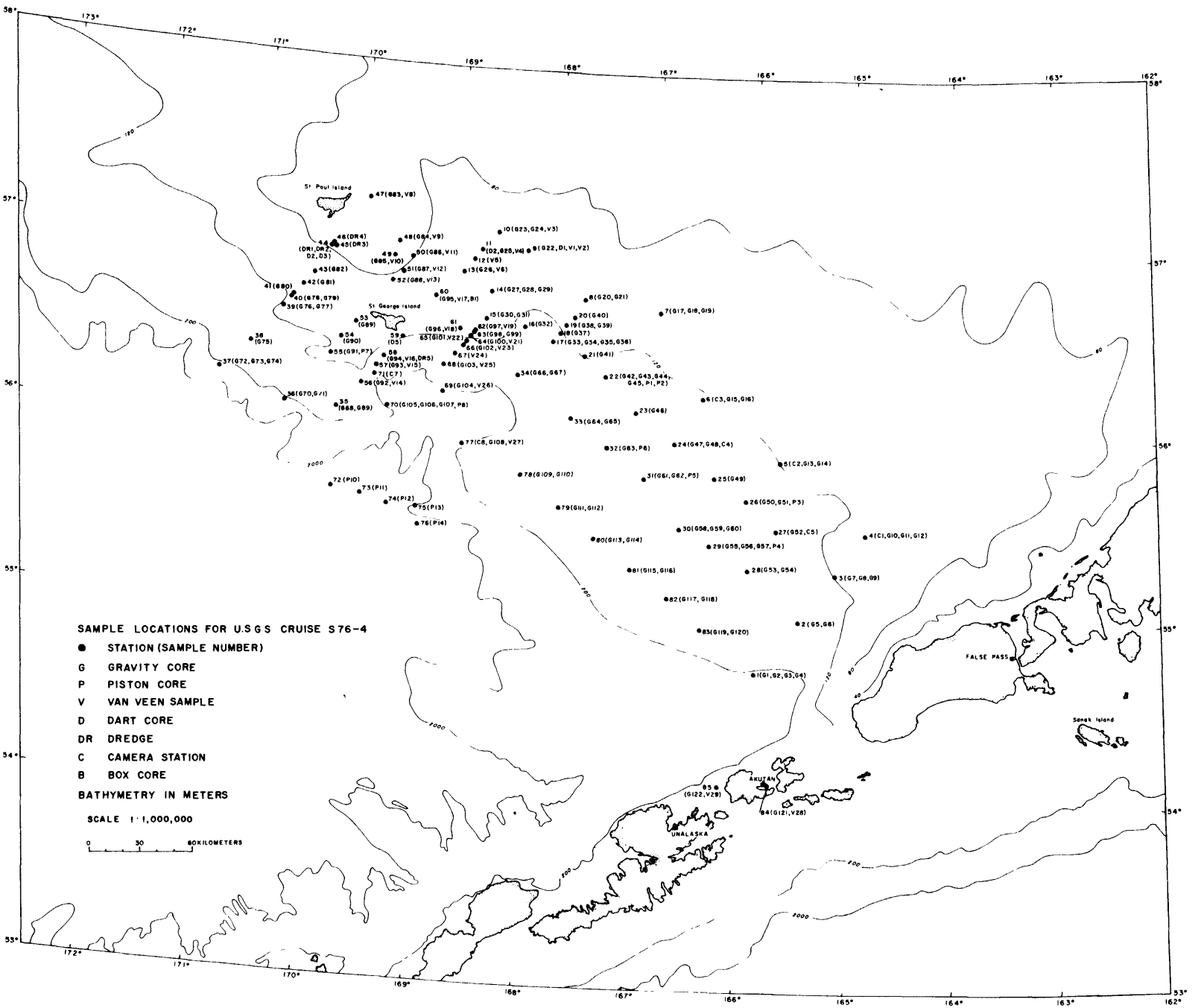

Figure 4. Sample locations for cruise S4-76.

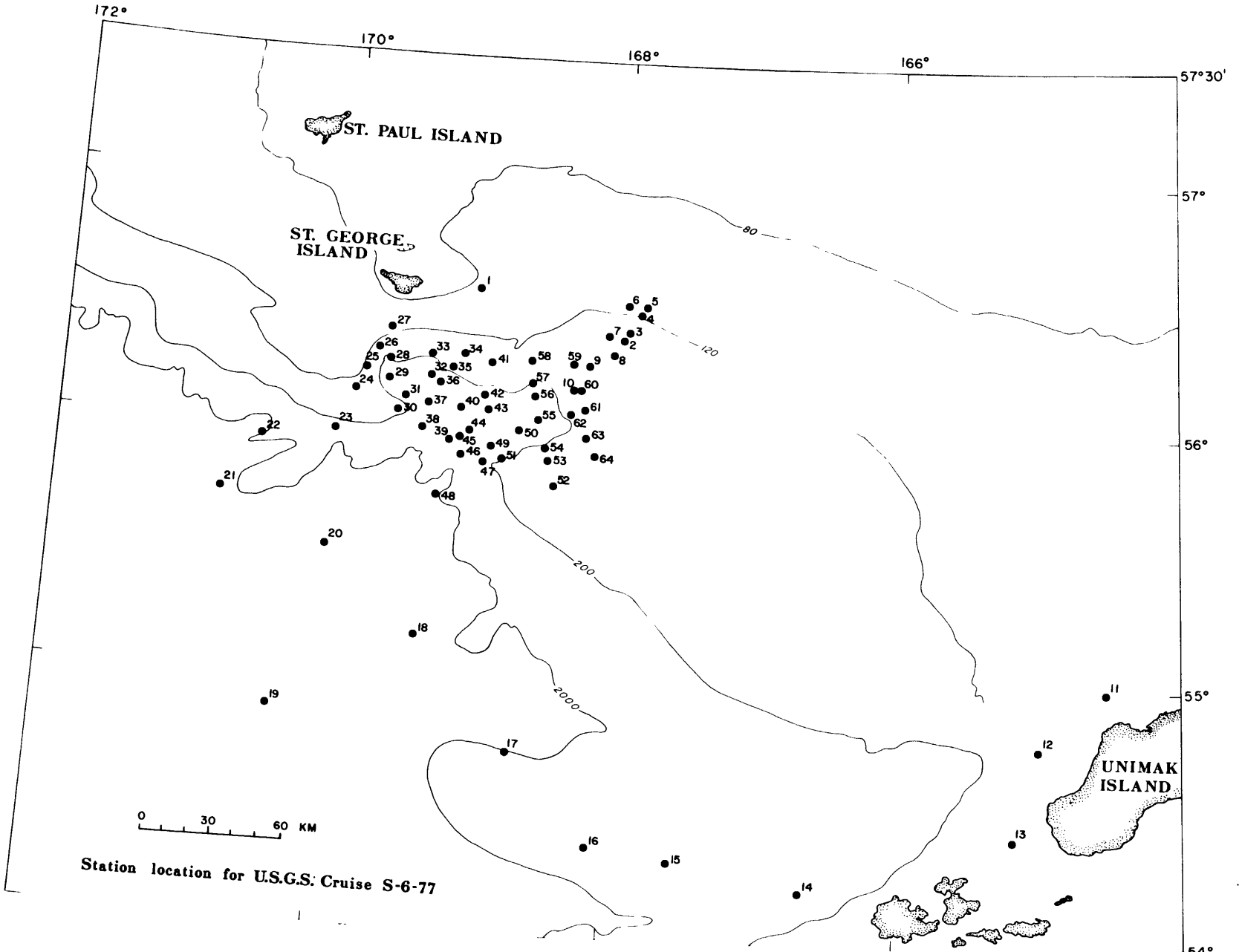

Figure 5. Sample locations for cruise S6-77.

grain-size composition of heavy (ρ>2.85) and light (ρ<2.85 minerals, clay minerals, and inorganic geochemistry were collected from the top 3 cm of van Veen samples, and from within the top 5 cm of gravity and piston cores (Table 4). The primary sampling network during the 1976 field season consisted of 51 stations centered over the St. George basin and the Pribilof Islands (Fig. 4). Duplicate cores were collected at 30 of these stations in order to measure local variability in major and minor elements. The duplicate cores were separated by as much as several hundred meters, depending upon drift of the ship while on station. In addition to samples collected on the St. George Basin grid, 18 samples were collected during the 1977 field season (Fig. 5) in the vicinity of the Pribilof Islands, from the adjacent continental slope, and near Unimak Island in the Aleutian chain. Sample locations used for our sediment analyses are plotted on a bathymetric chart of the area in Figure 6, which is keyed to Table 4.

Grain size was measured by first splitting samples into >63μ and <63μ size fractions. The >63μ fractions were analyzed using 2-m rapid sediment analyzers (Thiede et al., 1976) and the >63 μ fractions were analyzed with a hydrophotometer (Jordon et al., 1971). Replicate analyses and calibration tests show that the rapid sediment analyzers have a precision of ±5% and accuracy of ±5%. The hydrophotometer has a precision of ±10% and an accuracy of ±1%. Total carbon was determined with a LECO model WR-12 carbon analyzer. Three analyses of total carbon per sample were averaged. The LECO has a precision of ±2% and an accuracy of ±1%.

Bulk samples of sediment were sieved to retrieve the 63$\mu$to 88 μ fraction. This fraction was then floated on diluted tetrabromoenthane (ρ = 2.85) to separate heavy minerals and rock fragments from light minerals and rock fragments. Random-mounted slides were prepared and a minimum of 300 counts were made covering the whole area of each slide using the line method.

All samples for clay mineralogy, as well as all samples for other studies reported here, were kept moist in air-tight sample vials at 3° C from the time of collection until the time of preparation. The <2 μ fraction was used for clay mineral studies following the preparation procedures of Hein et al. (1975), and the semi-quantitative weighted-peak X-ray diffraction technique of Biscaye (1965). A polar planimeter was used to measure the areas under the peaks on the diffractograms. Barium saturation was attempted on several samples to help differentiate between chlorite and vermiculite. Although a peak at 7.8Å commonly did appear as a result of this treatment, it was not well developed and was highly interpretive. Hence, barium saturation was not used routinely. Samples were glycolated to help identify the expandable clays. Diffractograms were run from 3° to 14° 2θ and measurements of peak areas were taken on the glycolated sample. X-ray diffraction peaks corresponding to d-spacings of 7Å, 10Å, and 17Å were routinely measured for chlorite/kaolinite, illite,

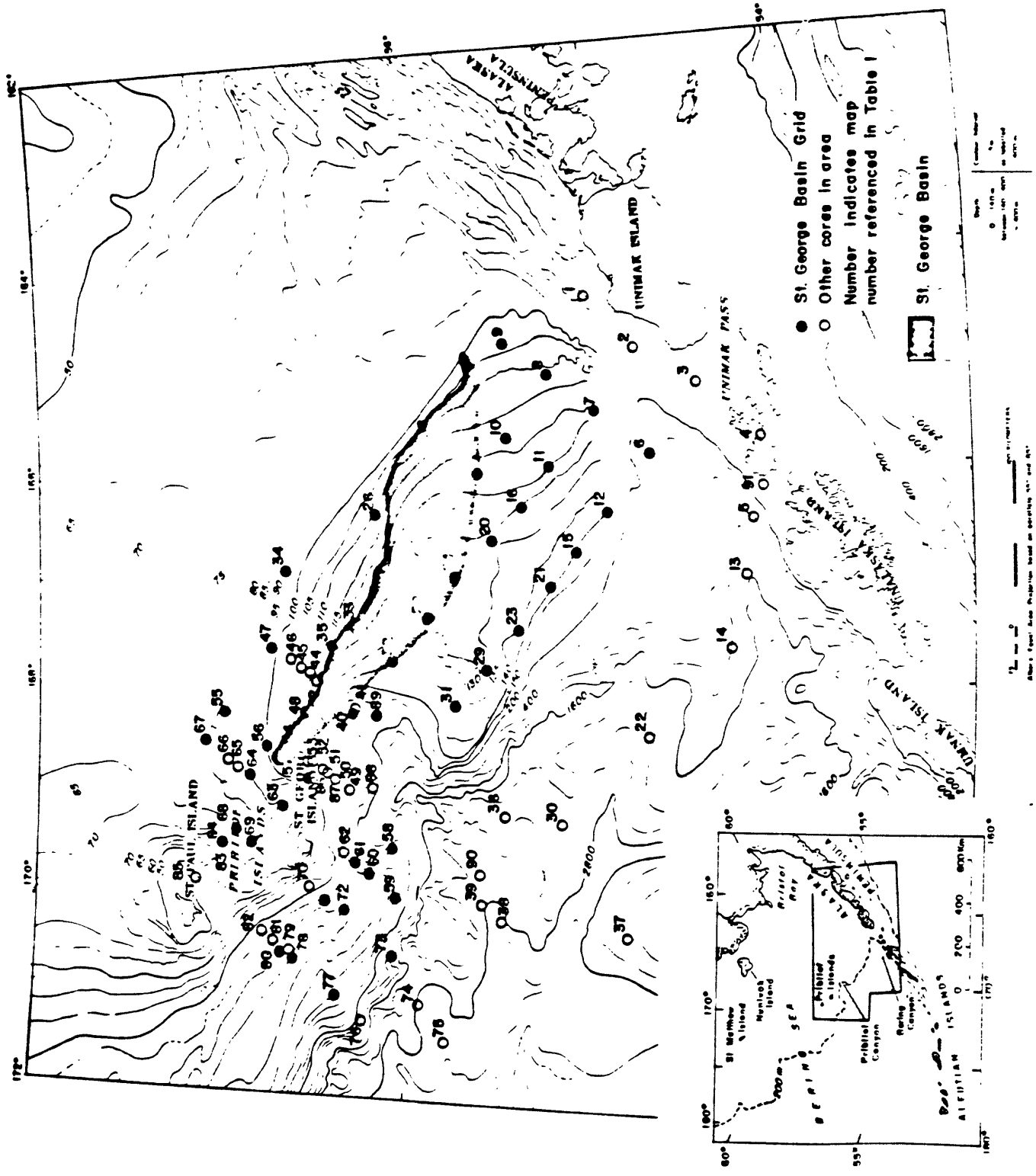

Figure 6. Bathymetric chart of the southern Bering Sea region with the St. George basin shaded. The number next to a circle or dot is a map reference number (see Table 4 for corresponding sample number).

Table 4. Summary of Analyses. Map number refers to numbers on Fig. 6. Letters in the sample column designate sample types; G = gravity core, P = piston core, and V = van Veen Sampler. X designates analysis performed.

Map Number	Core		Interval (cm.)	Grain Size	Clay	Heavy Mineral	Light Mineral	Inorganic Geochemistry		Carbon
	year	#						Complete Chemistry	6-step spec. only	
1	77	V05	0-3					X		X
2	77	V06	0-3	X		X	X	X		X
3	77	V07	0-3					X		X
4	76	G121	0-5	X	X	X	X	X		X
4	76	V28	0-3					X		
5	77	G014	0-5	X		X	X	X		X
6	76	G002	15-20	X		X	X	X		X
7	76	G005	0-5	X	X	X	X	X		X
7	76	G006	3-4					X		
8	76	G007	0-5							
8	76	G008	7-15	X	X	X	X	X		X
8	76	G009	4-5					X		
9	76	G010	0-10					X		
9	76	G011	13-18	X	X	X		X		X
9	76	G012	4-5					X		
10	76	G052	9-13	X	X	X	X	X		X
11	76	G053	0-1					X		
11	76	G054	0-3	X	X	X	X	X		X
12	76	G119	0-5	X		X	X	X		X
12	76	G120	4-5					X		
13	77	G016	0-5	X		X	X	X		X
14	77	G019	0-5	X		X	X	X		X
15	76	G117	0-1					X		
15	76	G118	6-11	X		X	X	X		X
16	76	G055	4-5					X		
16	76	G056	0-4	X		X	X	X		X
16	76	G057	0-5					X		
17	76	G058	0-1					X		
17	76	G059	6-11	X	X	X		X		X
17	76	P03	3-8					X		
18	76	G013	14-19	X	X	X	X	X		X
18	76	G014	4-5					X		
19	76	G049	0-5	X		X	X	X		X
20	76	G059	5-8	X	X	X		X		X
20	76	G060	0-2					X		
21	76	G115	4-5					X		
21	76	G116	0-5	X		X	X	X		X
22	77	G020	0-5	X		X	X	X		X
23	76	G113	3-8	X	X	X	X	X		
23	76	G114	0-1					X		
24	76	G061	4-5					X		
24	76	G062	0-5	X	X	X	X	X		X
24	76	P05	0-5					X		
25	76	G047	4-5					X		
25	76	G048	0-8	X		X	X	X		X
26	76	G015	4-5					X		
26	76	G010	7-9		X	X	X	X		
27	76	G046	11-16	X	X	X	X	X		X
28	76	G063	15-20	X	X	X		X		X
28	76	P06	6-11					X		
29	76	G111	1-5	X	X	X	X	X		X
29	76	G112	4-5					X		
30	77	G022	0-5	X		X	X	X		X
31	76	G109	3-8	X	X	X	X	X		X
31	76	G110	4-5					X		
32	76	G064	4-5					X		
32	76	G065	10-15	X	X	X	X	X		X
33	76	G042	0-1					X		
33	76	G043	0-6	X	X	X	X	X		X
34	76	G018	4-5					X		
34	76	G019	0-3	X		X	X	X		X
35	76	G041	6-11	X	X	X	X	X		X
36	76	P13	0-2	X	X	X	X		X	X
37	77	G023	0-5	X				X		X
38	77	G024	0-5	X				X		X
38	77	G025	0-10	X			X	X		X
39	76	P10	0-2	X	X	X	X		X	X

Table 4. (Continued)

Map Number	Core		Interval (cm.)	Grain Size	Clay	Heavy Mineral	Light Mineral	Inorganic Geochemistry		Carbon
	year	#						complete chemistry	6-step spec. only	
40	76	G006	4-5					x		
40	76	G007	5-10	x	x	x	x	x		x
41	77	G012	11-12					x		x
42	77	G007	0-1					x		x
43	76	G033	8-13	x				x		x
43	76	G034	4-5					x		
43	76	G036	2-7					x		
44	76	G037	2-8	x		x	x		x	x
45	76	G038	0-5	x					x	x
45	76	G039	0-5						x	
46	76	G040	6-10	x					x	x
47	76	G020	6-11	x	x	x	x	x		x
47	76	G021	4-5					x		
48	76	G032	6-11	x				x		x
49	76	G103	2-7	x	x	x	x		x	x
49	76	V25	0-3						x	
50	76	V23	0-3	x					x	x
51	76	V21	0-3	x				x		x
52	76	V20	0-3	x	x				x	x
53	76	V19	0-3	x					x	x
54	76	G030	1-6	x		x	x		x	x
54	76	G031	4-5						x	
55	76	V02	0-3	x		x	x	x		x
56	76	G027	14-19	x	x		x	x		x
56	76	G028	0-5					x		
56	76	G029	4-5					x		
57	76	V18	0-3	x	x	x	x	x		x
58	76	G105	10-15	x	x	x	x	x		x
58	76	G107	0-5					v		
58	76	P08	3-8					x		
59	76	G069	0-5	x		x		x		x
59	76	V07	0-3	x		x	x	x		x
60	76	V14	0-3	x		x	x	x		x
61	76	V15	0-3	x				x		x
62	76	G094	0-3	x		x			x	x
63	76	V17	0-3	x	x	x	x	x		x
64	76	V06	0-3	x	x	x	x	x		
65	76	V05	0-3	x					x	x
66	76	V04	0-3	x					x	x
67	76	V03	0-3	x	x	x	x	x		x
68	76	V11	0-3	x				x		x
69	76	V12	0-3	x	x	x	x	x		x
70	76	G089	0-3	x	x	x	x		x	x
71	76	G090	2-4	x				x		x
72	76	G091	0-1					x		
72	76	P07	5-10	x	x	x	x	x		x
73	76	G070	0-1					x		
73	76	G071	2-7	x	x	x	x	x		x
74	77	G029	0-5	x		x	x	x		x
75	77	G026	0-5	x		x	x	x		x
76	76	G072	4-5						x	
76	76	G074	0-5		x	x	x			
77	76	G075	6-10	x	x	x	x	x		
78	76	G077	0-5	x	x	x	x	x		x
79	76	G078	0-1						x	
79	76	G079	0-5	x		x			x	x
80	76	G080	0-5	x				x		x
81	76	G081	0-5	x			x		x	x
82	76	G082	0-5	x	x				x	x
83	76	V10	0-3	x					x	x
84	76	V09	0-3	x		x	x	x		x
85	76	V08	0-3		x					
86	76	V22	0-3	x	x	x	x		x	x
87	76	V24	0-3	x						x
88	76	V26	0-3	x						x
89	77	V04	0-3	x						
90	76	P11	0-5	x						x
91	76	V29	0-3	x		x				x

and mixed layer clays respectively. A slow scan (0.25° 2θ per min.) between 24° and 26° 2θ was used to differentiate kaolinite from chlorite. No internal standards were used in this study. Therefore, the values obtained by these techniques are relative within this study only and should not be taken as absolute percentages of clay minerals present.

A total of 103 samples from 65 stations in the 1976 St. George basin grid were analyzed for 31 major, minor, and trace elements using a combination of semiquantitative optical emission spectroscopy, X-ray fluorescence, atomic absorption spectrometry, and neutron activation analysis. The details of these analytical methods are described in sections by J. S. Wahlberg, Claude Huffman, Jr., J. I. Dinnin, Harriet G. Neiman, A. J. Bartel, and H. T. Millard, Jr., in Miesch (1976). Eighteen of these 103 samples were chosen at random for duplicate analyses in the analytical laboratories. All 121 analytical samples (103 samples plus 18 duplicates) were submitted in a randomized sequence to the analytical laboratories of the U.S. Geological Survey in Denver. An additional suite of 24 samples from 20 stations in the vicinity of the Pribilof Islands were analyzed for concentrations of 19 major, minor, and trace elements by semiquantitative optical emission spectroscopy.

Samples were air dried and ground in a ceramic mill to pass a 100-mesh (149 μ) sieve. Because the samples were air dried, analytical values of Na, S, and Mg will be too high due to Na^+, $SO_4^=$, and Mg^{++} dissolved in interstitial water and left as a residue after evaporation. To correct these values, we assumed that all of the Cl determined by X-ray fluorescence was due to Cl^- dissolved in interstitial water, and that the interstitial water contained the same proportions of Na, S, Mg, and Cl as average sea water. Interstitial water contributions of Na, S, and Mg were then subtracted from the analytical values.

SEDIMENTOLOGY AND GEOCHEMISTRY OF SURFACE SEDIMENTS

Summary

Present-day sediment dynamics, combined with the dynamics associated with lowering of sea level during the Pleistocene, have created a mixture of sediments on the outer continental shelf of the southern Bering Sea that has been derived from the Alaskan mainland, the Aleutian Islands, and the Pribilof ridge. Concentrations of finer-grained, higher-organic sediments in the region of the St. George basin have further modified the regional distribution patterns of sediment composition. Q-mode factor analysis of 58 variables related to sediment size and composition--including major, minor, and trace elements, heavy and light minerals, and clay minerals-- reveals three dominant sediment associations.

Felsic sediment derived from the generally quartz-rich rocks of the Alaskan mainland forms a background over most of the

continental shelf. These sediments contain relatively high concentrations of Si, Ba, Rb, quartz, garnet, epidote, metamorphic rock fragments, K-feldspar, and illite. A second important association, superimposed on the felsic background, is andesitic sediment derived from the Aleutian Islands. These sediments contain relatively high concentrations of Na, Ca, Ti, Sr, V, Mn, Cu, Fe, Al, Co, Zn, Y, Yb, Ga, volcanic rock fragments, glass, clinopyroxene, smectite, and vermiculite. A local basaltic association, derived from the Pribilof Islands, factors out as a subset of the Aleutian andesite association. Concentrations of finer-grained sediment in St. George basin results in a sediment association containing relatively high concentrations of C, S, U, Li, B, Zr, Ga, Hg, silt, and clay.

Sediments of the Aleutian andesite association are concentrated mainly between the 100- and 200-meter isobaths; they exhibit a strong gradient, or "plume", decreasing away from Unimak pass and toward St. George basin. Lack of present-day currents sufficient to move even clay-size material and the presence of the Bering submarine canyon between the Aleutian Islands and the outer continental shelf and slope indicate that Holocene sediment dynamics cannot be used to explain the observed distribution of surface sediments derived from the Aleutian Islands. We suggest that this distribution pattern is relict and resulted from sediment dynamics during lower sea levels in the Pleistocene.

Regional Setting

The geologic history and structure of the region have been summarized by Scholl et al. (1968), Scholl and Hopkins (1969), Nelson et al. (1974), Marlow et al. (1975), Scholl et al. (1975), and Marlow et al. (1977a). The southeastern Bering Sea can be broadly subdivided into four major physiographic provinces: outer continental shelf, continental margin, Pribilof ridge, and the Bering and Pribilof canyons (Figure 7). The outer continental shelf is a broad, flat area that has a gradient of 1:2000 (0.03°) between the 100 m isobath and the shelf break at about 170 m. The Pribilof ridge is a prominent northwest-southeast-trending topographic high that is capped by the Pribilof Islands. The ridge is a relatively smooth surface cut by at least one terrace that may be a Pleistocene feature. The ridge plunges below the shelf at about 56°40'N, 168°50'W, but can be followed to the east in the subsurface to 55°40'N, 165°30'W. The continental slope to the northwest abruptly drops away from the shelf break with gradients of 1:20 (3°). Toward the southeast, however, the gradient decreases to 1:40 (1.4°). The continental slope is characterized by hummocky topography, scarps, and canyons on almost all scales. The continental margin in this region is incised by two giant submarine canyons, Bering and Pribilof canyons (Scholl et al, 1970), which may have played significant roles in the transport of sediment to the Aleutian basin.

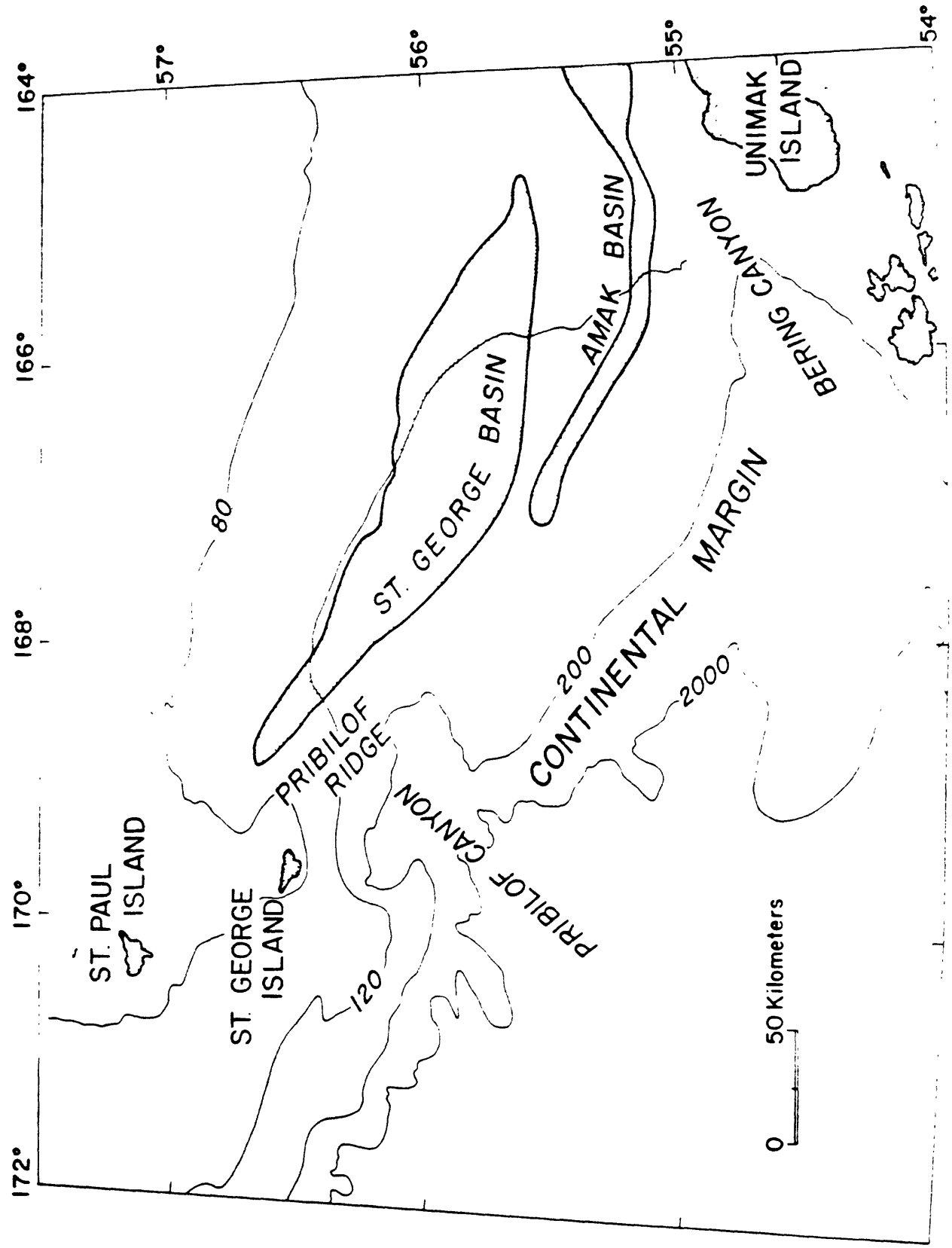

Figure 7. Physiographic provinces, southern Bering Sea.

Rock units underlying the continental shelf and slope can be broadly divided into an acoustically layered sequence of Cenozoic age and a Mesozoic unit that has been highly deformed and comprises the acoustic basement (Scholl et al., 1968; 1975). The acoustic basement probably consists of deformed rocks of Mesozoic age that can be divided into two belts (Marlow et al., 1977a; 1977b). A northeasterly belt of Upper Jurassic and younger Mesozoic rocks extends northwestward from the Black Hills region on the Alaska Peninsula to the northern part of the Pribilof ridge. A second belt lies basinward (southwest) of the first and consists of a younger (Campanian and younger assemblage of continental-margin rocks that extends, parallel to the inner belt of shallow-marine Jurassic rocks, from southern Alaska via the outer Bering shelf to eastern Siberia. Marlow et al. (1977a) speculated further that a Jurassic, Cretaceous, and earliest Tertiary magmatic arc extended parallel to and inside (landward) both deep-water and shallow-water depositional troughs.

The present-day deformational and sedimentological patterns in the southern Bering Sea were created after the growth of the Aleutian arc in late Mesozoic or earliest Tertiary time, when the old plate boundary shifted from an ancient Bering Sea margin to a site near the present Aleutian Trench, thereby trapping a large piece of the Kula Plate within the abyssal Bering Sea (Scholl, et al., 1975; Cooper, et al., 1976). After an initial episode of uplift and erosion in the early Tertiary, the margin underwent extensional collapse and differential subsidence that has continued to the present (Marlow et al., 1976). Elongate basins formed in the vicinity of the modern outer shelf as a consequence of collapse. St. George basin is the largest of the southern basins. This basin is a graben of sedimentary fill encompassing an area of approximately 15,000 km^2 and containing a volume of at least 150,000 km^3 (Marlow, et al., 1976). The basin is a long (greater than 300 km) and narrow (30 to 50 km) structure that parallels the present continental margin and is, in places, filled with more than 10 km of upper Mesozoic (?) and Cenozoic sedimentary deposits.

Studies of the distribution of sediments on the continental shelf of the southern Bering Sea by Sharma et al. (1972) and Sharma (1974, 1975) have concentrated mainly on samples from Bristol Bay, located on the inner shelf. These authors characterize Bristol Bay as a classical graded shelf. Askren (1972) investigated sediments in a broad region to the northwest of our area but did include 12 samples from within the area of this study. He concluded that the shelf is mid-stage in the establishment of a graded condition.

The oceanographic circulation of the Bering Sea was first studied by Ratmanoff (1937) who described the exchange between the Bering Sea and the Pacific Ocean. Interpretations of the physical oceanography of the Bering Sea through 1974 (e.g. Favorite, 1974; Takenouti and Ohtani, 1974) suggest that surface waters move in a cyclonic gyre or semi-gyre eastward along the

north side of the Aleutians-Alaskan Peninsula, curve around to the northwest along the southwestern Alaskan coast, and eventually turn northward and flow through the Bering Strait. The presence of a return flow of bottom waters to the southwest and south over the shelf has not been documented. Recently, Schumaker et al. (in prep.) reported on current-meter moorings deployed to measure surface and near-bottom currents on the outer continental shelf of the southern Bering Sea. They report a predominantly east-west tidal flow with little net flow. The semi-gyre described above is suggested by their data but the circulation is very sluggish. Pulses of high-velocity flow do occur for a few days during storms, with peak flows up to 40 cm/sec, but these pulses show no net flow over a season.

General Description and Texture of Surface Sediments

The surficial sediments of the outer continental shelf are generally olive gray greenish gray, to grayish olive green silt to silty sand. Evidence for extensive burrowing, such as color mottling, discrete burrows, and total homogenization with no internal structures, is common throughout all cores. Some cores have thin interbeds 5 to 15 cm thick of coarser-grained material, but this is not a general feature. Four cores from the outermost part of the continental shelf (cores G113, G116, G118, and G119) have an upper layer, 50 cm thick, of diatom-bearing greenish gray silt overlying a gray silty clay with very few diatoms. Almost all of the other cores show a uniform lithology. Askren (1972) reported benthonic foraminifera in sediments from this area. We examined 124 surface sediment samples and did not find any benthonic foraminifera. The reasons for this discrepancy remain a mystery.

The gray and greenish hues of the sediments indicate reducing conditions or at least reduced iron oxides in the clay minerals. The water column is certainly not anaerobic at any level; thus the reducing environment is diagenetic. Because the region is one of very high biological productivity (Hattori and Wada, 1974), it seems most likely that large volumes of organic debris from plankton and nekton settle to the sediment surface. Burrowing attests to high epifaunal and infaunal activity on and in the sediments. Organic debris that is supplied to anaerobic bacteria uses up all available oxygen by metabolizing the organic material. The sediments become reduced because of high biological oxygen demand within the sediments even though the bottom water is oxygenated.

The salient features of the distribution of grain sizes is a bull's-eye pattern of finer grain size over St. George basin, and a broad band of rapid size change around the head of Pribilof Canyon and the northwestern margin of Bering Canyon (Fig. 8). The bull's-eye pattern reflects the occurrence of finer grain sizes in the center of the graben that forms St. George basin.

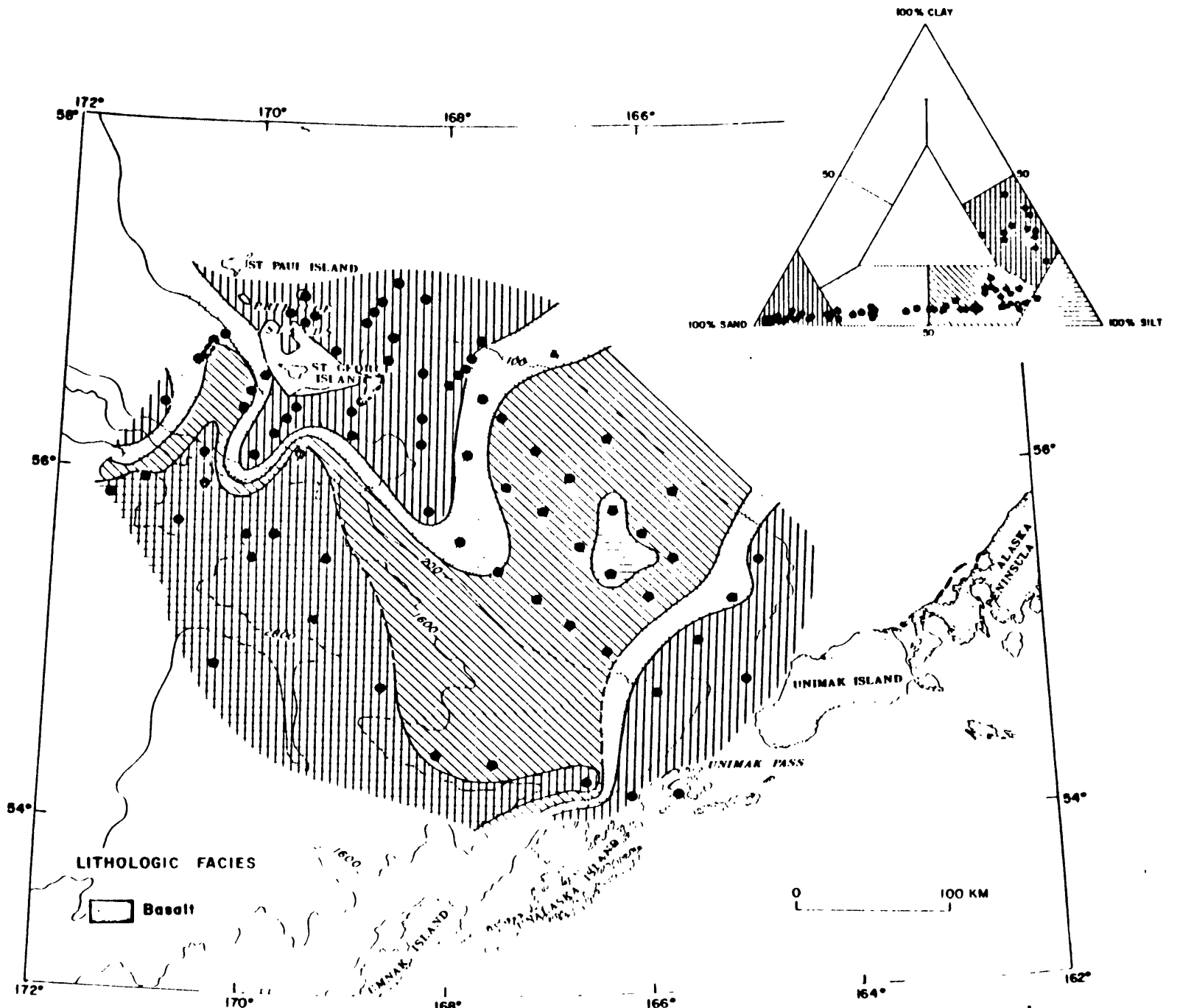

Figure 8. Map of lithologic facies of surface sediments from the continental margin.

The band of rapid size change coincides with areas of high topographic relief, with coarser sediments at the shallower depths.

The central portion of St. George basin is very poorly sorted (Fig. 9), which reflects the lack of significant winnowing. The northwestern border of the Bering Canyon, the head of Pribilof Canyon and the topographic high of Pribilof ridge all show moderately-sorted sediments. The size-frequency distribution for most sediments in St. George basin region are leptokurtic to very leptokurtic, but in the vicinity of the Pribilof Islands the distributions are mesokurtic. The distributions are fine to strongly fine-skewed throughout the region. Summary statistics of grain-size data (median grain size, mean grain size, sorting, skewness, and kurtosis) are given in Table 5.

Petrology of Surface Sediments

A subset of 32 samples, chosen to represent the whole region under study, was analyzed for heavy and light minerals. Those minerals and classes of rock fragments present in the study area, and their relative abundances, are listed in Table 6. Unidentifiable minerals and rock fragments account for only 1 to 10% of the counted grains.

The heavy minerals and rock fragments (those with specific gravity >2.85) fall into two major classes --metamorphic and volcanic. Metamorphic components occur as a low-concentration background (<10%) over the entire area (Figure 10). Volcanic components in the heavy mineral fractions dominate the region and show a gradient away from the Aleutians and onto the continental rise (Fig. 11). The heavy-mineral data are plotted on a ternary diagram with percentages of amphiboles, pyroxenes, and volcanic-rock fragments as end members. Sediments from the Yukon and Kuskokwim Rivers were also analyzed and the results plotted on the ternary diagram for a comparison. The rivers are potential sources of sediment on the shelf and both rivers drain, in part, metamorphic terrains.

The light minerals and rock fragments (those with a specific gravity <2.85) include quartz, feldspar, volcanic glass, volcanic rock fragments and non-volcanic rock fragments. Relative concentrations within the three-component system of feldspars, quartz plus non-volcanic rock fragments, and volcanic glass plus volcanic rock fragments are shown in Figure 12. Analysis of samples from the Yukon River are also plotted in Fig. 12 but samples from Kuskokwim River sediments were not analyzed for light minerals.

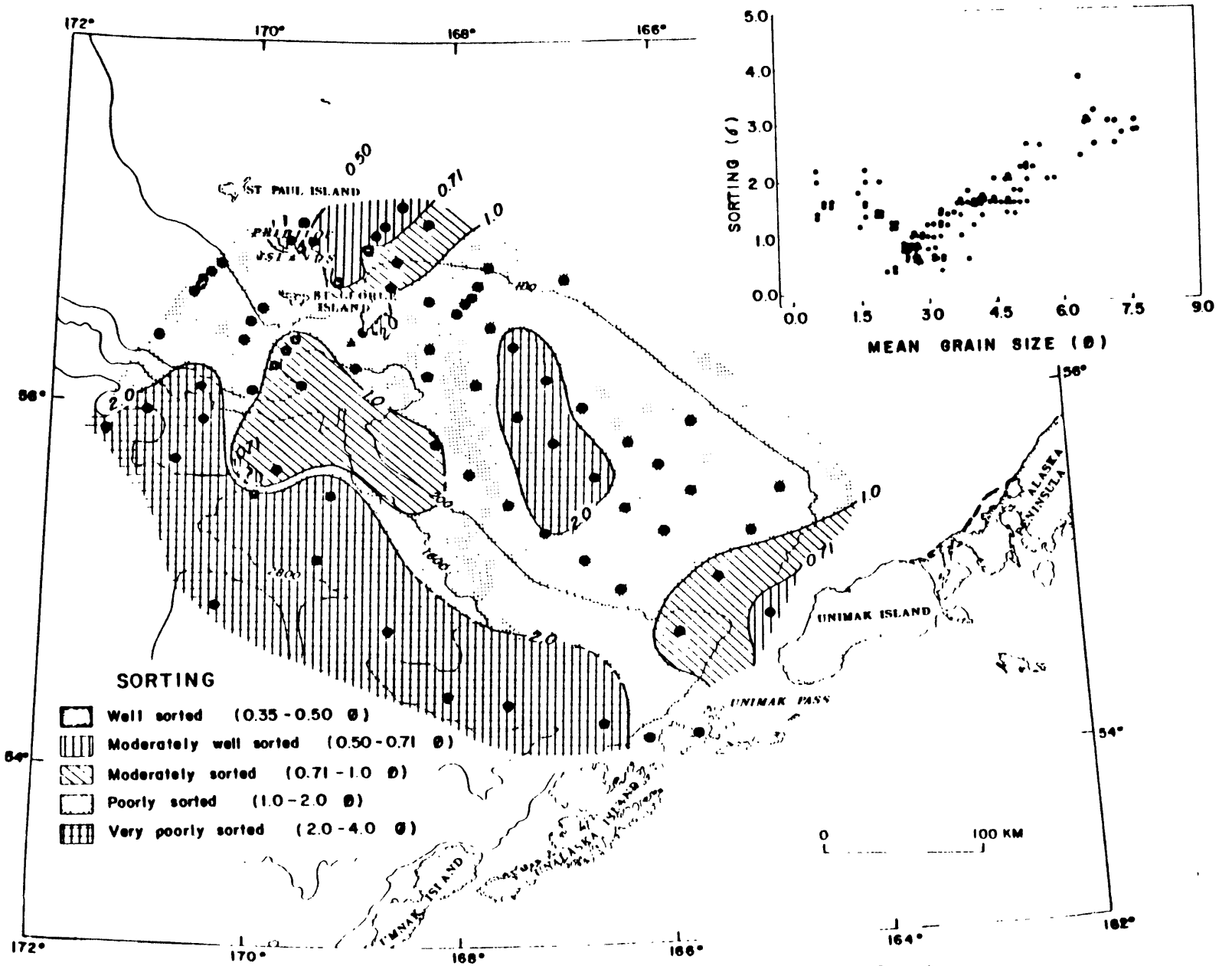

Figure 9. Distribution of sorting values from surface sediments. Inset is a plot of sorting vs mean grain size.

TABLE 5

GRAPHICAL STATISTICS FROM GRAIN SIZE ANALYSIS

(Folk and Ward, 1957)

SAMPLE	MAP INDEX NUMBER	MEDIAN (Md) (¢)	MEAN (M_z) (¢)	SORTING (σ_i)	SKEWNESS (Sk_i)	KURTOSIS (K_G)
76-G4	6	3.54	3.81	1.05	0.63	2.71
76-G5	7	3.72	3.88	0.69	0.55	3.02
76-G8	8	3.66	3.98	1.20	0.46	1.27
76-G10	9	3.20	3.52	1.32	0.43	1.66
76-G19	34	3.45	3.85	1.52	0.46	1.16
76-G20	47	3.01	3.33	1.32	0.49	1.44
76-G28	56	3.18	3.53	1.36	0.55	2.06
76-G30	54	3.18	3.29	1.05	0.38	2.38
76-G32	48	3.06	3.29	1.19	0.49	2.12
76-G33	43	3.14	3.71	1.66	0.59	1.54
76-G36	43	3.21	3.83	1.70	0.62	1.20
76-G37	44	3.04	3.32	1.30	0.46	1.48
76-G38	45	3.28	3.70	1.47	0.52	1.42
76-G39	45	3.29	3.75	1.52	0.53	1.35
76-G40	46	3.15	3.39	1.26	0.40	1.25
76-G43	33	4.84	4.80	2.06	0.13	1.08
76-G48	25	5.63	5.80	1.97	0.25	1.71
76-G51	17	4.81	4.81	1.60	0.07	1.37
76-G52	10	4.91	4.89	1.45	0.10	1.61
76-G54	11	4.60	4.52	1.66	0.07	1.30
76-G56	16	4.85	4.89	1.60	0.19	1.56
76-G57	16	5.12	5.26	1.57	0.28	1.72
76-G59	20	5.35	5.32	1.90	0.16	1.48
76-G60	20	5.26	5.11	2.17	0.06	1.16
76-G62	24	5.34	5.25	2.27	0.09	1.15
76-G67	40	2.00	1.93	1.45	0.19	5.24
76-G69	59	2.90	3.05	1.12	0.50	2.45
76-G71	73	6.52	6.76	3.27	0.17	0.93
76-G75	77	2.99	3.37	1.28	0.55	1.68
76-G77	78	3.79	4.15	1.60	0.43	1.16
76-G79	79	3.75	4.16	1.61	0.46	1.15
76-G80	80	4.60	4.64	1.67	0.16	1.05
76-G89	70	3.69	4.19	1.36	0.68	1.63
76-G90	71	4.94	5.01	1.70	0.20	1.44
76-G94	62	0.75	0.65	1.53	0.02	0.63
76-G103	49	1.72	1.77	2.06	0.19	2.27
76-G105	58	6.16	6.60	2.97	0.30	0.86
76-G107	58	5.36	6.66	3.08	0.60	0.97
76-G109	31	2.64	2.87	0.94	0.59	2.90
76-G111	29	3.02	3.71	1.59	0.69	1.06
76-G113	23	4.04	4.50	1.57	0.49	1.21
76-G116	21	4.68	4.80	2.04	0.12	1.34
76-G118	15	4.73	4.57	1.96	0.03	1.04

TABLE 5 cont.

SAMPLE	MAP INDEX NUMBER	MEDIAN (Md) (¢)	MEAN (Mz) (¢)	SORTING (σ)	SKEWNESS (Sk_i)	KURTOSIS (K_g)
76-G119	12	4.48	4.57	1.50	0.22	1.27
76-G121	4	4.64	4.75	1.51	0.27	1.13
77-G14	5	6.56	6.77	2.61	0.21	1.14
77-G16	13	5.11	5.18	2.65	0.11	1.43
77-G19	14	5.34	5.48	2.69	0.17	1.32
77-G20	22	7.40	7.58	2.76	0.17	1.09
77-G22	30	7.08	7.30	2.74	0.19	1.13
77-G23	37	7.12	7.25	2.56	0.19	1.38
77-G24	38	7.36	7.61	2.84	0.19	0.85
77-G25	38	7.12	7.24	2.90	0.12	0.97
77-G26	75	6.23	6.51	2.35	0.30	1.19
77-G29	74	6.90	7.01	2.91	0.14	0.99
76-V2	55	2.58	2.59	0.76	0.26	2.41
76-V3	67	2.75	2.75	0.68	0.19	1.94
76-V4	66	2.59	2.66	0.68	0.36	1.79
76-V5	65	2.65	2.71	0.79	0.38	2.10
76-V6	64	2.80	2.99	0.72	0.48	3.34
76-V7	59	3.19	3.19	1.11	0.31	2.41
76-V9	84	2.14	2.13	0.43	0.14	2.22
76-V10	83	2.23	2.22	0.44	0.09	4.58
76-V11	68	2.80	2.80	0.66	0.11	1.66
76-V12	69	2.17	2.20	1.18	-0.03	3.13
76-V14	60	3.00	2.94	0.87	0.22	2.88
76-V15	61	1.42	0.93	1.56	-0.32	0.51
76-V16	62	0.45	0.65	2.10	0.36	1.07
76-V17	63	2.64	2.73	0.64	0.50	2.11
76-V18	57	2.84	2.81	0.64	0.06	1.33
76-V19	53	3.04	3.03	0.91	0.21	2.48
76-V21	51	2.93	2.90	0.89	0.21	2.42
76-V22	86	2.85	2.86	0.97	0.29	2.63
76-V23	50	2.66	2.67	0.93	0.33	2.96
76-V24	87	1.87	1.61	1.57	-0.12	1.86
76-V25	49	1.68	1.43	1.78	-0.01	2.30
76-V26	88	1.96	1.60	1.33	-0.34	2.11
76-V28	4	4.66	4.83	1.48	0.29	1.08
76-V29	91	1.86	1.93	1.33	0.12	3.64
77-V4	89	1.79	1.49	1.23	-0.32	1.94
77-V6	2	3.22	3.25	0.68	0.49	5.47
76-P3	26	5.02	5.06	1.75	0.17	1.56
76-P6	32	5.36	5.36	2.21	0.17	1.14
76-P7	55	5.13	5.14	1.69	0.15	1.16
76-P8	70	6.46	6.47	3.79	0.05	1.32
76-P11	73	7.73	7.72	3.08	0.06	0.89

TABLE 6

UNIVARIATE STATISTICS ON PERCENTAGES OF

HEAVY AND LIGHT MINERALS

AND CLASSES OF ROCK FRAGMENTS

	MINERAL	MINIMUM	MAXIMUM	MEAN	STANDARD DEVIATION
v	clinopyroxene	9.0	35.0	16.8	5.6
v	orthopyroxene	5.0	19.0	11.4	3.9
v	volcanic rock fragments	6.0	69.0	28.9	13.1
v	amphibole	2.0	24.0	15.1	5.4
v	olivine	0	7.0	1.1	2.0
	opaques	2.0	18.0	7.3	3.8
m	chlorite	0	8.0	2.9	2.1
m	epidote	0	7.0	2.8	1.8
m	garnet	0	4.0	1.2	1.1
m	metamorphic rock fragments	0	8.0	3.3	2.2
	plutonic rock fragments	0	6.0	1.7	1.6
	fine-grained rock fragments	0	8.0	3.1	2.2
	quartz	0.3	25.6	15.1	7.0
	feldspar	1.6	50.4	36.1	7.0
v	**volcanic glass**	2.9	30.6	11.2	8.3
v	**volcanic rock fragments**	3.3	36.5	11.1	8.4
	non-volcanic rock fragments	4.1	34.8	19.7	7.5

v = volcanic origin
m = metamorphic origin

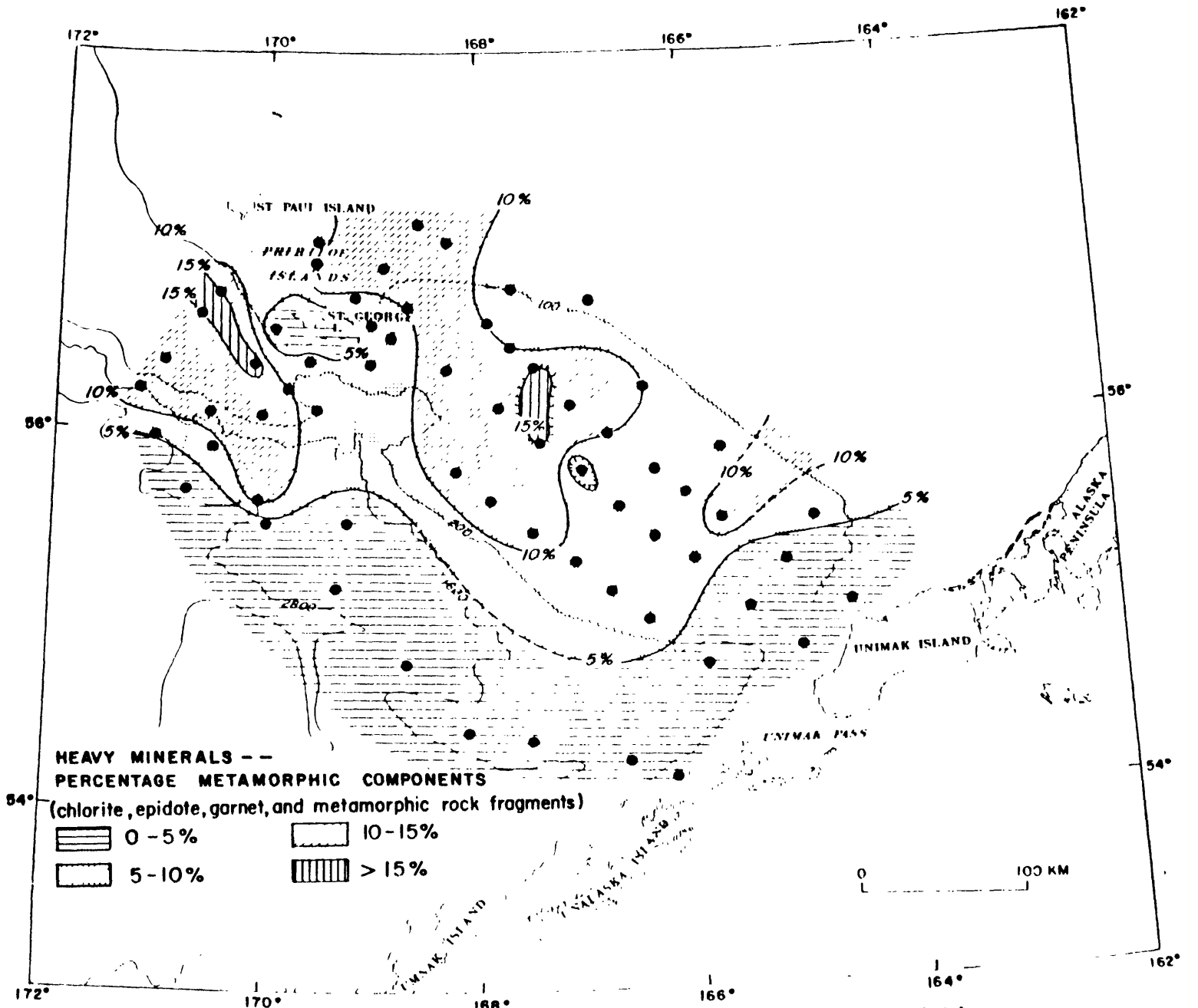

Figure 10. Distribution of the percentages of metamorphic components within the heavy mineral fraction of surface sediments.

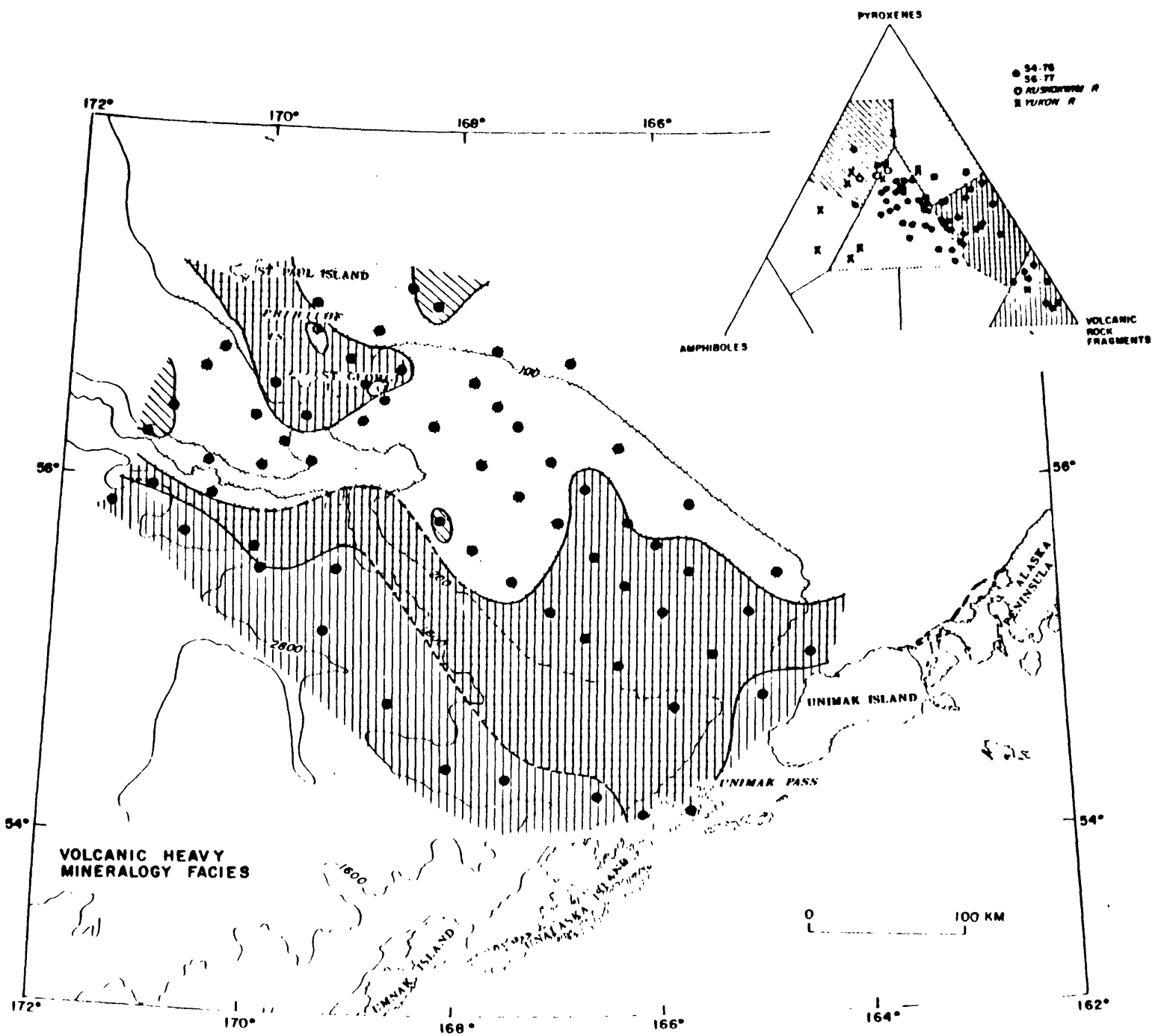

Figure 11. Distribution of the percentage of volcanic components within the heavy mineral fraction of surface sediments. Volcanic components include clinopyroxene, orthopyroxene, olivine, and volcanic rocks.

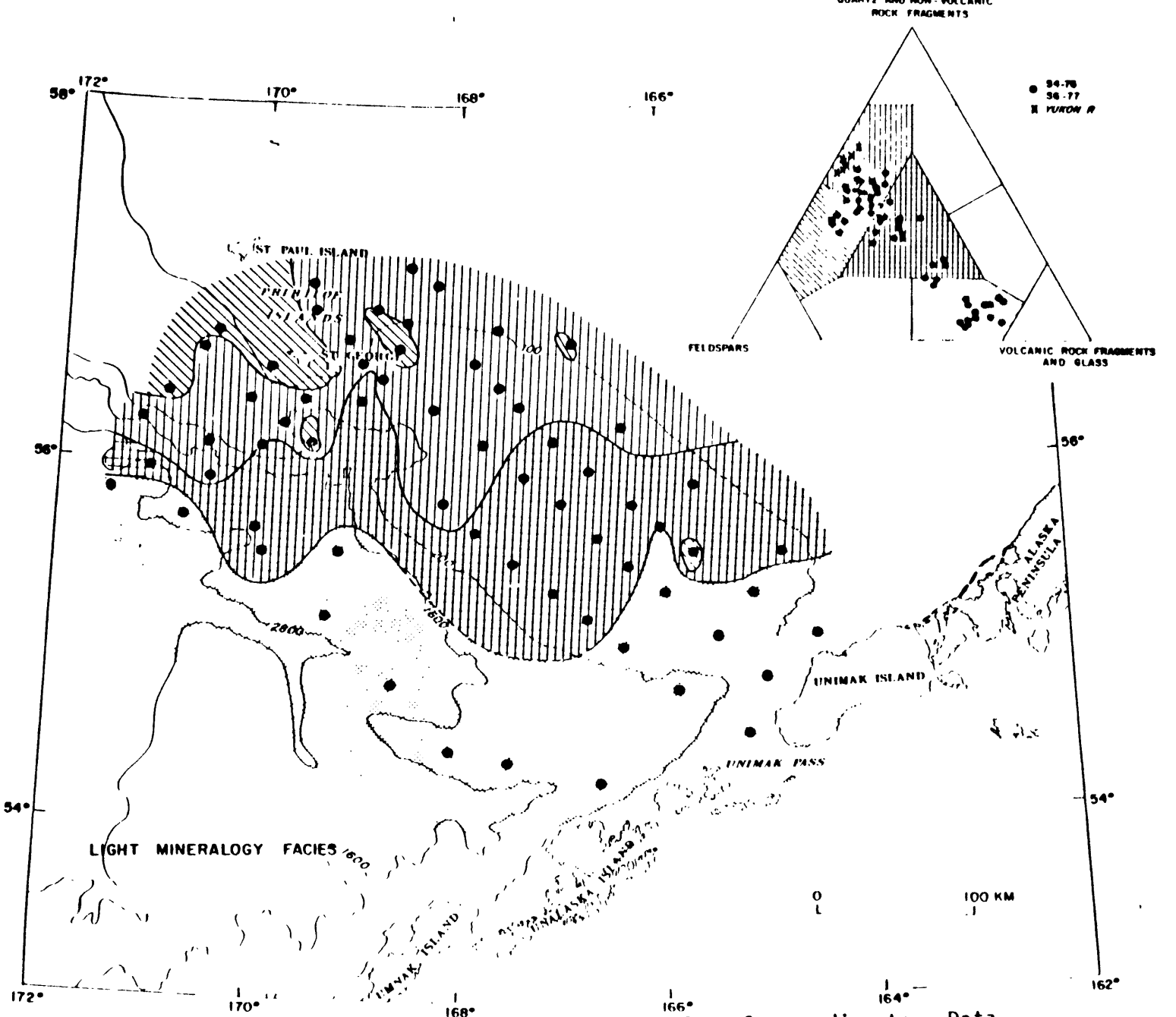

Figure 12. Distribution of light mineral components of surface sediments. Data on the ternary diagram include samples from the Yukon River as well as samples from the continental margin.

Mineralogy of Clays

The occurrences and relative abundances of the major clay mineral (chlorite, illite, smectite and vermiculite, illite crystallinity) and the expandable and non-expandable percentages of mixed-layer clays were determined; the univariate statistics for each clay mineral parameter are given in Table 7. Smectite and vermiculite are grouped together because of the difficulty of distinguishing one from the other on diffractograms. This grouping is reasonable because both clay minerals are the result of weathering of volcanic rocks (Biscaye, 1965). The aerial distributions of illite and kaolinite show no distinct gradients or concentrations. The distribution of smectite plus vermiculite (Fig. 13) shows a northwest-trending band of values that are greater than the mean. The highest values occur closest to the Aleutians and decrease with a northwest-trending gradient starting in the vicinity of Unimak Pass and Unimak Island. The distribution of chlorite also shows a northwest-trending band (Fig. 14), of lower-than-average values that may be the result of dilution within this zone by smectite plus vermiculite. Chlorite is derived from low-grade metamorphic rocks and is common in marine sediments in high latitudes (Biscaye, 1965).

Table 7. Univariate Statistics for the Relative Percentages of Clay Minerals

MINERAL	MINIMUM	MAXIMUM	MEAN	STANDARD DEVIATION
smectite + vermiculiate	13.0	57.5	31.2	9.4
illite	17.0	47.0	29.8	6.9
kaolinite	0	11.8	6.0	3.5
chlorite	24.3	44.3	33.2	5.6

Distribution of Major, Minor, and Trace Elements

The distribution of total carbon shows a strong negative correlation with grain size (Fig. 15) throughout the region. For example, concentrations of total carbon are highest in the fine-grained central region of the St. George Basin and lowest in regions where coarser-grained sand occurs. The sediments that we investigated are almost completely devoid of carbonate, and therefore most of the total carbon is organic-carbon that has been absorbed by clay particles (Bader, 1963). A negative correlation between organic-carbon and grain size is almost universally observed in non-carbonate, fine-grained sediments in marine and lacustrine environments because of absorption of organic matter by clays (Trask, 1932; Van Straaten, 1954; Emery, 1960; Bordovskiy, 1965; Thomas, 1969; Kemp, 1971).

Values (wt. percent) for 32 elements are given in Table 8, and summary statistics for each of 31 elements in 103 samples

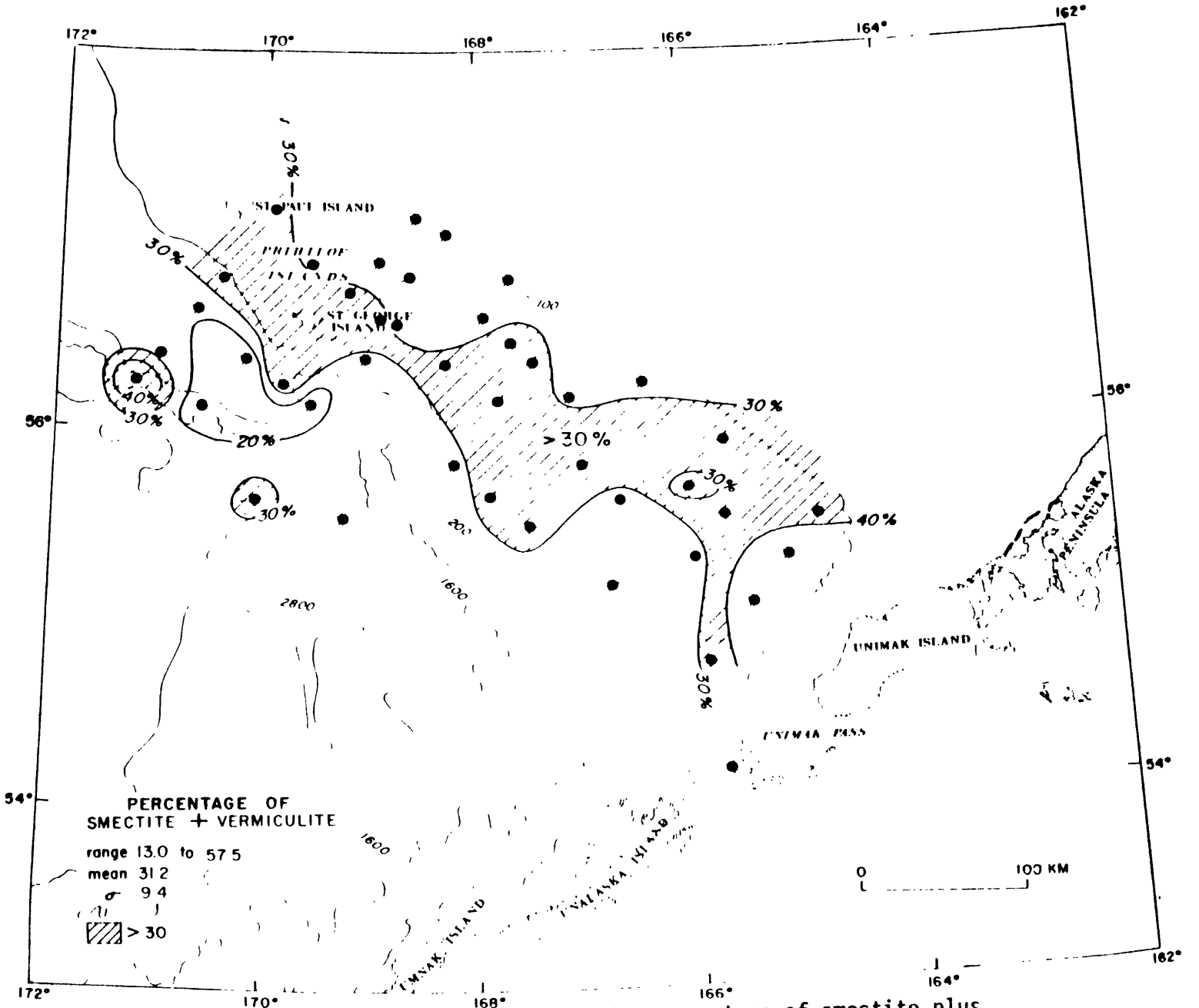

Figure 13. Map showing the distribution of the percentage of smectite plus vermiculite in the clay assemblage. The univariate statistics are also shown.

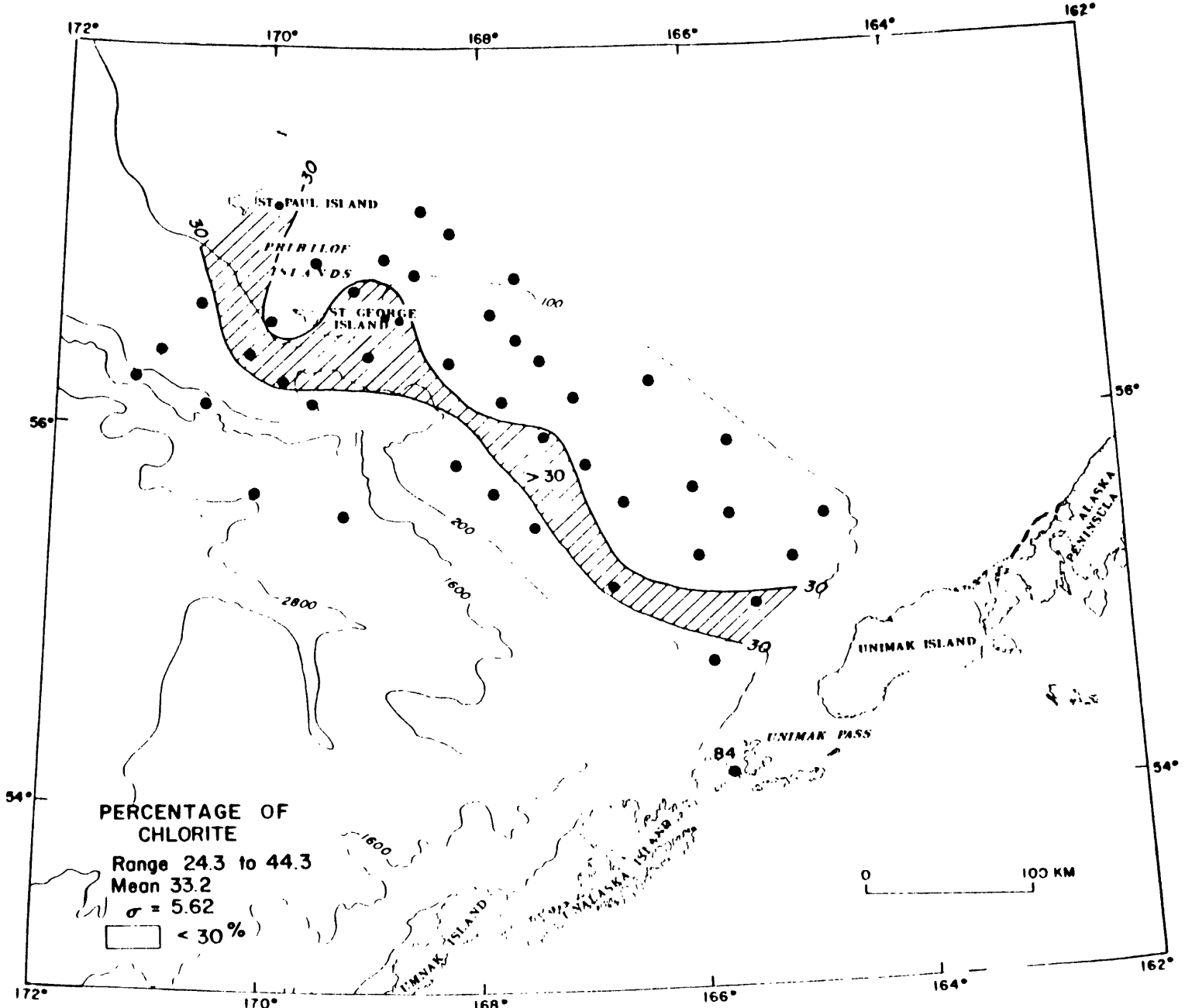

Figure 14. Map showing the distribution of the percentages of chlorite within the total clay assemblage. The univariate statistics are shown.

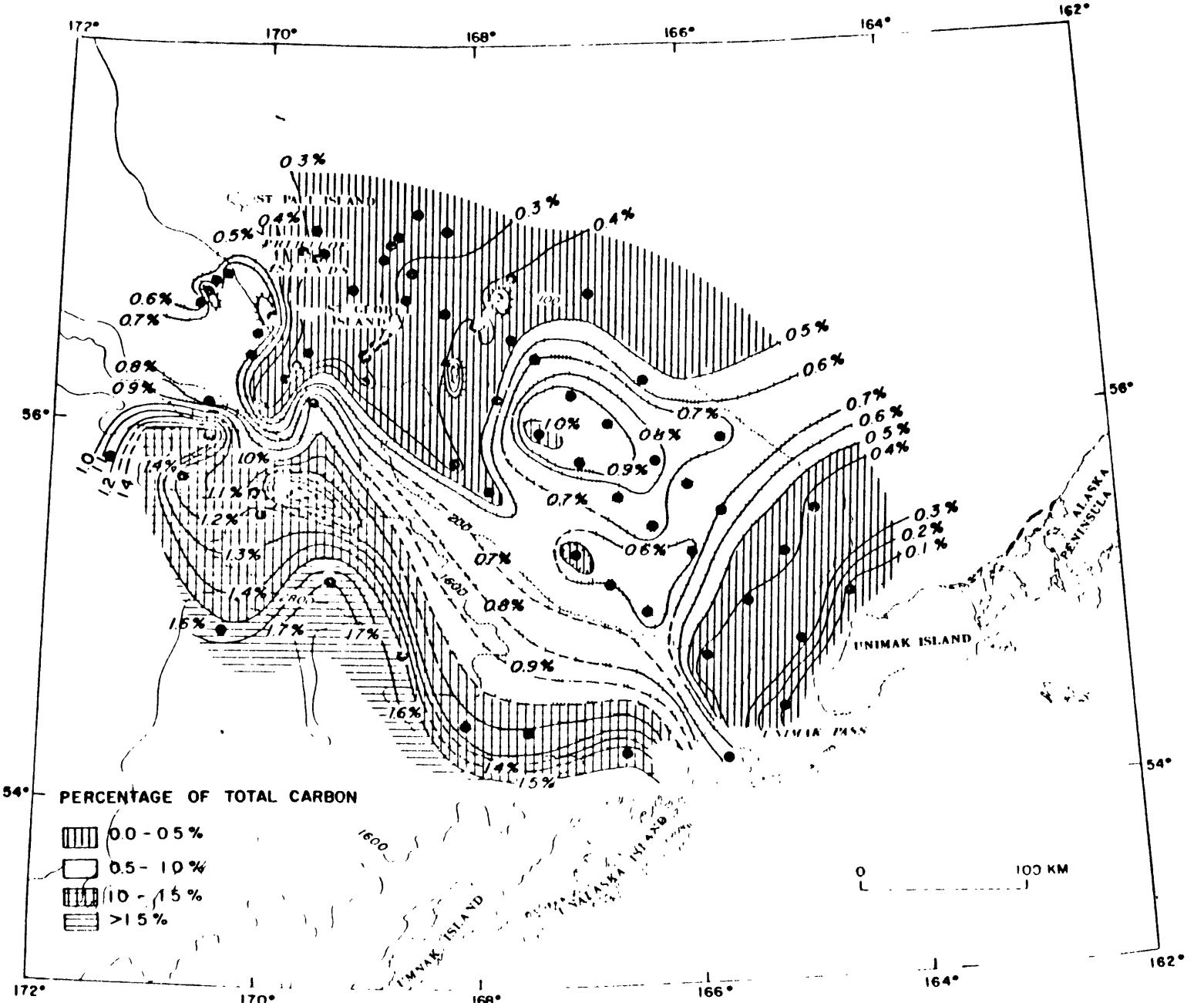

Figure 15. Map showing the distribution of the percentages of total carbon in bulk samples of surface sediments.

Table 8, Cruise S4-76. Values (in weight percent) for 32 elements determined by X-ray fluorescence (SRF or X), atomic absorption spectroscopy (aas or a), instrumental neutron activation (n), and emission spectroscopy (s) techniques.

CORE	INTERVAL (cm)	1 Si %-xrf	2 Al %-xrf	3 Ca %-xrf	4 K %-xrf	5 Fe %-xrf	6 Ti %-xrf	7 S %-xrf	8 Mg %-aas	9 Na %-aas	10 Mg ppm-a
G002	15-20	26.0000	7.0000	4.0000	1.0500	5.0000	0.7000	0.0200	1.5400	2.3100	0.0300
G005	0-5	24.0244	7.9282	4.6906	0.9747	5.6325	0.6475	0.1160	1.4600	2.5600	0.0400
G006	3-4	24.0945	7.2772	4.8357	1.0012	5.5919	0.6583	0.0070	1.5800	2.5800	0.0300
G008	7-15	31.7037	5.4672	2.1877	1.1648	2.2249	0.3825	0.0860	1.2400	2.4300	0.0400
G009	4-5	26.6231	6.4410	4.0624	1.0834	4.4519	0.5463	0.1210	1.1900	2.4000	0.0300
G010	0-5	30.1006	6.4251	3.0603	1.2005	3.1628	0.4405	0.1390	0.9700	2.3300	0.0500
G011	13-18	28.9928	5.6630	2.8738	1.1947	3.1495	0.4192	0.1460	0.9600	2.1100	0.0400
G012	4-5	28.3338	5.7741	2.9810	1.1540	3.1104	0.4109	0.1220	0.9600	2.1500	0.0400
G013	14-19	28.3011	5.6206	2.9053	1.1756	3.2160	0.4155	0.1100	1.0000	2.1700	0.0300
G014	4-5	28.6984	5.6577	2.8910	1.1947	3.2565	0.4321	0.1410	1.0000	2.0200	0.0400
G015	4-5	30.4651	5.3190	2.5822	1.2411	2.9138	0.4261	0.1410	0.9800	2.2600	0.0800
G016	7-9	27.6187	5.1724	2.4714	1.1158	2.9985	0.4310	0.1300	0.9700	1.9500	0.0500
G018	4-5	30.1847	5.2719	2.2106	1.2760	2.4410	0.3587	0.1540	0.9300	1.9600	0.0400
G018	4-5	31.3298	5.2835	2.2306	1.2677	2.4067	0.3809	0.0690	0.8800	1.9900	0.0400
G019	0-3	29.7640	5.0956	2.3349	1.2403	2.3865	0.3482	0.1310	0.8500	1.8500	0.0300
G020	6-11	30.6427	5.5465	2.0126	1.2503	2.3487	0.3435	0.1180	0.8700	2.0400	0.0600
G021	4-5	32.5123	5.5677	2.2084	1.2760	2.2452	0.3575	0.1230	0.8600	2.0400	0.0400
G021	4-5	30.6334	5.2470	2.0419	1.2229	2.3354	0.3586	0.1070	0.8200	2.0300	0.0400
G027	14-19	31.6617	4.9188	2.0955	1.2710	2.2445	0.3578	0.1630	0.8900	1.8900	0.0300
G028	cc	32.6432	5.1597	2.1034	1.2395	2.0165	0.3667	0.1200	0.7700	1.7900	0.0490
G029	4-5	31.6897	5.0628	2.0226	1.2088	2.0808	0.3133	0.0570	0.8400	1.9900	0.0400
G029	4-5	32.2272	5.5148	2.0991	1.2262	2.0871	0.3593	0.1170	0.8400	1.8000	0.0400
G032	6-11	31.4981	4.9998	1.9783	1.2561	2.1759	0.3276	0.1090	0.8600	1.8200	0.0300
G033	8-13	31.0167	4.8919	2.0934	1.2470	2.3375	0.3399	0.0880	0.8900	2.0000	0.0400
G034	4-5	32.8255	4.8749	2.1598	1.2810	2.2557	0.3459	0.1180	0.8200	1.9500	0.0300
G034	4-5	32.6432	5.4513	2.1834	1.2677	2.2046	0.3693	0.0990	0.8000	1.8400	0.0400
G036	2-7	31.0728	5.0438	2.0812	1.2096	2.2095	0.3303	0.0880	0.8200	1.8400	0.0400
G041	6-11	30.4231	5.1115	2.1227	1.2378	2.5179	0.3591	0.1350	0.8700	1.8600	0.0400
G042	0-1	28.5301	5.1274	2.4514	1.1631	2.9250	0.3950	0.0780	0.9900	1.9400	0.0400
G043	0-6	28.8386	5.3454	2.3020	1.1872	2.9425	0.3927	0.2500	0.9900	2.1100	0.0600
G046	11-16	28.3525	5.4830	2.5222	1.1905	3.4594	0.4282	0.2020	1.0600	2.0000	0.0400
G047	4-5	27.0531	5.8353	2.6408	1.1349	3.7601	0.4595	0.2340	1.1300	2.1100	0.0400
G048	0-8	26.2071	6.0493	2.6094	1.1125	3.7077	0.4558	0.1760	1.0900	2.0000	0.0400
G049	0-5	26.3754	5.7900	2.9510	1.1133	3.8769	0.4724	0.1490	1.1300	2.1700	0.0400
G049	0-5	25.6042	5.9911	2.8724	1.0842	3.7720	0.4586	0.1690	1.1000	2.1500	0.0500
G050	0-1	27.3195	6.0387	3.3376	1.0942	4.0070	0.4878	0.1150	0.9600	2.4800	0.0400
G050	0-1	22.5567	5.1231	2.6351	0.9215	3.2286	0.3651	0.1030	1.1500	2.4700	0.0800
G051	6-11	26.1043	5.8800	3.0954	1.0826	3.8525	0.4743	0.1840	1.2300	2.4600	0.0500
G052	9-13	24.9077	7.1502	3.4220	0.9929	4.2364	0.5161	0.2120	1.2300	2.4300	0.0400
G053	0-1	25.0573	5.9170	3.9566	1.0278	4.6386	0.5457	0.1790	1.2700	2.3900	0.0300
G054	0-3	25.7397	6.2769	3.9444	0.9954	4.5876	0.5463	0.2090	1.2400	2.4200	0.0500
G055	4-5	26.8241	6.6844	3.4977	1.0651	3.9854	0.5163	0.1040	1.2300	2.6000	0.0500
G055	4-5	27.1372	6.7850	3.5463	1.0776	4.1357	0.5435	0.1530	1.1700	2.2800	0.0400
G056	0-4	25.5574	6.4198	3.3048	1.0602	4.4750	0.5237	0.1200	1.1900	2.4100	0.0400
G057	0-5	26.3614	6.0864	3.4792	1.0560	4.2169	0.5055	0.0730	1.1900	2.3500	0.0400
G059	5-8	26.0809	6.1181	2.9103	1.0984	3.7329	0.4381	0.1220	1.0800	2.2100	0.0400
G060	0-2	26.0809	6.0758	2.6315	1.1482	3.6769	0.4272	0.3550	1.1000	2.3200	0.0600
G061	4-5	26.8802	5.3295	2.6844	1.1291	3.4230	0.4294	0.1650	1.0400	1.9700	0.0300
G062	0-5	28.6376	6.0070	2.6287	1.1714	3.3559	0.4609	0.1720	1.0500	2.1100	0.0400
G063	15-20	26.7587	4.8590	2.2835	1.1316	3.1929	0.4268	0.2080	1.0900	2.0600	0.0400

Table 8 (Continued), Cruise S4-76

CORE	INTERVAL (cm)	11 Li ppm-a	12 Rb ppm-a	13 Zn ppm-a	14 As ppm-x	15 Ge ppm-x	16 Sn ppm-x	17 B ppm-s	18 Ba ppm-s	19 Co ppm-s	20 Cr ppm-s
G064	4-5	20.0000	43.0000	68.0000	4.2780	1.3600	0.5784	30.0000	500.0000	10.0000	50.0000
G065	10-15	20.0000	44.0000	69.0000	0.0000B	0.0000B	0.0000B	30.0000	700.0000	10.0000	50.0000
G066	4-5	17.0000	30.0000	73.0000	4.9450	1.1650	1.0010	50.0000	700.0000	15.0000	70.0000
G067	5-10	16.0000	45.0000	72.0000	0.0000B	0.0000B	0.0000B	50.0000	500.0000	15.0000	50.0000
G069	cc	18.0000	40.0000	58.0000	0.0000B	0.0000B	0.0000B	30.0000	700.0000	7.0000	50.0000
G070	0-1	42.0000	70.0000	111.0000	8.5490	1.3810	0.9752	50.0000	700.0000	15.0000	100.0000
G071	2-7	44.0000	38.0000	118.0000	0.0000B	0.0000B	0.0000B	50.0000	500.0000	15.0000	70.0000
G075	6-10	17.0000	48.0000	55.0000	0.0000B	0.0000B	0.0000B	30.0000	500.0000	7.0000	50.0000
G075	6-10	17.0000	43.0000	59.0000	0.0000B	0.0000B	0.0000B	30.0000	500.0000	10.0000	50.0000
G077	0-5	20.0000	36.0000	62.0000	4.0650	1.4320	0.7464	30.0000	500.0000	7.0000	50.0000
G080	0-5	20.0000	40.0000	72.0000	0.0000B	0.0000B	0.0000B	50.0000	700.0000	7.0000	70.0000
G090	2-4	21.0000	30.0000	79.0000	0.0000B	0.0000B	0.0000B	50.0000	700.0000	10.0000	100.0000
G091	0-1	20.0000	40.0000	79.0000	4.0490	1.4280	0.7971	50.0000	700.0000	10.0000	100.0000
G105	10-15	43.0000	65.0000	134.0000	18.5300	1.6980	1.4940	70.0000	700.0000	15.0000	100.0000
G107	0-5	45.0000	75.0000	140.0000	13.3100	1.6660	1.4360	50.0000	1500.0000	15.0000	100.0000
G109	3-8	16.0000	43.0000	57.0000	0.0000B	0.0000B	0.0000B	50.0000	700.0000	10.0000	70.0000
G110	4-5	16.0000	48.0000	60.0000	4.9950	1.5620	1.0920	20.0000	500.0000	7.0000	50.0000
G111	1-5	17.0000	40.0000	66.0000	0.0000B	0.0000B	0.0000B	30.0000	700.0000	10.0000	50.0000
G112	4-5	18.0000	35.0000	66.0000	4.0130	1.6690	0.8168	50.0000	700.0000	10.0000	30.0000
G112	4-5	17.0000	25.0000	65.0000	0.0000B	0.0000B	0.0000B	50.0000	500.0000	10.0000	50.0000
G113	3-8	20.0000	33.0000	82.0000	5.6080	1.6280	1.3620	50.0000	500.0000	10.0000	30.0000
G114	0-1	19.0000	14.0000	82.0000	3.8160	1.3790	1.4470	50.0000	700.0000	10.0000	70.0000
G115	4-5	18.0000	30.0000	97.0000	4.8970	1.3140	1.2440	50.0000	500.0000	15.0000	30.0000
G115	4-5	19.0000	20.0000	104.0000	0.0000B	0.0000B	0.0000B	30.0000	500.0000	15.0000	30.0000
G116	0-5	20.0000	40.0000	90.0000	0.0000B	0.0000B	0.0000B	30.0000	500.0000	10.0000	30.0000
G117	0-1	18.0000	14.0000	110.0000	0.0000B	0.0000B	0.0000B	50.0000	500.0000	15.0000	50.0000
G118	6-11	20.0000	25.0000	97.0000	0.0000B	0.0000B	0.0000B	30.0000	500.0000	15.0000	30.0000
G119	0-5	17.0000	25.0000	99.0000	0.0000B	0.0000B	0.0000B	30.0000	500.0000	20.0000	30.0000
G120	4-5	19.0000	25.0000	108.0000	0.0000B	0.0000B	0.0000B	30.0000	500.0000	15.0000	50.0000
G120	4-5	19.0000	35.0000	108.0000	0.0000B	0.0000B	0.0000B	30.0000	500.0000	15.0000	30.0000
G121	0-5	17.0000	25.0000	102.0000	0.0000B	0.0000B	0.0000B	20.0000	300.0000	15.0000	30.0000
V002	0-3	15.0000	40.0000	45.0000	5.1910	1.6670	1.0290	20.0000	500.0000	7.0000	70.0000
V003	0-3	16.0000	35.0000	45.0000	5.4190	1.3980	0.5711	30.0000	700.0000	7.0000	200.0000
V006	0-3	16.0000	45.0000	46.0000	6.3580	1.5700	0.9425	30.0000	700.0000	7.0000	50.0000
V007	0-3	18.0000	35.0000	59.0000	0.0000B	0.0000B	0.0000B	50.0000	700.0000	7.0000	50.0000
V007	0-3	19.0000	45.0000	113.0000	0.0000B	0.0000B	0.0000B	30.0000	500.0000	7.0000	70.0000
V009	0-3	16.0000	48.0000	55.0000	0.0000B	0.0000B	0.0000B	50.0000	500.0000	15.0000	70.0000
V011	0-3	16.0000	30.0000	55.0000	6.7000	1.4220	0.6229	30.0000	700.0000	15.0000	70.0000
V012	0-3	15.0000	30.0000	48.0000	6.9840	1.4380	1.3300	50.0000	700.0000	10.0000	100.0000
V014	0-3	17.0000	38.0000	61.0000	5.2570	1.8520	1.1620	20.0000	500.0000	10.0000	50.0000
V014	0-3	18.0000	40.0000	58.0000	0.0000B	0.0000B	0.0000B	50.0000	500.0000	7.0000	50.0000
V015	0-3	16.0000	44.0000	68.0000	0.0000B	0.0000B	0.0000B	30.0000	500.0000	15.0000	150.0000
V017	0-3	13.0000	33.0000	71.0000	5.6390	1.5530	0.8603	20.0000	500.0000	20.0000	150.0000
V018	0-3	18.0000	40.0000	63.0000	5.5590	1.4630	1.0490	20.0000	700.0000	15.0000	70.0000
V018	0-3	16.0000	43.0000	62.0000	0.0000B	0.0000B	0.0000B	30.0000	500.0000	15.0000	100.0000
V021	0-3	18.0000	40.0000	58.0000	3.4330	1.0590	0.6202	30.0000	700.0000	10.0000	70.0000
V028	0-3	16.0000	23.0000	102.0000	0.0000B	0.0000B	0.0000B	30.0000	300.0000	30.0000	30.0000
P003	3-8	19.0000	14.0000	102.0000	0.0000B	0.0000B	0.0000B	50.0000	500.0000	15.0000	50.0000
P005	0-5	22.0000	25.0000	109.0000	0.0000B	0.0000B	0.0000B	30.0000	700.0000	10.0000	50.0000
P005	0-5	22.0000	35.0000	97.0000	0.0000B	0.0000B	0.0000B	30.0000	500.0000	10.0000	50.0000
P006	6-7	23.0000	40.0000	96.0000	0.0000B	0.0000B	0.0000B	50.0000	500.0000	10.0000	50.0000
P007	5-10	21.0000	45.0000	85.0000	0.0000B	0.0000B	0.0000B	70.0000	700.0000	10.0000	100.0000
		48.0000	90.0000	130.0000	8.3310	1.4770	1.4390	30.0000	700.0000	15.0000	70.0000

Table 8 (Continued), Cruise S4-76

CORE	INTERVAL (cm)	31 Th ppm-n	32 U ppm-n
G002	15-20	1.9400	1.5300
G005	0-5	3.5900	1.4600
G006	3-4	5.1000	1.2800
G008	7-15	1.9400	1.8800
G009	4-5	1.9400	1.9200
G010	0-5	1.9400	2.2200
G011	13-18	1.9400	1.9700
G012	4-5	3.2300	1.6200
G013	14-19	5.7800	1.9400
G014	4-5	5.7000	2.1600
G015	4-5	5.1700	2.3700
G016	7-9	1.9400	2.6400
G018	4-5	4.9000	2.5900
G018	4-5	3.7800	2.6900
G019	0-3	1.9400	2.2600
G020	6-11	4.9400	2.0900
G021	4-5	5.8100	2.1900
G021	4-5	5.4700	2.1600
G027	14-19	1.9400	2.8700
G028	cc	4.1700	1.7700
G029	4-5	4.7300	2.0900
G029	4-5	3.9200	2.0300
G032	6-11	3.7500	2.2500
G033	8-13	3.8700	2.2100
G034	4-5	5.2600	1.8100
G034	4-5	1.9400	2.0800
G036	2-7	4.5800	1.5700
G041	6-11	1.9400	2.2600
G042	0-1	5.2700	2.0700
G043	0-6	5.5200	3.2900
G046	11-16	6.4300	2.4500
G047	4-5	1.9400	3.0200
G048	0-8	4.4900	2.4000
G049	0-5	1.9400	2.7700
G049	0-5	1.9400	2.4200
G050	0-1	1.9400	2.9000
G050	0-1	1.9400	2.7300
G051	6-11	1.9400	2.5800
G052	9-13	1.9400	2.2600
G053	0-1	5.1800	1.8900
G054	0-3	1.9400	2.3700
G055	4-5	4.4100	2.2200
G055	4-5	1.9400	2.4700
G056	0-4	1.9400	2.1200
G057	0-5	4.5000	1.7600
G059	5-8	1.9400	2.4000
G060	0-2	1.9400	3.6200
G061	4-5	4.8800	2.5900
G062	0-5	1.9400	2.6500
G063	15-20	1.9400	2.1600
G064	4-5	3.3600	2.0500
G065	10-15	1.9400	2.3500
G066	4-5	1.9400	2.6100
G067	5-10	3.9400	1.6600
G069	cc	3.6500	1.6800
G070	0-1	6.6500	2.9100
G071	2-7	7.7300	3.9400
G075	6-10	5.7600	1.8400
G075	6-10	4.3600	1.9200
G077	0-5	5.6700	2.0800
G080	0-5	1.9400	2.5200
G090	2-4	4.5400	2.6000
G091	0-1	4.9000	2.0900
G105	10-15	7.1300	3.4000
G107	0-5	6.9900	2.8200
G109	3-8	4.3000	1.9000
G110	4-5	5.4600	1.8100
G111	1-5	4.6600	2.0900
G112	4-5	1.9400	2.0900
G112	4-5	1.9400	1.9800
G113	3-8	3.9400	1.8800
G114	0-1	1.9400	2.1000
G115	4-5	1.9400	2.1300
G115	4-5	1.9400	2.3500
G116	0-5	5.2500	2.0100
G117	0-1	1.9400	1.9900
G118	6-11	1.9400	2.4200
G119	0-5	1.9400	2.1900
G120	4-5	1.9400	2.7000
G120	4-5	1.9400	2.5700
G121	0-5	1.9400	1.6000
V002	0-3	3.6600	1.7600
V003	0-3	2.7700	1.5100
V006	0-3	4.9700	1.4700
V007	0-3	1.9400	1.7900
V007	0-3	3.7600	1.6500
V009	0-3	3.8300	1.3300
V011	0-3	4.8100	1.6700
V012	0-3	2.8700	1.5200
V014	0-3	4.5100	1.4200
V014	0-3	3.5700	1.4300
V015	0-3	4.4600	1.4200
V017	0-3	4.4400	1.4300
V018	0-3	3.6400	1.7400
V018	0-3	4.2300	1.5900
V021	0-3	2.8600	1.6900
V028	0-3	1.9400	1.2100
P003	3-8	6.1600	2.2200
P005	0-5	1.9400	2.6600
P005	0-5	1.9400	3.0300
P006	6-	1.9400	2.3500
P007	5- 0	1.9400	2.3200
P008	3-8	6.3700	3.8100

Table 8 (Continued), Cruise S4-76

CORE	INTERVAL (cm)	11 Li ppm-a	12 Rb ppm-a	13 Zn ppm-a	14 As ppm-x	15 Ce ppm-x	16 Sn ppm-x	17 B ppm-s	18 Ba ppm-s	19 Co ppm-s	20 Cr ppm-s
G064	4-5	20.0000	43.0000	68.0000	4.2730	1.3600	0.5794	30.0000	500.0000	10.0000	50.0000
G065	10-15	20.0000	44.0000	69.0000	0.0000B	0.0000B	0.0000B	30.0000	700.0000	10.0000	50.0000
G066	4-5	17.0000	30.0000	73.0000	4.9450	1.1650	1.0010	50.0000	700.0000	15.0000	70.0000
G067	5-10	16.0000	45.0000	72.0000	0.0000B	0.0000B	0.0000B	50.0000	500.0000	15.0000	50.0000
G069	cc	13.0000	40.0000	58.0000	0.0000B	0.0000B	0.0000B	30.0000	700.0000	7.0000	50.0000
G070	0-1	42.0000	70.0000	111.0000	3.5490	1.3810	0.9752	50.0000	700.0000	15.0000	100.0000
G071	2-7	44.0000	38.0000	118.0000	0.0000B	0.0000B	0.0000B	50.0000	500.0000	15.0000	70.0000
G075	6-10	17.0000	43.0000	55.0000	0.0000B	0.0000B	0.0000B	30.0000	500.0000	7.0000	50.0000
G075	6-10	17.0000	43.0000	59.0000	0.0000B	0.0000B	0.0000B	30.0000	500.0000	10.0000	50.0000
G077	0-5	20.0000	36.0000	62.0000	4.0650	1.4320	0.7464	30.0000	500.0000	7.0000	50.0000
G080	0-5	20.0000	40.0000	72.0000	0.0000B	0.0000B	0.0000B	50.0000	700.0000	7.0000	70.0000
G090	2-4	21.0000	30.0000	79.0000	0.0000B	0.0000B	0.0000B	50.0000	700.0000	10.0000	100.0000
G091	0-1	20.0000	40.0000	79.0000	4.0490	1.4280	0.7971	50.0000	700.0000	10.0000	100.0000
G105	10-15	43.0000	65.0000	134.0000	18.5300	1.6930	1.4940	70.0000	700.0000	15.0000	100.0000
G107	0-5	45.0000	75.0000	140.0000	13.3100	1.6660	1.4360	50.0000	1500.0000	15.0000	100.0000
G109	3-8	16.0000	43.0000	57.0000	0.0000B	0.0000B	0.0000B	50.0000	700.0000	10.0000	70.0000
G110	4-5	16.0000	43.0000	60.0000	4.9950	1.5620	1.0920	20.0000	500.0000	7.0000	50.0000
G111	1-5	17.0000	40.0000	66.0000	0.0000B	0.0000B	0.0000B	30.0000	700.0000	10.0000	50.0000
G112	4-5	17.0000	35.0000	66.0000	4.0130	1.6690	0.8168	50.0000	700.0000	10.0000	50.0000
G112	4-5	17.0000	25.0000	65.0000	0.0000B	0.0000B	0.0000B	50.0000	500.0000	10.0000	50.0000
G113	3-8	20.0000	33.0000	82.0000	5.6080	1.6280	1.3620	50.0000	500.0000	10.0000	50.0000
G114	0-1	19.0000	14.0000	82.0000	3.8160	1.3790	1.4470	50.0000	700.0000	10.0000	70.0000
G115	4-5	18.0000	30.0000	97.0000	4.8970	1.3140	1.2440	50.0000	500.0000	15.0000	30.0000
G115	4-5	19.0000	20.0000	104.0000	0.0000B	0.0000B	0.0000B	30.0000	500.0000	15.0000	30.0000
G116	0-5	20.0000	40.0000	90.0000	0.0000B	0.0000B	0.0000B	30.0000	500.0000	10.0000	30.0000
G117	0-1	13.0000	14.0000	110.0000	0.0000B	0.0000B	0.0000B	50.0000	500.0000	15.0000	50.0000
G118	6-11	20.0000	25.0000	97.0000	0.0000B	0.0000B	0.0000B	30.0000	500.0000	15.0000	30.0000
G119	0-5	17.0000	25.0000	99.0000	0.0000B	0.0000B	0.0000B	30.0000	500.0000	20.0000	30.0000
G120	4-5	19.0000	25.0000	108.0000	0.0000B	0.0000B	0.0000B	30.0000	500.0000	15.0000	50.0000
G120	4-5	19.0000	35.0000	108.0000	0.0000B	0.0000B	0.0000B	30.0000	500.0000	15.0000	30.0000
G121	0-5	17.0000	25.0000	102.0000	0.0000B	0.0000B	0.0000B	20.0000	300.0000	15.0000	30.0000
V002	0-3	15.0000	40.0000	45.0000	5.1910	1.6670	1.0290	20.0000	500.0000	7.0000	70.0000
V003	0-3	16.0000	35.0000	45.0000	5.4190	1.3980	0.5711	30.0000	700.0000	7.0000	200.0000
V006	0-3	16.0000	45.0000	46.0000	6.3530	1.5700	0.9425	30.0000	700.0000	7.0000	50.0000
V007	0-3	18.0000	35.0000	59.0000	0.0000B	0.0000B	0.0000B	50.0000	700.0000	7.0000	50.0000
V007	0-3	19.0000	45.0000	113.0000	0.0000B	0.0000B	0.0000B	30.0000	500.0000	7.0000	70.0000
V009	0-3	16.0000	48.0000	55.0000	0.0000B	0.0000B	0.0000B	50.0000	500.0000	15.0000	70.0000
V011	0-3	16.0000	30.0000	55.0000	6.7000	1.4220	0.6229	30.0000	700.0000	15.0000	70.0000
V012	0-3	15.0000	30.0000	48.0000	6.9340	1.4330	1.3300	50.0000	700.0000	10.0000	100.0000
V014	0-3	17.0000	38.0000	61.0000	5.2520	1.3520	1.1620	20.0000	500.0000	10.0000	50.0000
V014	0-3	18.0000	40.0000	58.0000	0.0000B	0.0000B	0.0000B	50.0000	500.0000	7.0000	50.0000
V015	0-3	16.0000	44.0000	68.0000	0.0000B	0.0000B	0.0000B	30.0000	500.0000	15.0000	150.0000
V017	0-3	13.0000	33.0000	71.0000	5.6390	1.5530	0.8603	20.0000	500.0000	20.0000	150.0000
V013	0-3	13.0000	40.0000	63.0000	5.5590	1.4630	1.0490	20.0000	700.0000	15.0000	70.0000
V018	0-3	16.0000	43.0000	62.0000	0.0000B	0.0000B	0.0000B	30.0000	500.0000	15.0000	100.0000
V021	0-3	18.0000	40.0000	58.0000	3.4130	1.0590	0.6202	30.0000	700.0000	10.0000	70.0000
V023	0-3	16.0000	23.0000	102.0000	0.0000B	0.0000B	0.0000B	30.0000	300.0000	10.0000	30.0000
P003	3-8	19.0000	14.0000	102.0000	0.0000B	0.0000B	0.0000B	50.0000	500.0000	15.0000	50.0000
P005	0-5	22.0000	25.0000	109.0000	0.0000B	0.0000B	0.0000B	30.0000	700.0000	10.0000	50.0000
P005	0-5	22.0000	35.0000	97.0000	0.0000B	0.0000B	0.0000B	30.0000	500.0000	10.0000	50.0000
P006	6-7	23.0000	40.0000	96.0000	0.0000B	0.0000B	0.0000B	50.0000	500.0000	10.0000	50.0000
P007	5-10	21.0000	45.0000	85.0000	0.0000B	0.0000B	0.0000B	70.0000	700.0000	10.0000	100.0000
		48.0000	90.0000	130.0000	8.3110	1.4770	1.4390	30.0000	700.0000	15.0000	70.0000

Table 8 (Continued), Cruise S4-76

CORE	INTERVAL (cm)	21 Cu ppm-s	22 Ga ppm-s	23 Mn ppm-s	24 Ni ppm-s	25 Sc ppm-s	26 Sr ppm-s	27 V ppm-s	28 Y ppm-s	29 Yb ppm-s	30 Zr ppm-s
G002	15-20	70.0000	20.0000	700.0000	15.0000	20.0000	500.0000	150.0000	30.0000	3.0000	70.0000
G005	3-5	70.0000	20.0000	700.0000	10.0000	20.0000	500.0000	200.0000	50.0000	5.0000	100.0000
G006	3-4	70.0000	15.0000	700.0000	15.0000	30.0000	700.0000	300.0000	30.0000	5.0000	70.0000
G008	7-15	50.0000	20.0000	700.0000	15.0000	20.0000	500.0000	200.0000	30.0000	3.0000	70.0000
G009	4-5	70.0000	30.0000	700.0000	15.0000	20.0000	500.0000	200.0000	20.0000	3.0000	100.0000
G010	0-5	30.0000	20.0000	700.0000	15.0000	15.0000	500.0000	150.0000	20.0000	3.0000	70.0000
G011	13-18	30.0000	15.0000	500.0000	15.0000	15.0000	500.0000	150.0000	30.0000	3.0000	100.0000
G012	4-5	30.0000	20.0000	500.0000	15.0000	15.0000	500.0000	100.0000	30.0000	3.0000	100.0000
G013	14-19	30.0000	20.0000	500.0000	20.0000	15.0000	500.0000	150.0000	30.0000	3.0000	100.0000
G014	4-5	30.0000	15.0000	500.0000	15.0000	15.0000	300.0000	100.0000	30.0000	3.0000	150.0000
G015	4-5	20.0000	20.0000	500.0000	30.0000	15.0000	300.0000	150.0000	20.0000	3.0000	100.0000
G016	7-9	50.0000	20.0000	500.0000	15.0000	15.0000	500.0000	150.0000	30.0000	3.0000	150.0000
G018	4-5	20.0000	15.0000	300.0000	15.0000	10.0000	300.0000	70.0000	20.0000	3.0000	100.0000
G018	4-5	30.0000	15.0000	300.0000	20.0000	15.0000	300.0000	100.0000	20.0000	2.0000	200.0000
G019	0-3	15.0000	15.0000	500.0000	30.0000	15.0000	300.0000	150.0000	20.0000	3.0000	150.0000
G020	6-11	15.0000	15.0000	500.0000	20.0000	15.0000	200.0000	100.0000	20.0000	2.0000	70.0000
G021	4-5	15.0000	15.0000	500.0000	20.0000	10.0000	300.0000	70.0000	20.0000	3.0000	70.0000
G021	4-5	15.0000	15.0000	500.0000	15.0000	15.0000	300.0000	100.0000	20.0000	3.0000	100.0000
G027	14-19	15.0000	15.0000	300.0000	20.0000	10.0000	300.0000	100.0000	20.0000	3.0000	100.0000
G028	cc	15.0000	15.0000	500.0000	15.0000	15.0000	200.0000	70.0000	30.0000	3.0000	150.0000
G029	4-5	20.0000	15.0000	500.0000	20.0000	15.0000	300.0000	70.0000	15.0000	1.5000	100.0000
G029	4-5	15.0000	15.0000	500.0000	20.0000	15.0000	300.0000	70.0000	15.0000	2.0000	70.0000
G032	6-11	15.0000	15.0000	300.0000	20.0000	10.0000	300.0000	100.0000	20.0000	3.0000	100.0000
G033	8-13	20.0000	15.0000	500.0000	20.0000	15.0000	200.0000	70.0000	15.0000	1.5000	70.0000
G034	4-5	15.0000	15.0000	500.0000	30.0000	15.0000	300.0000	100.0000	15.0000	2.0000	100.0000
G034	4-5	15.0000	15.0000	700.0000	15.0000	15.0000	300.0000	100.0000	20.0000	2.0000	70.0000
G036	2-7	15.0000	20.0000	500.0000	20.0000	15.0000	300.0000	70.0000	20.0000	2.0000	70.0000
G041	6-11	20.0000	15.0000	500.0000	20.0000	15.0000	300.0000	100.0000	20.0000	3.0000	150.0000
G042	0-1	30.0000	20.0000	500.0000	20.0000	15.0000	500.0000	150.0000	20.0000	3.0000	100.0000
G043	0-6	50.0000	20.0000	500.0000	20.0000	15.0000	300.0000	100.0000	30.0000	3.0000	200.0000
G046	11-16	30.0000	20.0000	500.0000	30.0000	15.0000	300.0000	150.0000	20.0000	2.0000	100.0000
G047	4-5	50.0000	20.0000	500.0000	20.0000	15.0000	300.0000	150.0000	30.0000	3.0000	100.0000
G048	0-8	50.0000	20.0000	500.0000	20.0000	20.0000	500.0000	150.0000	30.0000	3.0000	100.0000
G049	0-5	70.0000	20.0000	700.0000	15.0000	15.0000	300.0000	150.0000	30.0000	3.0000	100.0000
G049	0-5	50.0000	20.0000	500.0000	15.0000	15.0000	300.0000	150.0000	30.0000	3.0000	100.0000
G050	0-1	50.0000	20.0000	700.0000	15.0000	20.0000	500.0000	150.0000	30.0000	3.0000	70.0000
G050	0-1	50.0000	20.0000	500.0000	15.0000	15.0000	500.0000	200.0000	50.0000	5.0000	70.0000
G051	6-11	50.0000	20.0000	700.0000	20.0000	20.0000	500.0000	200.0000	30.0000	5.0000	100.0000
G052	9-13	50.0000	20.0000	500.0000	10.0000	20.0000	300.0000	150.0000	30.0000	3.0000	150.0000
G053	0-1	70.0000	20.0000	700.0000	15.0000	20.0000	500.0000	200.0000	30.0000	3.0000	100.0000
G054	0-3	70.0000	30.0000	700.0000	15.0000	30.0000	700.0000	200.0000	30.0000	3.0000	70.0000
G055	4-5	50.0000	20.0000	700.0000	15.0000	20.0000	500.0000	200.0000	30.0000	3.0000	100.0000
G055	4-5	50.0000	20.0000	500.0000	20.0000	20.0000	500.0000	200.0000	30.0000	3.0000	100.0000
G056	0-4	50.0000	20.0000	500.0000	15.0000	20.0000	500.0000	200.0000	30.0000	3.0000	100.0000
G057	0-5	50.0000	30.0000	700.0000	15.0000	20.0000	500.0000	200.0000	30.0000	3.0000	70.0000
G059	3-5	50.0000	20.0000	500.0000	15.0000	15.0000	300.0000	150.0000	30.0000	3.0000	100.0000
G060	0-2	50.0000	20.0000	500.0000	15.0000	20.0000	300.0000	150.0000	30.0000	3.0000	70.0000
G061	4-5	50.0000	20.0000	500.0000	30.0000	15.0000	500.0000	150.0000	30.0000	3.0000	100.0000
G062	0-5	50.0000	20.0000	500.0000	15.0000	15.0000	300.0000	150.0000	20.0000	3.0000	100.0000
G063	15-20	50.0000	15.0000	500.0000	15.0000	15.0000	300.0000	150.0000	30.0000	3.0000	70.0000

Table 8 (Continued), Cruise S4-76

CORE	INTERVAL (cm)	21 Cu ppm-s	22 Ga ppm-s	23 Mn ppm-s	24 Ni ppm-s	25 Sc ppm-s	26 Sr ppm-s	27 V ppm-s	28 Y ppm-s	29 Yb ppm-s	30 Zr ppm-s
G064	4-5	20.0000	15.0000	500.0000	15.0000	15.0000	300.0000	100.0000	30.0000	3.0000	70.0000
G065	10-15	20.0000	15.0000	500.0000	20.0000	15.0000	300.0000	150.0000	20.0000	3.0000	70.0000
G066	4-5	30.0000	15.0000	700.0000	30.0000	15.0000	500.0000	150.0000	20.0000	3.0000	100.0000
G067	5-10	20.0000	15.0000	700.0000	15.0000	15.0000	200.0000	100.0000	20.0000	2.0000	70.0000
G069	cc	15.0000	15.0000	300.0000	15.0000	10.0000	200.0000	100.0000	20.0000	3.0000	100.0000
G070	0-1	50.0000	20.0000	500.0000	20.0000	15.0000	300.0000	200.0000	30.0000	3.0000	100.0000
G071	2-7	50.0000	30.0000	500.0000	20.0000	15.0000	300.0000	150.0000	30.0000	3.0000	70.0000
G075	6-10	15.0000	15.0000	500.0000	20.0000	10.0000	200.0000	70.0000	15.0000	1.5000	100.0000
G075	6-10	15.0000	15.0000	500.0000	20.0000	15.0000	300.0000	100.0000	15.0000	2.0000	100.0000
G077	0-5	15.0000	15.0000	500.0000	20.0000	15.0000	300.0000	100.0000	30.0000	3.0000	150.0000
G080	0-5	20.0000	15.0000	500.0000	20.0000	10.0000	300.0000	100.0000	20.0000	3.0000	100.0000
G090	2-4	30.0000	15.0000	300.0000	30.0000	15.0000	500.0000	100.0000	30.0000	3.0000	100.0000
G091	0-1	20.0000	15.0000	500.0000	30.0000	15.0000	500.0000	150.0000	20.0000	3.0000	100.0000
G105	10-15	70.0000	30.0000	500.0000	50.0000	15.0000	200.0000	150.0000	20.0000	3.0000	70.0000
G107	0-5	70.0000	20.0000	300.0000	50.0000	15.0000	300.0000	200.0000	30.0000	3.0000	100.0000
G109	3-8	30.0000	15.0000	500.0000	15.0000	15.0000	300.0000	100.0000	20.0000	2.0000	70.0000
G110	4-5	15.0000	15.0000	500.0000	15.0000	15.0000	300.0000	100.0000	20.0000	3.0000	100.0000
G111	1-5	30.0000	20.0000	500.0000	15.0000	15.0000	300.0000	150.0000	20.0000	3.0000	150.0000
G112	4-5	20.0000	15.0000	500.0000	15.0000	15.0000	300.0000	150.0000	20.0000	3.0000	70.0000
G112	4-5	20.0000	15.0000	500.0000	15.0000	15.0000	300.0000	150.0000	20.0000	3.0000	100.0000
G113	3-8	50.0000	20.0000	700.0000	15.0000	15.0000	300.0000	150.0000	30.0000	3.0000	100.0000
G114	0-1	50.0000	15.0000	500.0000	15.0000	15.0000	500.0000	150.0000	20.0000	3.0000	100.0000
G115	4-5	50.0000	15.0000	500.0000	15.0000	15.0000	500.0000	150.0000	30.0000	3.0000	70.0000
G115	4-5	50.0000	20.0000	500.0000	15.0000	15.0000	500.0000	150.0000	30.0000	3.0000	100.0000
G116	0-5	50.0000	20.0000	500.0000	15.0000	15.0000	300.0000	150.0000	30.0000	3.0000	100.0000
G117	0-1	70.0000	20.0000	500.0000	15.0000	15.0000	500.0000	200.0000	30.0000	3.0000	70.0000
G118	6-11	50.0000	15.0000	700.0000	15.0000	15.0000	300.0000	150.0000	30.0000	3.0000	70.0000
G119	0-5	70.0000	20.0000	700.0000	15.0000	20.0000	500.0000	200.0000	30.0000	3.0000	70.0000
G120	4-5	70.0000	20.0000	700.0000	20.0000	20.0000	700.0000	200.0000	30.0000	5.0000	70.0000
G120	4-5	50.0000	15.0000	700.0000	15.0000	15.0000	500.0000	150.0000	30.0000	3.0000	100.0000
G121	0-5	70.0000	20.0000	700.0000	15.0000	15.0000	500.0000	200.0000	30.0000	3.0000	70.0000
V002	0-3	7.0000	15.0000	500.0000	15.0000	10.0000	200.0000	70.0000	15.0000	2.0000	70.0000
V003	0-3	7.0000	15.0000	300.0000	15.0000	10.0000	200.0000	70.0000	20.0000	2.0000	70.0000
V006	0-3	7.0000	10.0000	300.0000	15.0000	7.0000	200.0000	70.0000	20.0000	2.0000	70.0000
V007	0-3	15.0000	15.0000	300.0000	15.0000	10.0000	300.0000	100.0000	15.0000	2.0000	70.0000
V007	0-3	20.0000	15.0000	300.0000	20.0000	10.0000	300.0000	70.0000	20.0000	3.0000	100.0000
V009	0-3	7.0000	15.0000	500.0000	50.0000	7.0000	200.0000	70.0000	15.0000	1.5000	70.0000
V011	0-3	15.0000	15.0000	300.0000	30.0000	10.0000	500.0000	100.0000	20.0000	3.0000	150.0000
V012	0-3	10.0000	10.0000	300.0000	30.0000	10.0000	300.0000	100.0000	15.0000	1.5000	70.0000
V014	0-3	15.0000	15.0000	500.0000	20.0000	15.0000	300.0000	100.0000	20.0000	2.0000	100.0000
V014	0-3	15.0000	15.0000	300.0000	30.0000	10.0000	300.0000	70.0000	15.0000	2.0000	100.0000
V015	0-3	15.0000	15.0000	500.0000	50.0000	15.0000	300.0000	150.0000	20.0000	3.0000	70.0000
V017	0-3	20.0000	20.0000	500.0000	150.0000	15.0000	300.0000	100.0000	15.0000	2.0000	150.0000
V018	0-3	15.0000	15.0000	300.0000	50.0000	15.0000	300.0000	150.0000	20.0000	3.0000	70.0000
V018	0-3	15.0000	15.0000	500.0000	30.0000	15.0000	300.0000	150.0000	15.0000	1.5000	100.0000
V021	0-3	15.0000	15.0000	300.0000	30.0000	10.0000	300.0000	100.0000	20.0000	2.0000	100.0000
V023	0-3	100.0000	20.0000	700.0000	70.0000	30.0000	500.0000	200.0000	20.0000	3.0000	70.0000
P003	3-8	70.0000	20.0000	700.0000	15.0000	20.0000	500.0000	200.0000	30.0000	3.0000	100.0000
P005	0-5	50.0000	15.0000	500.0000	20.0000	15.0000	500.0000	150.0000	30.0000	3.0000	70.0000
P005	0-5	50.0000	15.0000	500.0000	15.0000	15.0000	300.0000	150.0000	30.0000	3.0000	70.0000
P006	6-	50.0000	20.0000	500.0000	20.0000	15.0000	500.0000	150.0000	30.0000	3.0000	100.0000
P007	5- 0	30.0000	15.0000	500.0000	30.0000	15.0000	500.0000	150.0000	20.0000	3.0000	100.0000
P008	3-6	50.0000	20.0000	500.0000	30.0000	15.0000	200.0000	200.0000	30.0000	3.0000	70.0000

Table 8 (Continued), Cruise S4-76

CORE	INTERVAL (cm)	31 Th ppm-n	32 U ppm-n
G002	15-20	1.9400	1.5100
G005	0-5	3.5900	1.4600
G006	3-4	5.1300	1.2300
G008	7-15	1.9400	1.8800
G009	4-5	1.9400	1.9200
G010	0-5	1.9400	2.2200
G011	13-18	1.9400	1.9700
G012	4-5	3.2300	1.6200
G013	14-19	5.7800	1.9400
G014	4-5	5.7000	2.1600
G015	4-5	5.1700	2.3700
G016	7-9	1.9400	2.6400
G018	4-5	4.9000	2.5900
G018	4-5	3.7300	2.6900
G019	0-3	1.9400	2.2600
G020	6-11	4.9400	2.0900
G021	4-5	5.3100	2.1900
G021	4-5	5.4700	2.1600
G027	14-19	1.9400	2.8700
G028	cc	4.1700	1.7700
G029	4-5	4.7300	2.0900
G029	4-5	3.9200	2.0300
G032	6-11	3.7500	2.2500
G033	8-13	3.9700	2.2100
G034	4-5	5.2600	1.8100
G034	4-5	1.9400	2.0300
G036	2-7	4.5300	1.5700
G041	6-11	1.9400	2.2600
G042	0-1	5.2700	2.0700
G043	0-6	5.5200	3.2900
G046	11-16	6.4300	2.4500
G047	4-5	1.9400	3.0200
G048	0-8	4.4900	2.4000
G049	0-5	1.9400	2.7700
G049	0-5	1.9400	2.4200
G050	0-1	1.9400	2.9000
G050	0-1	1.9400	2.7300
G051	6-11	1.9400	2.5300
G052	9-13	1.9400	2.2600
G053	0-1	5.1800	1.8900
G054	0-3	1.9400	2.3700
G055	4-5	4.4100	2.2200
G055	4-5	1.9400	2.4700
G056	0-4	1.9400	2.1200
G057	0-5	4.5000	1.7600
G059	3-8	1.9400	2.4000
G060	0-2	1.9400	3.6200
G061	4-5	4.8600	2.5900
G062	0-5	1.9400	2.6500
G063	15-20	1.9400	2.1600
G064	4-5	3.3600	2.0500
G065	10-15	1.9400	2.3500
G066	4-5	1.9400	2.6100
G067	5-10	3.9400	1.6600
G069	cc	3.6500	1.6300
G070	0-1	6.6500	2.9100
G071	2-7	7.7300	3.9400
G075	6-10	5.7600	1.8400
G075	6-10	4.3600	1.9200
G077	0-5	5.6700	2.0300
G080	0-5	1.9400	2.5200
G090	2-4	4.5400	2.6000
G091	0-1	4.9000	2.0900
G105	10-15	7.1300	3.4000
G107	0-5	6.9900	2.8200
G109	3-8	4.3000	1.9000
G110	4-5	5.4600	1.8100
G111	1-5	4.6600	2.0900
G112	4-5	1.9400	2.0900
G112	4-5	1.9400	1.9800
G113	3-8	3.9400	1.8800
G114	0-1	1.9400	2.1000
G115	4-5	1.9400	2.1300
G115	4-5	1.9400	2.3500
G116	0-5	5.2500	2.0100
G117	0-1	1.9400	1.9900
G118	6-11	1.9400	2.4200
G119	0-5	1.9400	2.1900
G120	4-5	1.9400	2.7000
G120	4-5	1.9400	2.5700
G121	0-5	1.9400	1.6000
V002	0-3	3.6600	1.7600
V003	0-3	2.7700	1.5100
V006	0-3	4.9700	1.4700
V007	0-3	1.9400	1.7900
V007	0-3	3.7600	1.6500
V009	0-3	3.8300	1.3300
V011	0-3	4.8100	1.6700
V012	0-3	2.9700	1.5200
V014	0-3	4.5100	1.4200
V014	0-3	3.5700	1.4300
V015	0-3	4.4600	1.4200
V017	0-3	4.4400	1.4300
V013	0-3	3.6400	1.7400
V018	0-3	4.2300	1.5900
V021	0-3	2.8600	1.6900
V028	0-3	1.9400	1.2100
P003	3-8	6.1600	2.2200
P005	0-5	1.9400	2.6600
P005	0-5	1.9400	3.0300
P006	6-	1.9400	2.3500
P007	5- 0	1.9400	2.3200
P008	3-8	6.3700	3.8100

Table 8 (Continued), Cruise S6-77.

S6-77 data, seawater corrected

CORE	INTERVAL (cm)	Si %-xrf	Al %-xrf	Ca %-xrf	K %-xrf	Fe %-xrf	Ti %-xrf	% S-swc	% Mg-swc	% Na-swc	Hg ppm-a
V05	0-4	24.7743	6.8802	3.7164	0.8302	6.9943	0.8393	0.0861	2.8748	2.5240	0.0400
V06	0-4	24.3069	7.9387	4.0737	0.7471	5.3856	0.7194	0.1674	1.8529	2.9218	0.0400
V06	0-4	24.3069	7.4095	4.0023	0.7471	5.2457	0.7194	0.1674	1.8649	2.9960	0.0100
V07	0-4	24.7743	7.9387	4.2882	0.8302	5.3156	0.6595	0.0861	2.0907	2.8949	0.0300
G07	0-1	33.6557	5.1337	1.5723	1.0792	1.8884	0.2998	0.0768	0.8410	2.0701	0.0400
G12	11-12	28.5138	6.8802	1.3579	1.5773	3.5670	0.4196	0.1767	1.4501	2.0330	0.0800
G12	11-12	28.9813	7.4095	1.2864	1.6603	3.5670	0.4796	0.1767	1.5285	1.9588	0.0900
G14	0-5	26.6441	5.8217	2.7158	0.7471	3.6370	0.4196	0.1559	1.4146	2.3417	0.0100
G16	0-5	26.1766	6.3510	3.0017	0.9132	4.0566	0.4796	0.3116	1.5433	2.7060	0.0400
G19	0-5	26.6441	6.3510	3.0017	0.7471	4.0566	0.4796	0.1163	1.5801	2.5323	0.0100
G20	0-5	29.4487	3.9164	1.5008	0.7471	2.3081	0.2998	0.1140	0.9804	2.3467	0.0400
G22	0-5	29.4487	3.7576	1.5008	0.7471	2.1682	0.2998	0.0489	0.8685	1.9589	0.0100
G23	0-5	30.3836	2.9638	1.3579	0.5811	1.8185	0.2398	0.0372	0.8450	2.8138	0.0100L
G24	0-5	28.5138	3.1755	1.1435	0.7471	1.9584	0.2398	-0.0953	0.9187	2.2489	0.0800
G25	0-10	30.3836	3.9693	1.3579	0.8302	2.0982	0.2998	0.2930	1.0762	3.2522	0.1200
G25	0-10	28.5138	3.9164	1.2864	0.7471	2.0283	0.2398	0.0605	0.9750	2.6874	0.0400
G26	0-5	27.1115	5.2925	2.1441	0.9132	3.2873	0.4196	0.1745	1.3992	2.3890	0.1000
G29	0-5	28.0464	4.3398	1.2864	0.8302	2.4480	0.2998	0.3884	1.1358	2.7582	0.0300

CORE	INTERVAL (cm)	Li ppm-a	Rb ppm-a	Zn ppm-a	As ppm-x	Ge ppm-x	Sn ppm-x	B ppm-a	Ba ppm-a	Co ppm-a	Cr ppm-x
V05	0-4	6.0000	15.0000	135.0000	14.0000	1.6000	0.7000	20.0000	300.0000	30.0000	50.0000
V06	0-4	6.0000	15.0000	0.0000B	0.0000B	0.0000B	0.0000B	20.0000	500.0000	30.0000	20.0000
V06	0-4	5.0000	15.0000	107.0000	4.6000	1.2000	0.6000	20.0000	500.0000	30.0000	15.0000
V07	0-4	5.0000L	15.0000	102.0000	86.0000	0.2000L	0.3000	15.0000	500.0000	30.0000	30.0000
G07	0-1	7.0000	25.0000	56.0000	4.9000	1.5000	1.3000	30.0000	700.0000	15.0000	70.0000
G12	11-12	20.0000	40.0000	121.0000	4.8000	0.6000	1.0000	70.0000	700.0000	20.0000	100.0000
G12	11-12	21.0000	40.0000	126.0000	9.0000	1.3000	0.8000	70.0000	700.0000	20.0000	70.0000
G14	0-5	7.0000	15.0000	101.0000	0.0000B	0.0000B	0.0000B	70.0000	500.0000	20.0000	30.0000
G16	0-5	8.0000	15.0000	119.0000	5.2000	1.0000	1.1000	70.0000	500.0000	30.0000	30.0000
G19	0-5	7.0000	15.0000	110.0000	3.4000	1.0000	0.5000	70.0000	700.0000	30.0000	30.0000
G20	0-5	8.0000	15.0000	95.0000	0.0000B	0.0000B	0.0000B	150.0000	1000.0000	15.0000	30.0000
G22	0-5	7.0000	15.0000	88.0000	0.0000B	0.0000B	0.0000B	150.0000	1000.0000	15.0000	30.0000
G23	0-5	6.0000	10.0000	0.0000B	0.0000B	0.0000B	0.0000B	150.0000	1500.0000	15.0000	30.0000
G24	0-5	8.0000	15.0000	89.0000	0.0000B	0.0000B	0.0000B	150.0000	1500.0000	15.0000	30.0000
G25	0-10	7.0000	15.0000	83.0000	0.0000B	0.0000B	0.0000B	150.0000	700.0000	15.0000	30.0000
G25	0-10	8.0000	15.0000	84.0000	0.0000B	0.0000B	0.0000B	150.0000	700.0000	15.0000	50.0000
G26	0-5	10.0000	20.0000	105.0000	0.0000B	0.0000B	0.0000B	70.0000	700.0000	15.0000	50.0000
G29	0-5	10.0000	20.0000	99.0000	0.0000B	0.0000B	0.0000B	150.0000	700.0000	15.0000	50.0000

Table 8 (Continued), Cruise S6-77

S6-77 data, seawater corrected-continued

CORE	INTERVAL (cm)	Cu ppm-s	Ga ppm-s	Mn ppm-s	Ni ppm-s	Sc ppm-s	Sr ppm-s	V ppm-s	Y ppm-s	Yb ppm-s	Zr ppm-s
V05	0-4	20.0000	50.0000	700.0000	30.0000	30.0000	300.0000	300.0000	50.0000	5.0000	150.0000
V06	0-4	70.0000	30.0000	1500.0000	15.0000	30.0000	700.0000	300.0000	50.0000	5.0000	150.0000
V06	0-4	70.0000	30.0000	1500.0000	15.0000	30.0000	700.0000	150.0000	50.0000	5.0000	150.0000
V07	0-4	70.0000	30.0000	1500.0000	15.0000	70.0000	700.0000	300.0000	70.0000	5.0000	150.0000
G07	0-1	15.0000	20.0000	300.0000	30.0000	30.0000	300.0000	150.0000	30.0000	3.0000	200.0000
G12	11-12	70.0000	30.0000	500.0000	70.0000	30.0000	300.0000	300.0000	30.0000	3.0000	150.0000
G12	11-12	70.0000	30.0000	700.0000	70.0000	30.0000	300.0000	150.0000	30.0000	3.0000	150.0000
G14	0-5	100.0000	30.0000	700.0000	50.0000	30.0000	300.0000	200.0000	30.0000	3.0000	100.0000
G16	0-5	150.0000	30.0000	700.0000	30.0000	30.0000	300.0000	200.0000	30.0000	3.0000	150.0000
G19	0-5	150.0000	30.0000	700.0000	30.0000	30.0000	500.0000	150.0000	30.0000	3.0000	100.0000
G20	0-5	100.0000	10.0000	300.0000	50.0000	30.0000	300.0000	150.0000	30.0000	3.0000	100.0000
G22	0-5	100.0000	15.0000	300.0000	30.0000	15.0000	300.0000	150.0000	15.0000	2.0000	70.0000
G23	0-5	70.0000	15.0000	300.0000	30.0000	15.0000	200.0000	70.0000	15.0000	1.5000	70.0000
G24	0-5	100.0000	15.0000	300.0000	50.0000	20.0000	300.0000	100.0000	20.0000	2.0000	70.0000
G25	0-10	70.0000	15.0000	500.0000	30.0000	20.0000	300.0000	150.0000	20.0000	3.0000	70.0000
G25	0-10	70.0000	20.0000	300.0000	30.0000	15.0000	300.0000	150.0000	20.0000	2.0000	150.0000
G26	0-5	100.0000	30.0000	700.0000	30.0000	30.0000	300.0000	150.0000	30.0000	3.0000	100.0000
G29	0-5	70.0000	20.0000	300.0000	30.0000	20.0000	300.0000	150.0000	30.0000	3.0000	100.0000

Table 8 (Continued)

s4-76 Misc. Seds, Pribilof Isl

CORE	INTERVAL (cm)	1 Ca % - s	2 K % - s	3 Fe % - s	4 Ti % - s	5 Mg % - s	6 Na % - s	7 B ppm-s	8 Ba ppm-s	9 Co ppm-s	10 Cr ppm-s
G030	1-6	3.0000	3.0000	5.0000	0.3000	1.5000	2.0000	30.0000	700.0000	10.0000	70.0000
G031	4-5	3.0000	2.0000	5.0000	0.3000	1.5000	3.0000	30.0000	700.0000	10.0000	70.0000
G037	2-7	3.0000	3.0000	3.0000	0.5000	1.0000	2.0000	20.0000	1000.0000	7.0000	50.0000
G037	2-7	3.0000	2.0000	3.0000	0.3000	1.5000	3.0000	30.0000	700.0000	7.0000	50.0000
G038	0-5	3.0000	2.0000	5.0000	0.3000	1.5000	3.0000	30.0000	700.0000	10.0000	30.0000
G039	0-5	3.0000	3.0000	5.0000	0.3000	1.5000	3.0000	50.0000	700.0000	10.0000	100.0000
G040	6-10	3.0000	3.0000	3.0000	0.3000	1.5000	3.0000	30.0000	1000.0000	7.0000	50.0000
G040	6-10	3.0000	3.0000	3.0000	0.3000	1.5000	3.0000	30.0000	700.0000	10.0000	50.0000
G072	4-5	5.0000	3.0000	5.0000	0.5000	2.0000	3.0000	30.0000	700.0000	15.0000	100.0000
G072	4-5	3.0000	2.0000	5.0000	0.3000	2.0000	2.0000	50.0000	500.0000	15.0000	70.0000
G078	0-1	3.0000	2.0000	3.0000	0.3000	1.5000	3.0000	50.0000	700.0000	10.0000	70.0000
G079	0-5	3.0000	3.0000	3.0000	0.3000	1.5000	3.0000	50.0000	700.0000	10.0000	70.0000
G081	30-35	5.0000	3.0000	5.0000	0.5000	2.0000	5.0000	70.0000	700.0000	10.0000	70.0000
G082	20-25	5.0000	3.0000	5.0000	0.5000	1.5000	3.0000	50.0000	1000.0000	10.0000	70.0000
G089	0-3	5.0000	2.0000	5.0000	0.5000	2.0000	3.0000	30.0000	700.0000	15.0000	100.0000
G094	cc	5.0000	2.0000	7.0000	0.7000	5.0000	2.0000	30.0000	500.0000	30.0000	150.0000
G103	2-7	5.0000	3.0000	7.0000	0.5000	2.0000	2.0000	70.0000	700.0000	15.0000	100.0000
V004	0-3	3.0000	2.0000	3.0000	0.3000	1.0000	3.0000	50.0000	700.0000	7.0000	70.0000
V005	0-3	3.0000	2.0000	3.0000	0.3000	1.5000	3.0000	30.0000	500.0000	7.0000	150.0000
V010	0-3	3.0000	2.0000	3.0000	0.2000	3.0000	2.0000	30.0000	500.0000	15.0000	70.0000
V019	0-3	5.0000	2.0000	3.0000	0.3000	1.5000	3.0000	30.0000	700.0000	10.0000	70.0000
V020	0-3	5.0000	3.0000	3.0000	0.5000	2.0000	3.0000	30.0000	700.0000	10.0000	100.0000
V022	0-3	3.0000	2.0000	3.0000	0.3000	1.5000	3.0000	50.0000	500.0000	10.0000	70.0000
V022	0-3	3.0000	3.0000	5.0000	0.3000	2.0000	3.0000	50.0000	700.0000	10.0000	100.0000
V023	0-3	3.0000	3.0000	3.0000	0.3000	2.0000	3.0000	30.0000	700.0000	10.0000	70.0000
V023	0-3	5.0000	2.0000	5.0000	0.5000	1.5000	2.0000	30.0000	1000.0000	10.0000	70.0000
V025	0-3	5.0000	3.0000	7.0000	0.5000	2.0000	3.0000	50.0000	700.0000	15.0000	100.0000
P010	107-109	3.0000	2.0000	5.0000	0.3000	1.5000	5.0000	100.0000	1000.0000	10.0000	50.0000
P013	25-27	5.0000	2.0000	5.0000	0.3000	1.5000	7.0000	100.0000	1000.0000	7.0000	30.0000

CORE	INTERVAL (cm)	11 Cu ppm-s	12 Ga ppm-s	13 Ni ppm-s	14 Sc ppm-s	15 Sr ppm-s	16 V ppm-s	17 Y ppm-s	18 Yb ppm-s	19 Zr ppm-s
G030	1-6	15.0000	15.0000	30.0000	15.0000	500.0000	100.0000	20.0000	3.0000	200.0000
G031	4-5	20.0000	15.0000	30.0000	15.0000	500.0000	100.0000	30.0000	3.0000	150.0000
G037	2-7	15.0000	15.0000	20.0000	10.0000	500.0000	100.0000	20.0000	3.0000	70.0000
G037	2-7	15.0000	15.0000	15.0000	10.0000	300.0000	70.0000	20.0000	2.0000	100.0000
G038	0-5	20.0000	15.0000	20.0000	15.0000	300.0000	100.0000	20.0000	3.0000	100.0000
G039	0-5	30.0000	15.0000	30.0000	15.0000	500.0000	150.0000	30.0000	3.0000	100.0000
G040	6-10	15.0000	15.0000	20.0000	15.0000	500.0000	100.0000	20.0000	3.0000	150.0000
G040	6-10	20.0000	15.0000	20.0000	10.0000	300.0000	70.0000	20.0000	3.0000	70.0000
G072	4-5	50.0000	20.0000	50.0000	15.0000	500.0000	150.0000	30.0000	3.0000	150.0000
G072	4-5	50.0000	15.0000	50.0000	15.0000	300.0000	150.0000	30.0000	3.0000	100.0000
G078	0-1	15.0000	15.0000	20.0000	15.0000	300.0000	70.0000	30.0000	3.0000	150.0000
G079	0-5	15.0000	20.0000	20.0000	15.0000	500.0000	70.0000	30.0000	3.0000	150.0000
G081	30-35	30.0000	15.0000	30.0000	15.0000	500.0000	150.0000	30.0000	3.0000	300.0000
G082	20-25	30.0000	15.0000	30.0000	15.0000	500.0000	150.0000	20.0000	3.0000	100.0000
G089	0-3	20.0000	20.0000	50.0000	15.0000	500.0000	150.0000	30.0000	3.0000	200.0000
G094	cc	70.0000	20.0000	100.0000	20.0000	500.0000	200.0000	30.0000	3.0000	150.0000
G103	2-7	20.0000	15.0000	50.0000	15.0000	500.0000	150.0000	30.0000	3.0000	70.0000
V004	0-3	10.0000	15.0000	15.0000	10.0000	500.0000	70.0000	20.0000	2.0000	100.0000
V005	0-3	15.0000	15.0000	20.0000	10.0000	300.0000	70.0000	15.0000	2.0000	100.0000
V010	0-3	10.0000	10.0000	70.0000	7.0000	300.0000	70.0000	20.0000	2.0000	70.0000
V019	0-3	15.0000	15.0000	30.0000	15.0000	300.0000	70.0000	20.0000	3.0000	100.0000
V020	0-3	15.0000	15.0000	30.0000	15.0000	500.0000	100.0000	30.0000	3.0000	70.0000
V022	0-3	20.0000	15.0000	30.0000	10.0000	300.0000	70.0000	20.0000	3.0000	150.0000
V022	0-3	15.0000	20.0000	30.0000	15.0000	500.0000	100.0000	30.0000	3.0000	70.0000
V023	0-3	15.0000	15.0000	30.0000	15.0000	500.0000	70.0000	20.0000	3.0000	70.0000
V023	0-3	15.0000	15.0000	30.0000	15.0000	500.0000	150.0000	20.0000	3.0000	70.0000
V025	0-3	20.0000	15.0000	50.0000	15.0000	500.0000	200.0000	30.0000	3.0000	100.0000
P010	107-109	70.0000	20.0000	30.0000	15.0000	500.0000	150.0000	20.0000	3.0000	70.0000
P013	25-27	100.0000	20.0000	30.0000	15.0000	300.0000	100.0000	20.0000	3.0000	50.0000

Table 8 cruise s4-76 (semiquant. emission spectroscopy only)

(including 18 analytical duplicates) are given in Table 9. Skewness and kurtosis statistics, histograms of raw and log-transformed data, chi-square tests, analysis of variance, and correlation analysis indicate that the frequency distributions for most of the 31 elements listed in Table 9 are more closely approximated by a lognormal than a normal distribution. Consequently, all statistical analyses are based on log-transformed data.

Estimates of the central and expected ranges of concentrations of a particular element in outer continental shelf sediments from the southern Bering Sea can be obtained using the geometric means (GM) and geometric deviations (GD) given in Table 9. The central range of a lognormal distribution is the range in which approximately 68% of the population is estimated to occur and is within the range of GM/GD to GMxGD. The expected range of a lognormal population is the range in which approximately 95% of the population is estimated to occur, and is defined as the ratio of GM/GD^2 to $GMxGD^2$.

A three-level, nested analysis of variance was performed on the 31 elements in 103 samples from St. George basin in order to compare the variances caused by analytical imprecision, within station variability, and regional (between-station) variability The statistical model used was: $X_{ijk} = \mu + \alpha_i + \beta_{ij} + \varepsilon_{ijk}$

where X_{ijk} is the k^{th} analytical determination of the j^{th} sample from the i^{th} station, μ is the grand mean for the entire population, α_i is the difference between the grand mean and the mean for the i^{th} station, β_{ij} is the difference between the mean for the i^{th} station and the mean analysis of the j^{th} sample, and ε_{ijk} is the error in the k^{th} determination on the j^{th} sample from the i^{th} station. There are 51 stations ($1 \leq i \leq 51$), and a maximum of three samples per station ($1 \leq j \leq 3$), and a maximum of two replicate analyses per sample ($1 \leq k \leq 2$).

The computation of variance components at each of the three levels within the sampling design follows the techniques described by Anderson and Bancroft (1952). Results of the analysis of variance are presented in Table 10. The variance components at each level are given as percentages of the total logarithmic variance. Those variance components that are significantly different from zero at the 0.05 level of probability are marked with an asterisk (*) in Table 10.

Table 10 shows that most of the geographic variability in surface sediments from St. George basin occurs among sampling stations, with only a few elements exhibiting significant variability within stations. That is, chemical analyses of cores from the same station tend to show similar results, whereas analyses from different stations vary significantly. This indicates a component of compositional variability on a scale of greater than 50 km.

TABLE 9

Summary statistics for concentrations of major, minor, and trace elements in 103 samples or surface sediments from the St. George Basin, Outer Continental Shelf, Southern Bering Sea. N* refers to the total number of samples, out of 103, which contained measured element concentrations greater than the detection limit for that element. For subsequent statistical analyses, values less than the detection limit for a particular element were replaced by a value of 0.7 times the detection limit (e.g., the detection limit for both B and Rb is 20 ppm; values <20 ppm were replaced by 0.7 x 20 = 14 ppm). Analytical methods used are: (1) 6-step semiquantitative optical emission spectroscopy; (2) X-ray fluorescence; (3) Atomic Absorption Spectrophotometry; (4) Neutron Activation Analysis.

1/ values for Mg, Na, and S have been corrected for interstitial sea water containing dissolved Mg^{++}, Na^{+}, and $SO_4^{=}$.

Element	Method	Observed Range	Arithmetic Mean	Standard Deviation	Coefficient of Variation (%)	(GM) Geometric Mean	(GD) Geometric Deviation	N*
Al (%)	2	3.9 - 7.9	5.6	0.79	14	5.5	1.15	103
Ca (%)	2	1.7 - 5.1	2.7	0.76	28	2.6	1.29	103
Mg (%) 1/	3	0.66- 2.1	1.1	0.26	24	1.0	1.24	103
Fe (%)	2	1.7 - 5.6	3.2	0.96	30	3.0	1.34	103
K (%)	2	0.84- 1.9	1.2	0.15	13	1.2	1.12	103
Si (%)	2	22 - 34	29	2.8	10	29	1.10	103
Na (%) 1/	3	1.5 - 2.6	2.1	0.26	12	2.0	1.14	103
Ti (%)	2	0.26- 0.70	0.42	0.084	20	0.41	1.21	103
B (ppm)	1	<20 - 70	37	13	34	35	1.43	102
Ba (ppm)	1	300 - 1,500	580	141	24	570	1.24	103
Co (ppm)	1	7.0 - 30	12	3.8	33	11	1.37	103
Cr (ppm)	1	15 - 200	55	29	52	50	1.57	103
Cu (ppm)	1	7.0 - 100	36	21	58	30	1.92	103
Ga (ppm)	1	10 - 30	18	3.8	22	17	1.22	103
Ge (ppm)	2							
Hg (ppm)	3	0.02- 0.11	0.044	0.016	36	0.041	1.38	103
Li (ppm)	3	13 - 48	20	5.9	30	19	1.25	103
Mn (ppm)	1	300 - 700	520	124	24	500	1.30	103
Ni (ppm)	1	10 - 150	22	16	73	20	1.51	103
Rb (ppm)	3	<20 - 90	38	11	29	35	1.40	98
Sc (ppm)	1	7.0 - 30	15	3.9	26	15	1.29	103
Sn (ppm)	2							
Sr (ppm)	1	200 - 700	370	120	33	350	1.39	103
V (ppm)	1	70 - 300	140	46	33	130	1.42	103
Y (ppm)	1	15 - 50	25	6.8	28	24	1.32	103
Yb (ppm)	1	1.5 - 5.0	2.8	0.69	24	2.8	1.28	103
Zn (ppm)	3	45 - 140	83	22	30	80	1.30	103
Zr (ppm)	1	70 - 200	94	27	29	91	1.29	103
U (ppm)	4	1.2 - 3.9	2.2	0.54	25	2.1	1.27	103
Th (ppm)	4	<2 - 7.7	3.5	1.6	46	3.2	1.59	58
S (%) 1/	2	0.007 - 0.55	0.14	0.08	57	0.12	1.80	103

TABLE 10

Analysis of variance of surface sample chemistry, St. George Basin, outer continental shelf, southern Bering Sea. Asterick (*) indicates that a variance component is significantly different from zero at the 0.05 probability level; v is the observed variance ratio. See text for explanation.

Element	Total Logarithmic Variance	variance components as percentage of total variance			v
		Between Ship Stations	Between Samples Within Stations	Analytical Error	
Al	0.00393	82*	0	18	4.56
Ca	0.01269	88*	5	7	7.33
Mg	0.00887	97*	2*	1	32
Fe	0.01641	90*	6*	4	9.00
K	0.00292	88*	0	12	7.33
Si	0.00192	79*	0	21	3.76
Na	0.00470	93*	5*	2	13
Ti	0.00719	87*	0	13	6.69
B	0.02336	30*	11	59	0.43
Ba	0.00906	32*	29	39	0.47
Co	0.02041	71*	0	29	2.45
Cr	0.03900	54*	18	28	1.17
Cu	0.08124	90*	6*	4	9.0
Ga	0.00763	41*	46*	13	0.69
Ge					
Hg	0.01758	50*	7	43	1.00
Li	0.00919	96*	1	3	24
Mn	0.01448	58*	0	42	1.38
Ni	0.03239	59*	14	27	1.44
Rb	0.02168	49*	28*	23	0.96
Sc	0.01352	62*	0	38	1.63
Sn					
Sr	0.02053	46*	37*	17	0.85
V	0.02323	74*	4	22	2.85
Y	0.01427	52*	22	26	1.08
Yb	0.01633	42*	0	58	0.72
Zn	0.01633	82*	0	18	4.56
Zr	0.01254	16	9	75	0.19
U	0.01102	61*	33*	6	1.56
Th	0.04087	19	44*	37	0.23
S	0.03932	76*	0	24	3.17

The significant variation among stations for most elements suggests that regional baselines for these elements must be described by maps based on station means rather than by grand means for the entire region. According to Connor et al. (1972; see also Miesch, 1976), data are adequate for constructing maps when the variance among categories (stations in this study) exceeds the error variance for the category means. Because only one sample was taken at most stations and only one analysis was made for most samples, the error variance for station means is simply the sum of the variances due to analysis and the variance within stations (Table 10). The ratios of the variances among stations to the error variance are given as the variance ratio, v, in Table 10.

The variance ratio, v, is a relative measure of the adequacy of the sampling design for construction of maps. Where the ratio is large, no additional sampling is required to describe compositional differences among stations. Where the ratio is small, more sampling and (or) analytical work is required. Maps of element concentration for selected elements with values of $v>1.0$, the minimum suggested by Connor et al. (1972), are shown in Figs. 16 through 25.

Elements that exhibit a concentration gradient decreasing from southeast to northwest, similar to the gradients observed in the volcanic components of the light and heavy mineral fractions, include Al, Ca, Mg, Fe, Na, Ti, Co, Cu, Mn, V, and Zn. Maps of concentration of Si and K exhibit an increasing concentration gradient in the same southeast to northwest direction. Maps for U, S, and Li exhibit a bull's-eye pattern centered over St. George basin, similar to the pattern exhibited by maps of total-C and grain size. Local concentrations of basaltic material contributed to the shelf from the Pribilof Islands, suggested by the distributions of heavy minerals, is further supported by relatively high concentrations of Mg, Ti, Co, Cu, Cr, Ni, and V in sediments in the vicinity of the Pribilof Islands.

A Q-mode factor analysis was used to determine regional groupings of similar sediment based on all measured composition variables, and to examine inter-relationships among variables. The data set used consisted of 50 compositional variables that include grain size, clay minerals, heavy and light minerals, and inorganic geochemistry of sediments from 30 stations. The computer program used for the Q-mode analysis was adapted from the CABFAC program of Klovan and Imbrie (1971). A program option was used to scale all variables to range from zero to one so that those variables with larger means and variances would not determine the outcome. After scaling, the program normalizes the data so that the sum-of-squares of each row is unity. Rotated principal component (variance) also was used.

We found that 90% of the variance in the scaled and row-normalized data could be accounted for by only three factors. Varimax loadings for the 30 samples on each of the three factors

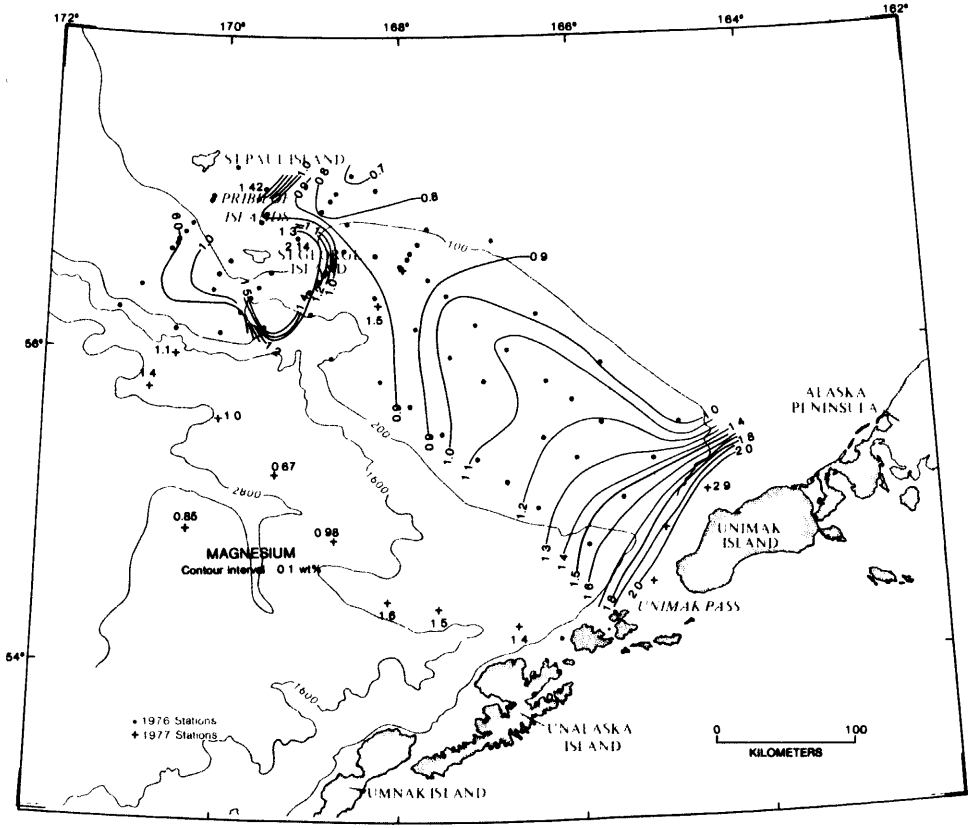

Figure 16. Distribution of magnesium (sea-water corrected) in surface sediment.

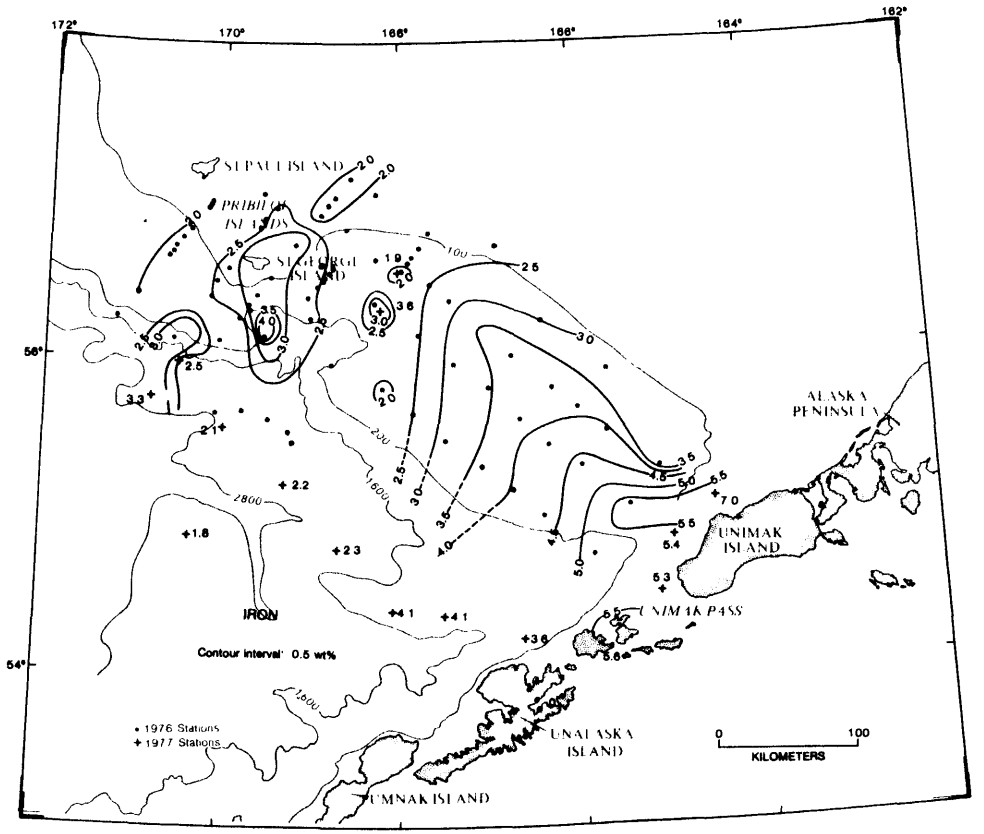

Figure 17. Distribution of iron in surface sediment.

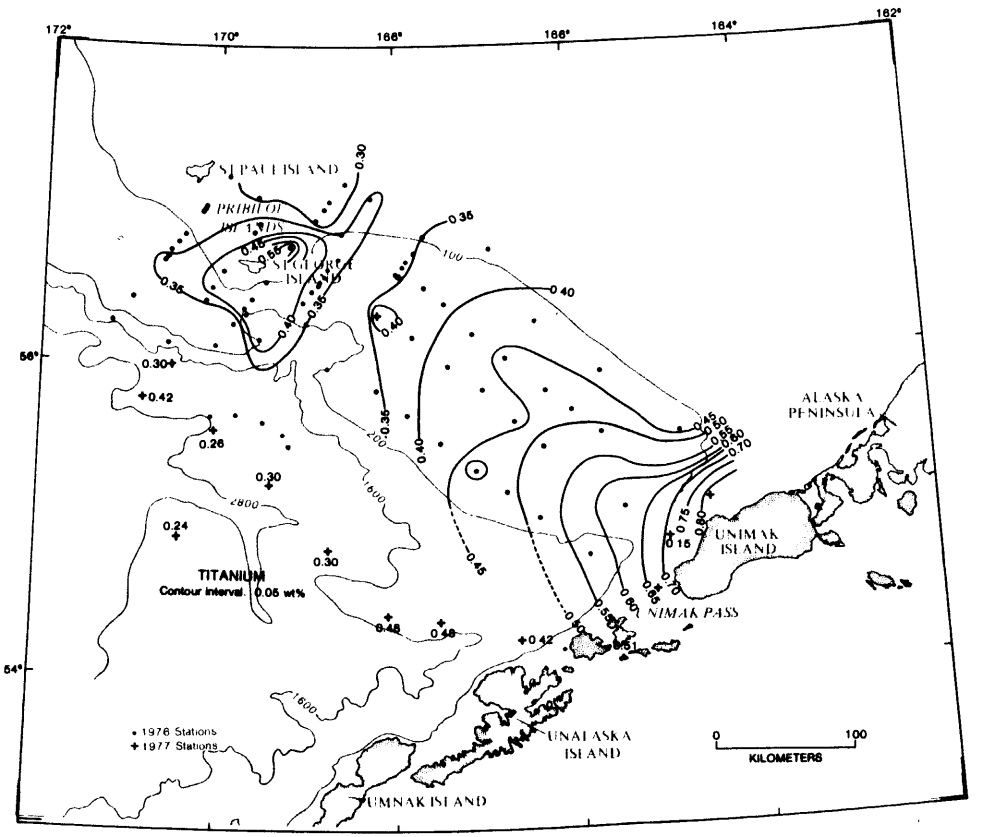

Figure 18. Distribution of titanium in surface sediment.

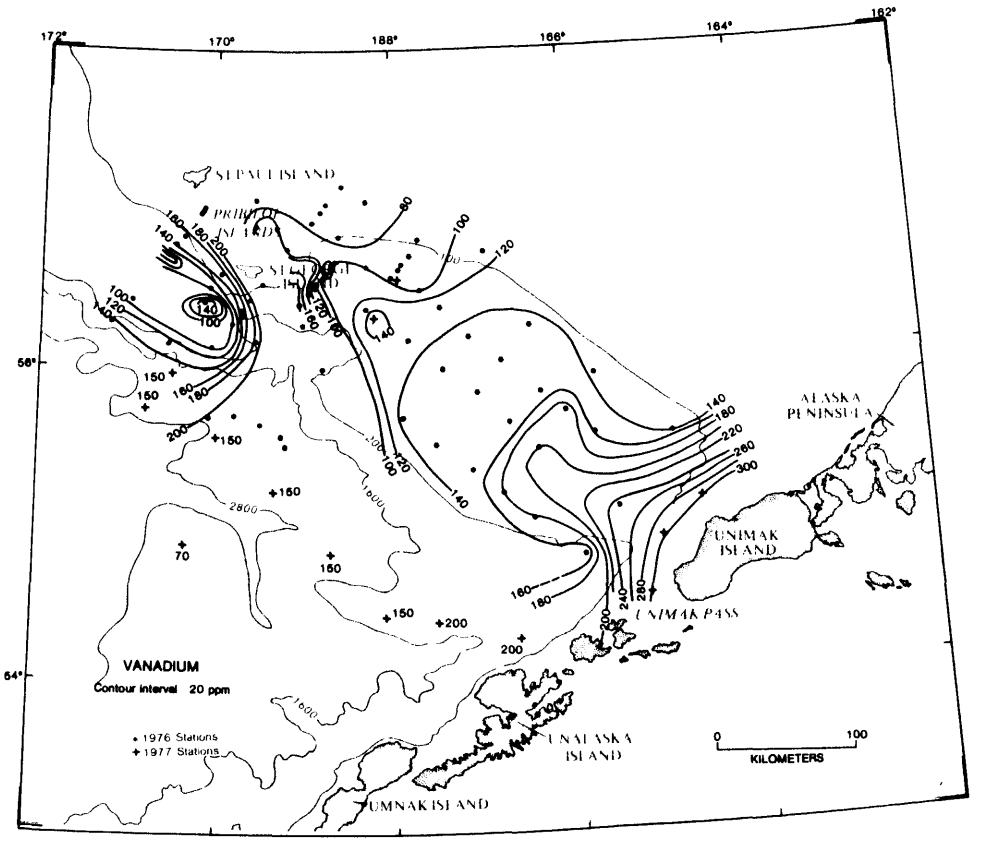

Figure 19. Distribution of vanadium in surface sediment.

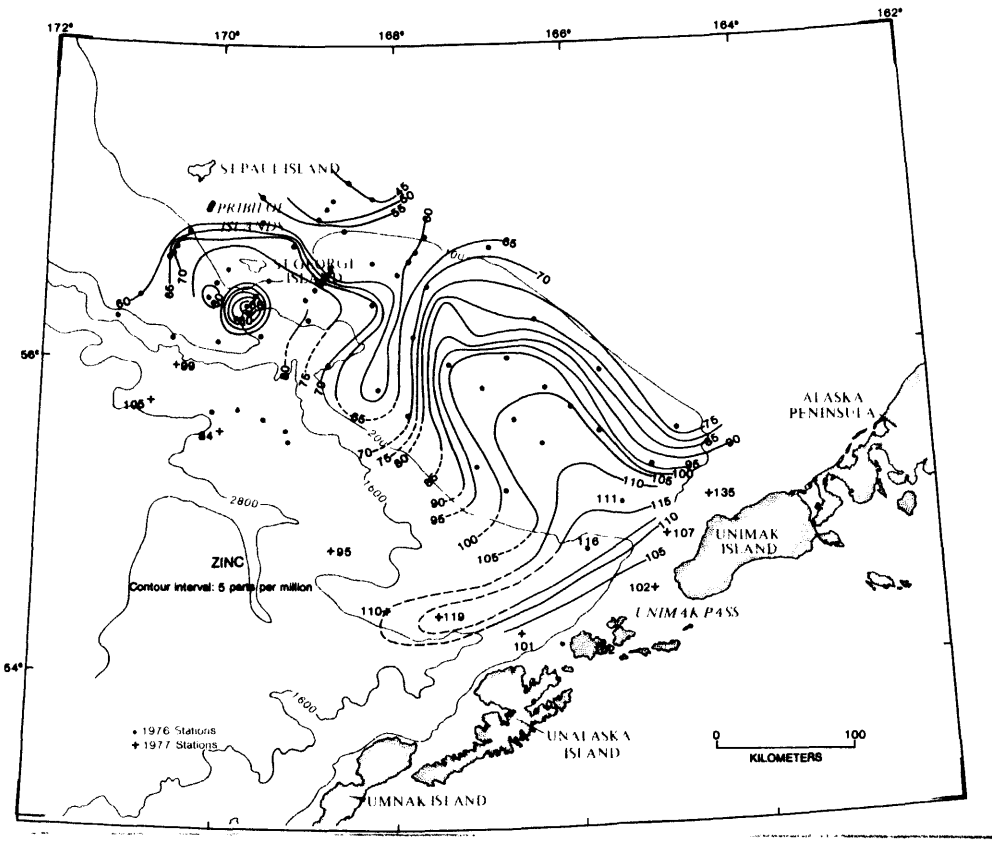

Figure 20. Distribution of zinc in surface sediment.

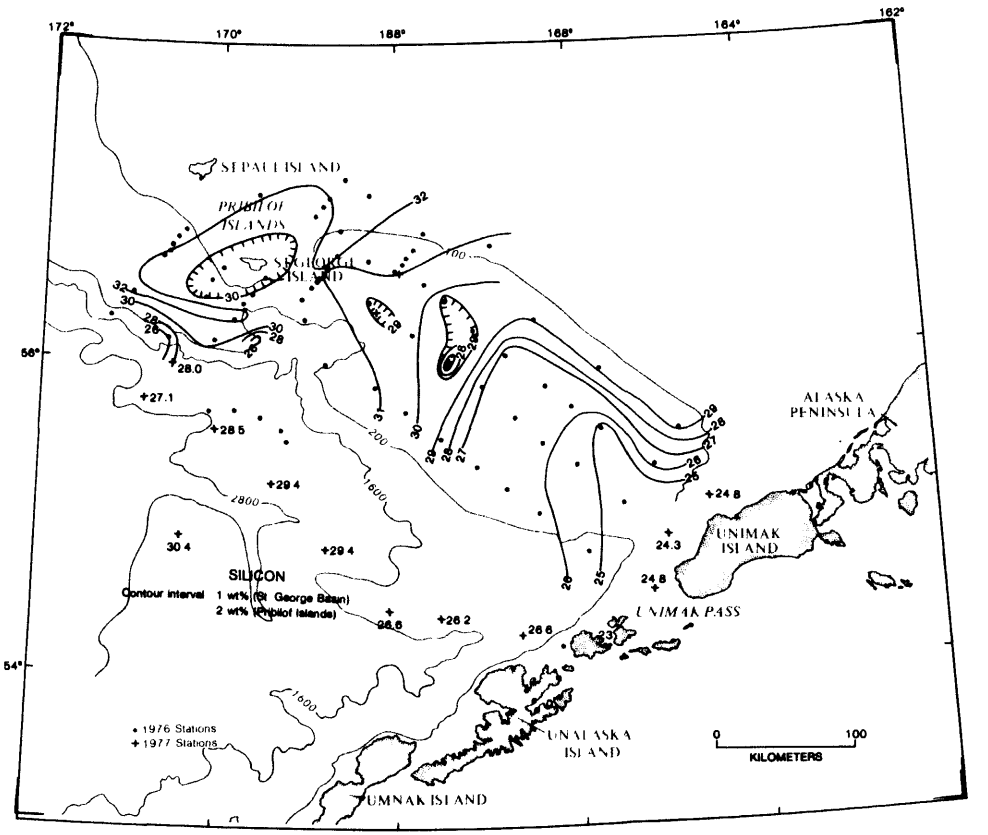

Figure 21. Distribution of silicon in surface sediment.

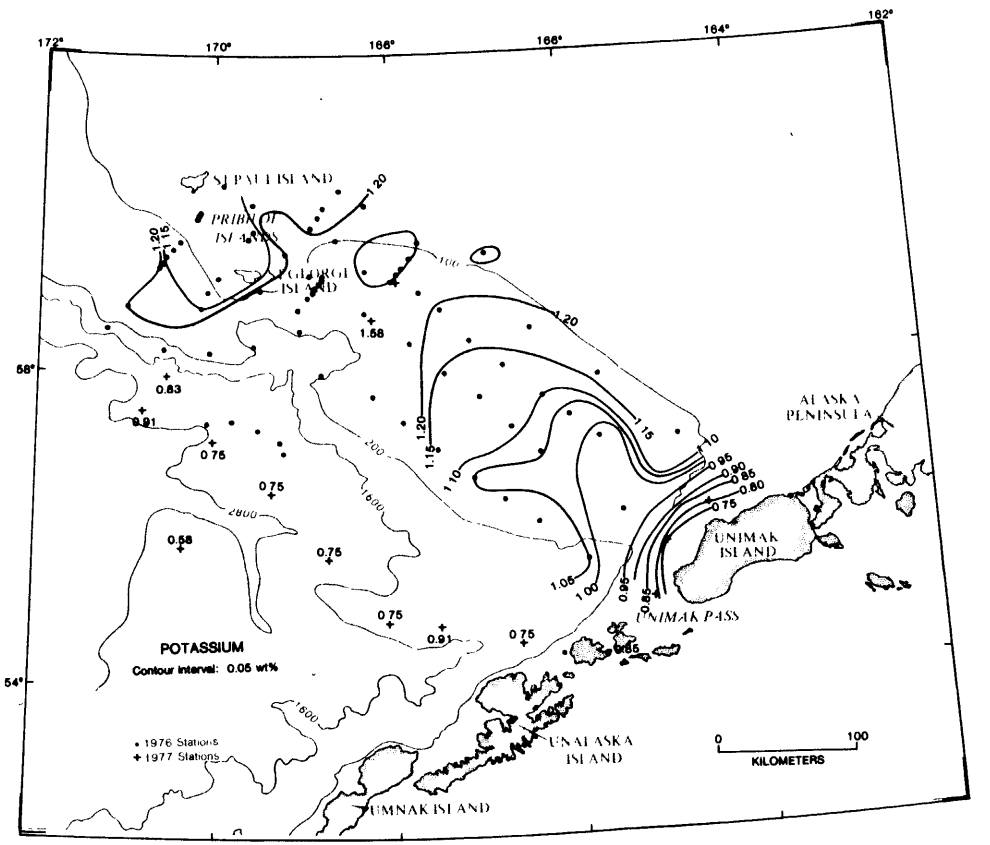

Figure 22. Distribution of potassium in surface sediment.

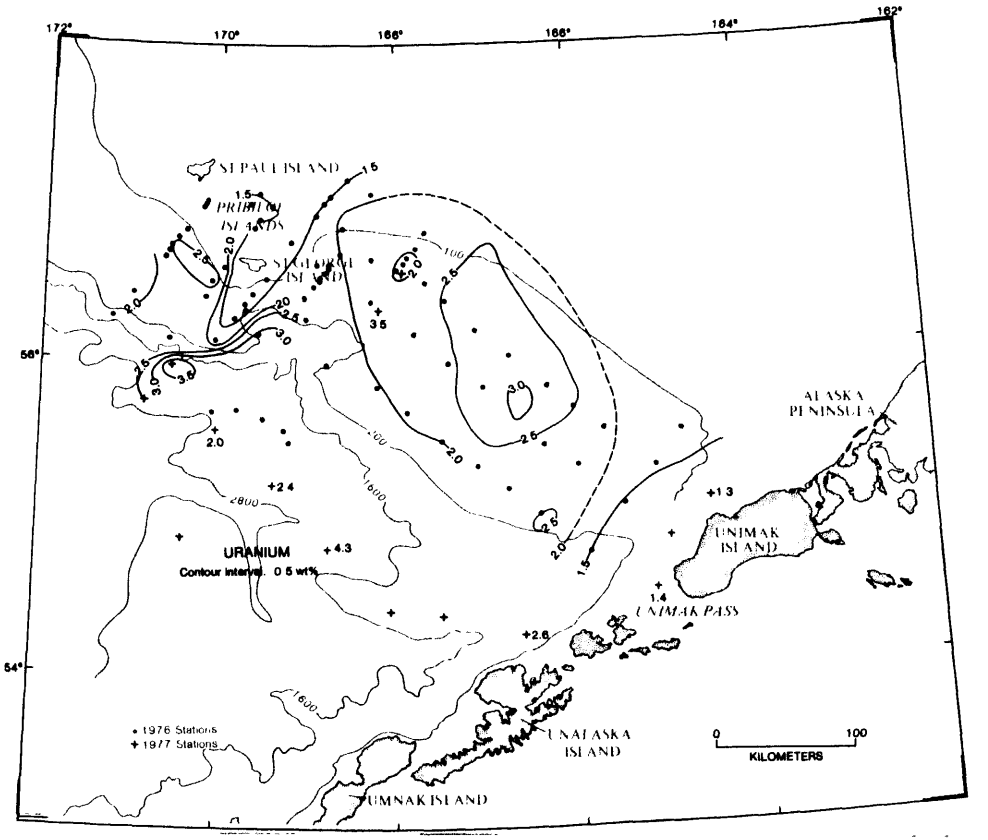

Figure 23. Distribution of uranium in surface sediment.

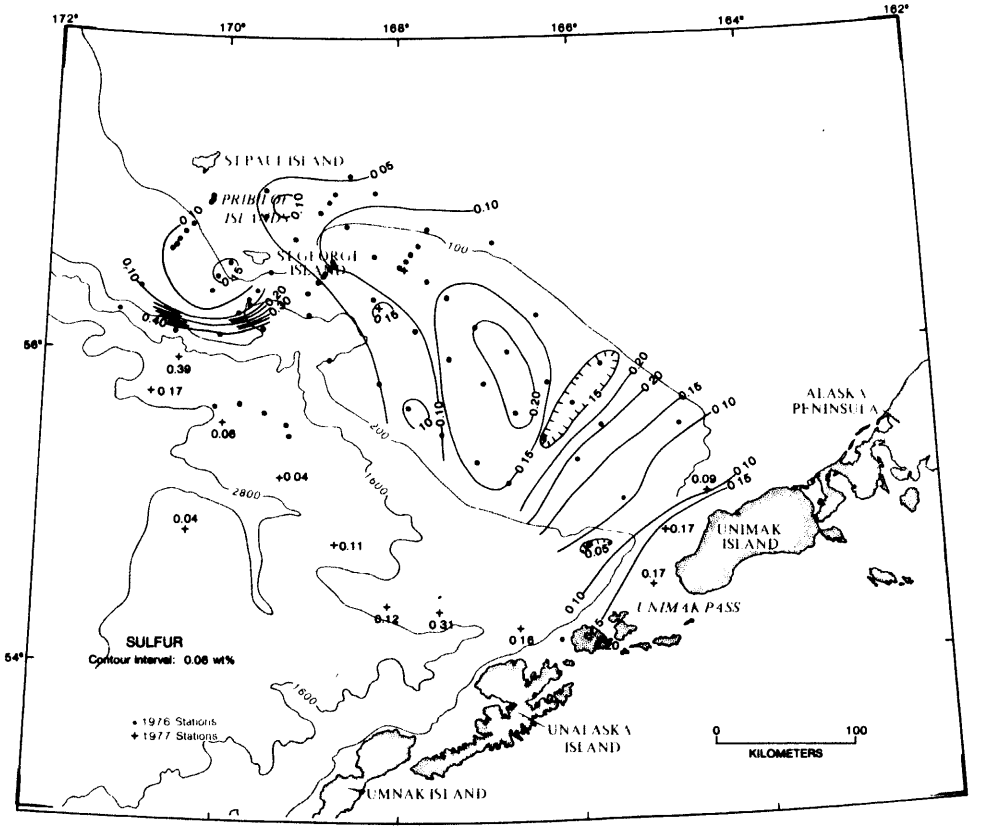

Figure 24. Distribution of sulfur (sea-water corrected) in surface sediment.

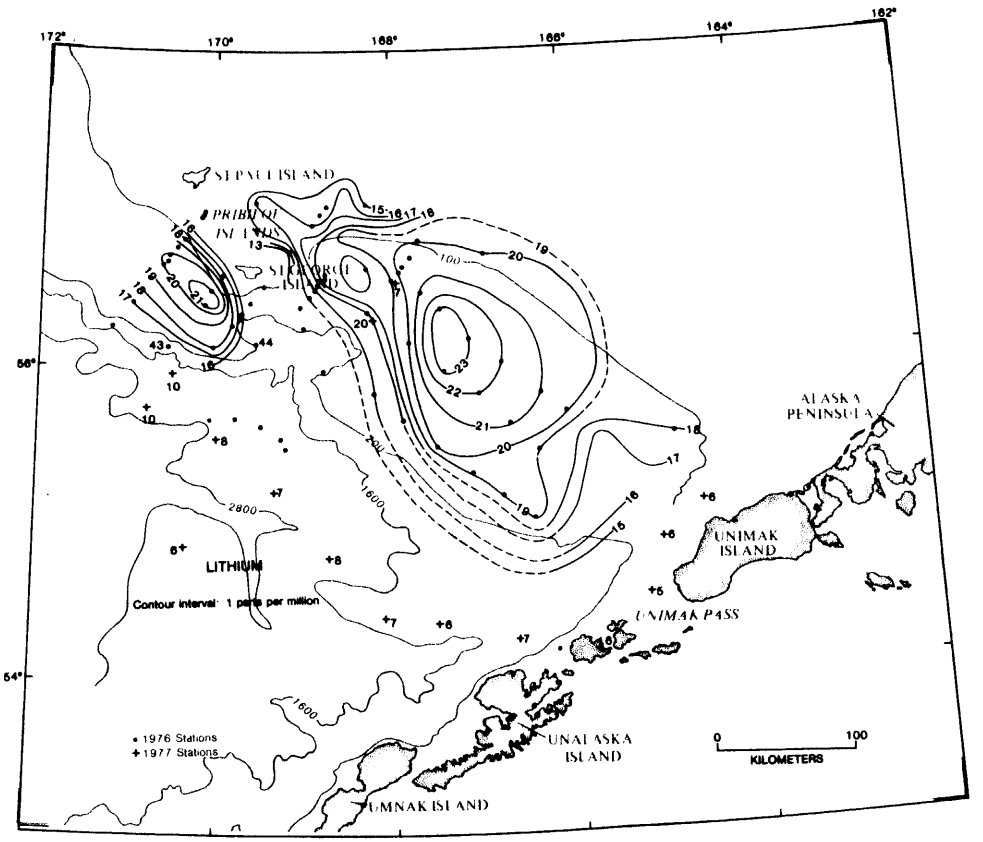

Figure 25. Distribution of lithium in surface sediment.

are listed in Table 11 and plotted in Figs. 26 through 28. These loadings can be thought of as composite compositional variables. In other words, the 50 compositional variables used as input to the Q-mode model have been reduced to 3 composite variables, each expressing some compositional attribute of the sediments based on a synthesis of a number of measured compositional variables. However, the loadings provide no indications as to which compositional variables were synthesized into which factor (composite variable). The factor loadings were treated as composite compositional variables in order to determine the relative contributions of each variable to the Q-mode model, and correlation coefficients between the loadings and the 50 observed variables were computed. Results are given in Table 12.

Table 12 indicates that loadings on factor 1 correlate positively with Na, Ca, Ti, glass, volcanic rock fragments, Sr, V, Mn, Cu, Fe, Al, smectite and vermiculite, Co, Y, Zn, Ga, clinopyroxene, and illite and kaolinite (i.e. factor 1 samples tend to be enriched in these components). Factor 1 loadings correlate negatively with Si, quartz, epidote, non-volcanic rock fragments, illite, k-feldspar, Rb, Ba, k. garnet, and ortho-pyroxene (i.e. factor 1 samples tend to be depleted in these components). Therefore, the compositional variables indicative of mafic volcanic material have all been synthesized into "factor 1".

Figure 26 shows that sediments with highest loadings for factor 1 occur closest to the Aleutian Islands. The distribution of sediments with high loadings for factor 1 is thus a measure of the distribution of sediments containing a relatively high input of volcanic material from the Aleutian Islands. The best "indicator" variables for Aleutian andesite are Na, Ca, Ti, glass, volcanic rock fragments, Sr, V, and Mn in roughly that order of importance.

Samples with highest loadings for factor 2 tend to have relatively high concentrations of Si, quartz, garnet, sand, epidote, orthopyroxene, metamorphic rock fragments, k-feldspar, and Ba. A map of sample loadings on factor 2 sediments (Fig. 27) indicates that these sediments occur as a "background" over most of the outer shelf, except near the Aleutian Islands where they are diluted by andesitic material. Sediment samples with high loadings on factor 2 tend to be coarser-grained, more felsic, mainland-derived materials that blanket most of Bristol Bay shelf (Sharma et al., 1972). The best indicator variables for the mainland component are Si, quartz, garnet, sand, epidote, orthopyroxene, and metamorphic rock fragments in roughly that order of importance.

The distribution of sediment samples with high loadings on factor 3 (Fig. 28) reflects the distribution of finer-grained, higher-organic sediments concentrated in a bull's-eye pattern in the St. Geroge Basin, and at the head of Pribilof Canyon south of

Table 11. Varimax factor loadings for three factors used in the Q-mode factor analysis of 50 variables in 30 samples of sediment from the outer continental shelf, southern Bering Sea.

CORE	COMM.	FACTOR 1	FACTOR 2	FACTOR 3
G11	0.9080	0.7587	0.4796	0.3201
G13	0.9008	0.5294	0.5074	0.6026
G16	0.9392	0.4767	0.5685	0.6236
G20	0.9240	0.3783	0.7593	0.4521
V03	0.8658	0.0877	0.9068	0.1894
V06	0.9359	0.0979	0.9325	0.2362
G41	0.8962	0.3859	0.6815	0.5317
G43	0.9065	0.3532	0.5077	0.7238
G46	0.8967	0.3406	0.4349	0.7691
G51	0.9267	0.6536	0.3418	0.6186
G52	0.8598	0.5680	0.3120	0.6632
G08	0.9467	0.8505	0.3004	0.3650
G05	0.9506	0.9386	0.1507	0.2166
G54	0.8910	0.7716	0.2190	0.4976
G59	0.9276	0.5470	0.3312	0.7202
G62	0.9134	0.5844	0.3052	0.6919
G63	0.9005	0.4297	0.4048	0.7430
G65	0.9308	0.3972	0.7326	0.4861
G67	0.8358	0.4346	0.7347	0.3273
V18	0.8028	0.4316	0.7473	0.2410
V12	0.8488	0.0976	0.8758	0.2687
G10	0.9443	0.3510	0.8605	0.2839
G11	0.8869	0.4319	0.7022	0.4552
G11	0.9474	0.6019	0.5320	0.5496
G10	0.7719	0.2832	0.3057	0.7735
P07	0.8830	0.3248	0.5012	0.7255
G77	0.9160	0.2168	0.7168	0.5960
G75	0.8905	0.1695	0.8172	0.4403
G71	0.8705	0.3085	0.3183	0.8210
G12	0.9116	0.8900	0.0309	0.3442
	% Cumulative Variance	25.904	60.168	89.765

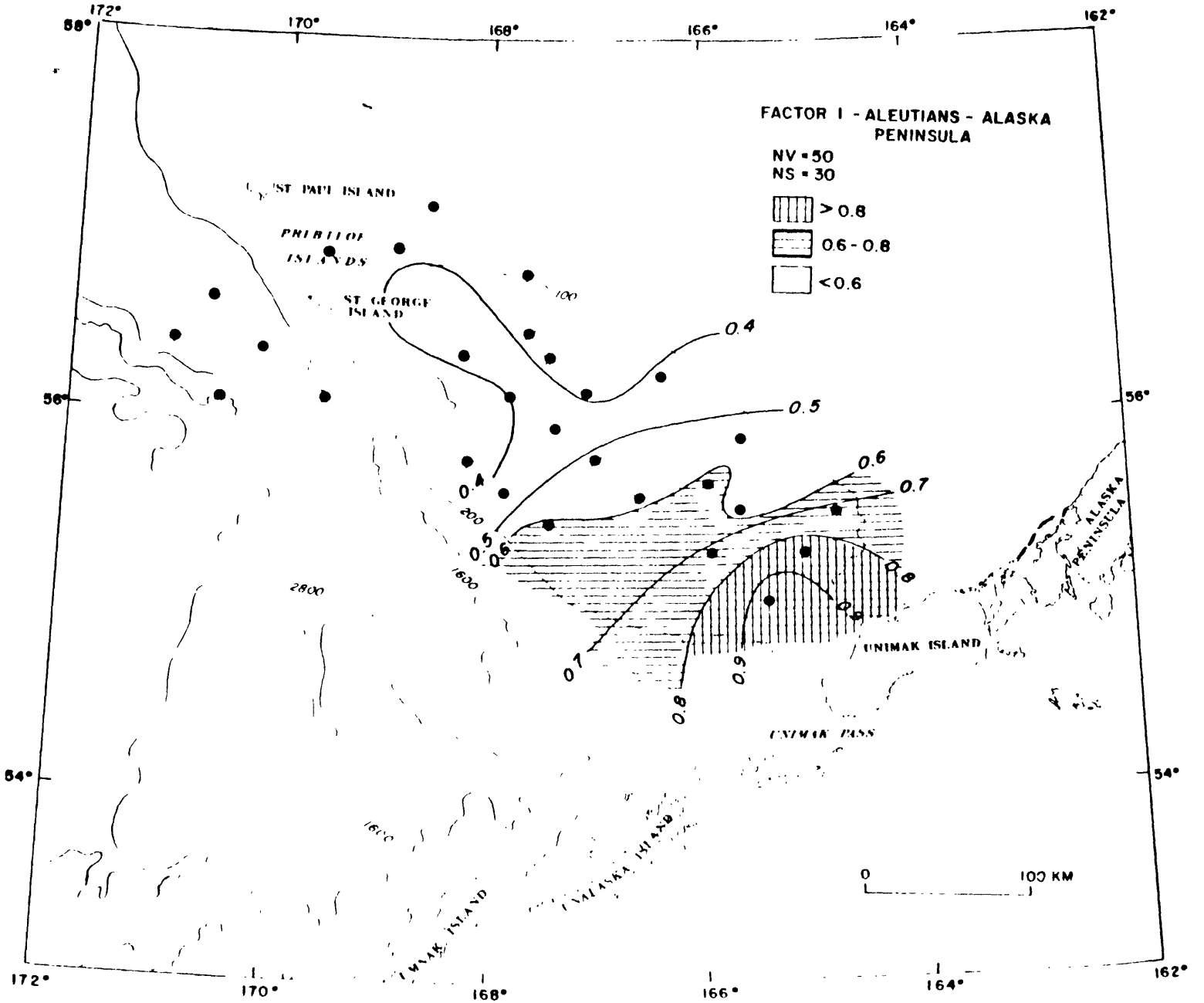

Figure 26. Map of the distribution of factor loadings for Factor I, the Aleutian-Alaska Peninsula factor.

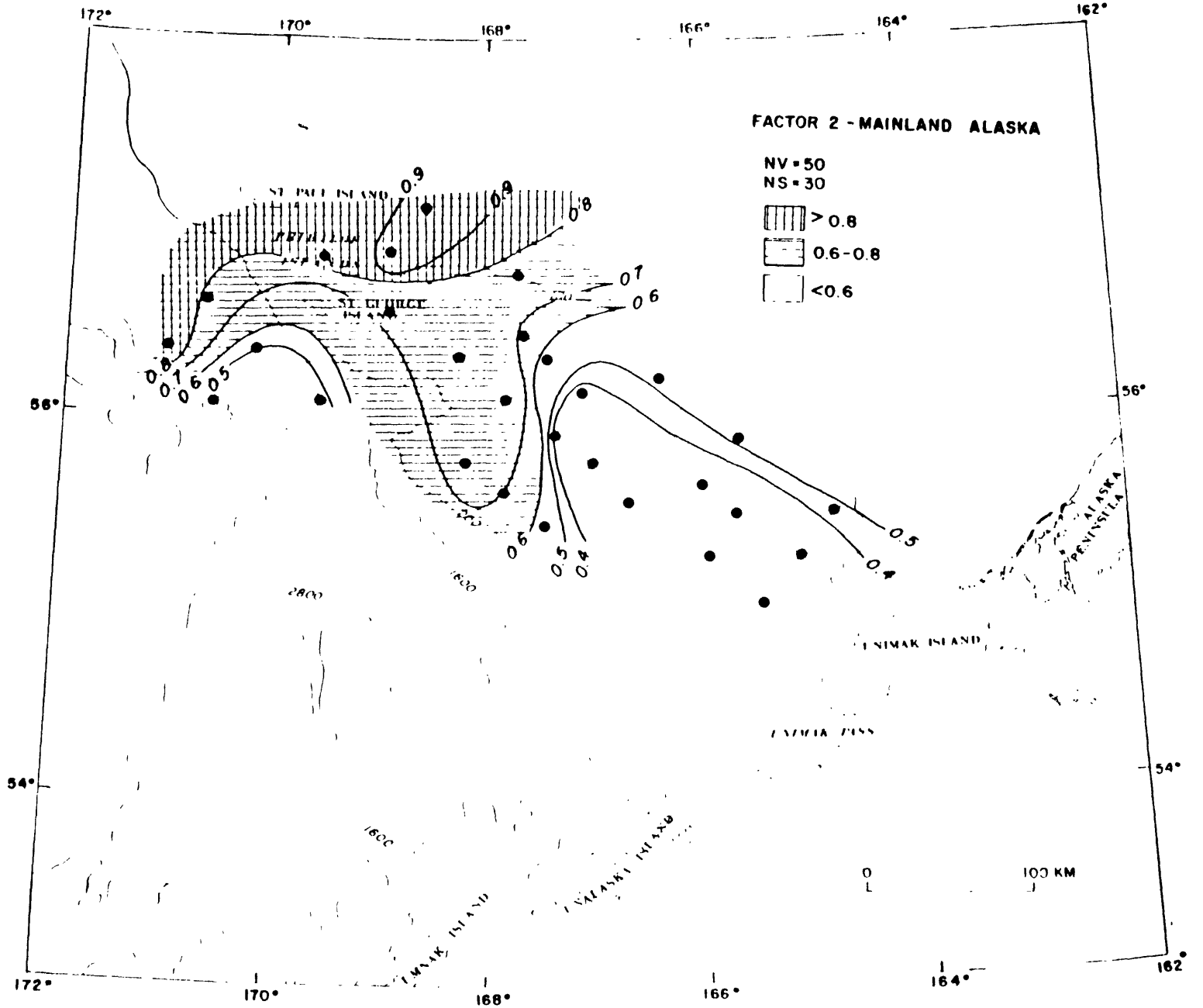

Figure 27. Map of the distribution of factor loadings for Factor II, the Alaska mainland factor.

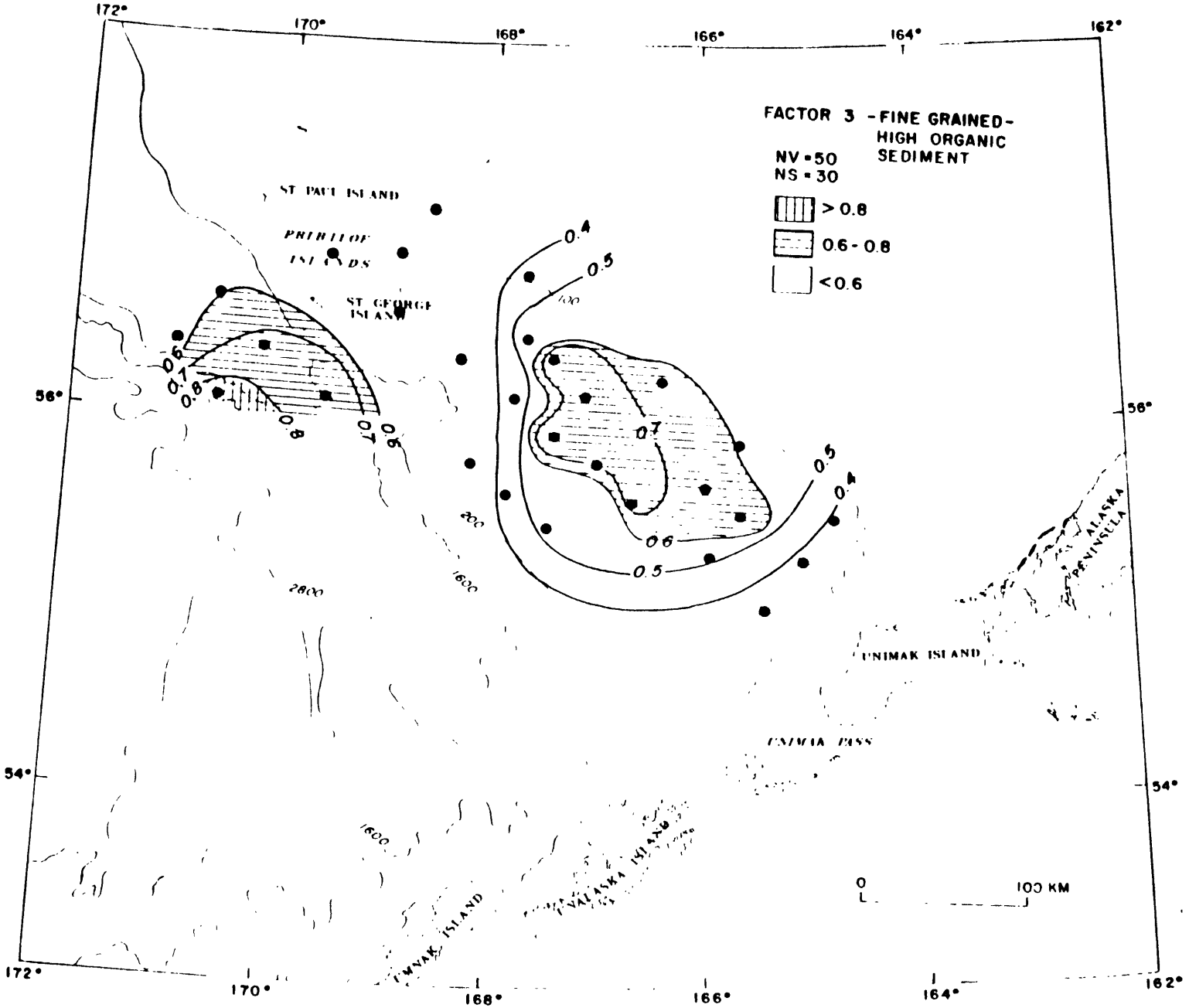

Figure 28. Map of the distribution of factor loadings for Factor III, the fine-grained high organic sediments factor.

Table 12: Correlation coefficients among factor loadings for each of the three factors used in the Q-mode factor analysis and the 50 observed compositional and size variables. Correlation coefficients significant at the 99% confidence level ($r > |0.41|$) are indicated by an asterick (*); correlation coefficients $> |0.60|$ are indicated by a double asterick (**).

VARIABLES	LOADINGS		
	factor 1	factor 2	factor 3
smec+ver	0.7007**	-0.4660*	-0.1331
illite	-0.6214**	0.4047*	0.0123
chlorite	-0.4535*	0.2027	0.2483
clinopx	0.5492*	-0.2751	-0.5591*
orthopx	-0.4779*	0.6088**	-0.2799
vol rx f	0.6894**	-0.8223**	0.2183
amphibol	-0.4557*	0.4326*	0.2786
opaques	0.0061	0.3379	-0.5101*
chlorits	-0.4332*	0.0392	0.6708**
epidote	-0.6736**	0.6454**	-0.1915
garnet	-0.4902*	0.7471**	-0.4466*
met rx f	-0.5803*	0.5813*	0.0502
plutonic	-0.3946	0.2686	0.2886
fine gr	-0.6321**	0.4728*	0.0957
ill klin	0.5297*	-0.2419	-0.0072
mean gz	0.1890	-0.7059**	0.8642**
% sand	-0.2569	0.7249**	-0.8970**
% silt	0.3396	-0.7147**	0.8319**
% clay	-0.1139	-0.4238*	0.6854**
Si (%)	-0.7361**	0.9612**	-0.3606
Al (%)	0.7604**	-0.8411**	0.2298
Ca (%)	0.8870**	-0.7124**	-0.1856
Fe (%)	0.7691**	-0.9097**	0.1764
K (%)	-0.4992*	0.2073	0.3131
Ti (%)	0.8559**	-0.8744**	0.1581
B	-0.2959	-0.0078	0.5395*
Ba (ppm)	-0.5918*	0.4403*	0.1044
Co (ppm)	0.6414**	-0.7061**	-0.0122
Cr (ppm)	-0.5604*	0.3894	-0.1697
Cu (ppm)	0.7720**	-0.9448**	0.3035
Ga (ppm)	0.5645*	-0.7997**	0.5064*
Hg (ppm)	0.2292	-0.5753**	0.4471*
Li (ppm)	-0.1790	-0.3222	0.6532**
Mn (ppm)	0.8021**	-0.6240**	0.0521
Ni (ppm)	-0.3997	0.1359	0.1963
Rb (ppm)	-0.6067**	0.2520	0.3170
Sr (ppm)	0.8248**	-0.6717**	-0.0016
V (ppm)	0.8171**	-0.8584**	0.1649
Y (ppm)	0.6112**	-0.7218**	0.3289
Yb (ppm)	0.6987**	-0.6502**	0.1952
Zn (ppm)	0.5748*	-0.9095**	0.5649*
U (ppm)	-0.0571	-0.3118	0.8416**
T-C (%)	0.1606	-0.6109**	0.8256**
Na (%)	0.9008**	-0.7325**	0.0850
T-S (%)	0.1006	-0.6207	0.6796**
% quartz	-0.8025**	0.8392**	-0.0960
% K-spar	-0.6196**	0.4688*	0.1237
% glass	0.8384**	-0.6712**	-0.1790
% vol rx	0.8382**	-0.6673**	-0.2911
% nonvol	-0.6559**	0.4082	0.3993

the Pribilof Islands. Samples with high loadings on factor 3 tend to be finer grained and relatively rich in C, U, S, Li, and B (Table 12).

Hydrocarbon Gas in Sediments (Keith A. Kvenvolden and George D. Redden)

Studies of hydrocarbon gases in near-surface sediments of the southern Bering shelf and slope were conducted during the 1976 and 1977 field seasons. The general objectives of this work were (1) to determine the distribution of hydrocarbon gases in surface and near-surface sediments, and (2) to interpret possible sources for the gas. During the 1976 season, 33 stations were occupied where hydrocarbon gases were extracted from 108 sediment samples recovered from gravity cores (maximum depth, 1.4 m), or van Veen grabs. The stations were part of a network of 85 stations established to evaluate the general geology of the southern Bering shelf between Unimak Island and the Pribilof Islands including the area of the St. George basin. The gas analysis results from this season are summarized briefly here. Small quantities of methane (C_1), ethane (C_2), propane (C_3), n-butane (n-C_4), isobutane (i-C_4), ethene ($C_{2:1}$) and propene ($C_{3:1}$) were found in all samples. C_1 was the most abundant hydrocarbon, having an average concentration of about 5700 nL/L of wet sediment. The concentrations of C_1 usually increased slightly with depth. The other hydrocarbon gases were present at lower concentrations than methane, and these gases showed no identifiable trends with depth. No anomalous distribution or concentrations of hydrocarbon gases were observed that would suggest possible hydrocarbon seeps or potential hazards.

Between the 1976 and 1977 field seasons, examination of multi-channel, seismic profiles across St. George basin indicated the presence of a number of acoustic anomalies where reflectors abruptly terminate leaving regions of acoustic turbidity beginning at depths of about 200-300 m (Marlow, personal communication). Single-channel seismic records showed these same features, but they were not as well defined. The cause of these anomalies is not known, but it is commonly assumed that they may result from gas occupying a portion of the pore space. Although the features are deep, we reasoned that if hydrocarbon gases are involved, these gases may leak to the surface, giving rise to anomalous concentrations of hydrocarbon gases that would correlate with the acoustic features. Furthermore, the composition of the gases might provide a clue to their sources. Part of the 1977 field season was devoted to testing this idea.

During the 1977 field season two sets of samples were collected for hydrocarbon gas analysis (Fig. 29). The first set consisted of 22 samples from 9 gravity cores. These cores were taken on the southern Bering shelf in a region where acoustic anomalies had been noted on the seismic records. Four of these cores were located over the anomalies, and five were at positions not associated with anomalies. The second set of 22 samples came

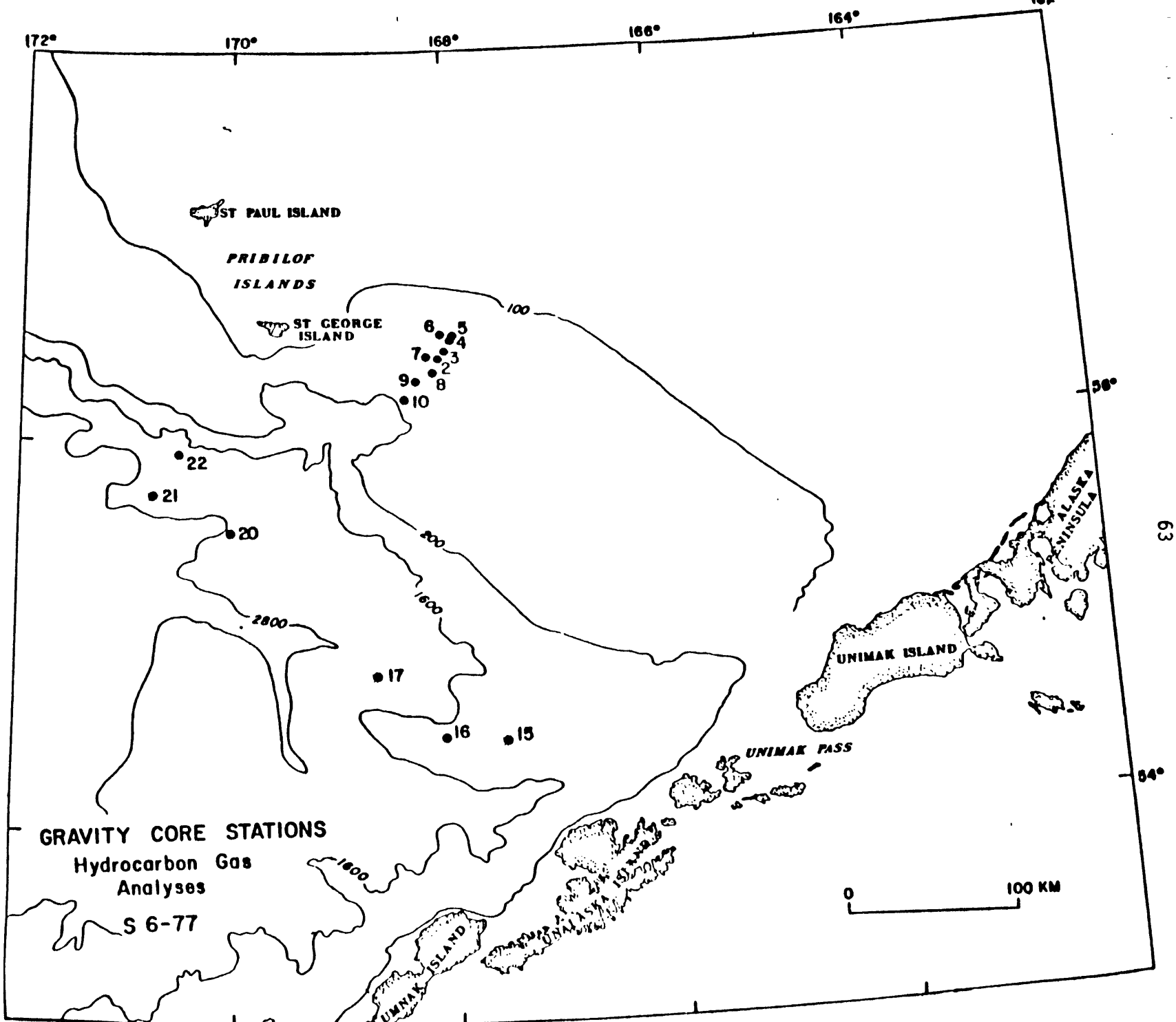

Figure 29. Map showing locations of samples that were collected for

from 6 gravity cores taken on the southern Bering slope. From these two sets of samples, comparisons were made between the occurrence of hydrocarbon gases from these two regions of the continental margin.

The following procedure was used for gas analysis. The 8-cm internal diameter core liner from the gravity core was cut at intervals (usually 0-10, 50-60, 100-110 cm). The sediment core was extruded from each of these intervals into a preweighed, 1 qt. can. The can had been pre-prepared with two small holes near the top and septa had been fixed over the holes. The can was filled with distilled water that had been purged with helium to remove any dissolved hydrocarbon gases. From the can 100 ml of water was removed. A double friction top was sealed in place, and the 100 ml headspace was purged with the helium through the septa. The cans were shaken for 10 minutes. From the can about 5 ml of gas was removed. Exactly one ml of this gas was injected into a modified Carle 311 Analytical Gas Chromatograph equipped with both flame ionization and thermal conductivity detectors. The instrument was calibrated by means of a standard mixture of hydrocarbon gases prepared by Matheson Gas Company. Calculations of concentrations of gases were determined from chromatograms by measuring the heights of peaks representing the gases. Partition coefficients were used to correct for the varying solubilities of the gases. Concentrations are reported as nL/L of wet sediment.

Results obtained during the 1977 field season are recorded in Table 13 (shelf) and Table 14 (slope). On the shelf, cores G-1, G-4, G-7, and G-10 were obtained in sediments over acoustic anomalies. The remaining cores were taken in areas where no anomalies were evident. There appears to be no correlation between gas concentrations and the presence of acoustic anomalies; that is, no hydrocarbon gas anomalies are associated with acoustic anomalies. If the acoustic anomalies are indeed caused by high concentrations of hydrocarbon gases, our data suggest that these gases do not leak to the surface to produce unusual concentrations of gases. The thick (200-300 m) of sediment cover may obscure or prevent gas migration.

Concentrations and compositions of the gases from the shelf and slope are generally similar. Average concentrations of C_1 differ slightly only because deeper samples with higher C_1 concents were recovered on the slope and are included in the average. For example, on the shelf, the average concentration of C_1 is about 2800 nL/L while on the slope the samples have an average C_1 concentration of about 3400 nL/L. The concentrations of the higher molecular weight hydrocarbons are similar for sediments from both shelf and slope.

Shelf sediments have an average $c_1(C_2 + C_3)$ ratio of 34 in contrast to the slope sediments with an average ratio of 107. Samples from the slope, however, include deeper intervals with higher C_1 contents and thus higher $C_1(C_2+ C_3)$ ratios. This ratio has been used in the past to interpret sources of hydrocarbon

gases (Bernard, Brooks, and Sackett, 1977, Earth and Planetary Science Letters, 31, 48-54). Ratios less than 50 were interpreted to indicate the presence of thermogenically-derived gases. Ratios greater than 50 suggested mainly biogenically-produced gases. Although this ratio may be a useful guide when high concentrations of gases are being considered, in the present study involving relatively low concentrations of gases, this ratio probably is not indicative of sources of hydrocarbon gases. It is quite likely that most of the hydrocarbon gases measured here are biologically-derived. The fact remains however, that in the first 60 cm of the cores, the C_1 (C_2 + C_3) ratios for southern Bering shelf and slope sediments are generally low as indicated on Table 13 and 14, and as also observed for the samples examined from the 1976 field season.

Two cores show usual concentrations of single components. C_2 is higher in samples from core G-12 than in other cores from both the shelf and the slope. In core G-28, the intervals from 100 cm and deeper show unusually high amounts of i-C_4. The significance of these observations is not clear at present.

The data shown in Tables 13 and 14 were obtained from analyses performed on shipboard immediately after core recovery. After gases were analyzed, these samples were frozen. A number of samples were thawed later and reanalyzed. This process tends to increase the amount of hydrocarbon gases that can be extracted. Most of the hydrocarbon gases are probably dissolved in the interstitial water of the sediments, and these are partially removed during the first extraction. Freezing and thawing release additional hydrocarbon gases that are held in the sediment in unknown ways. For these kinds of analyses, it is evident that comparisons of results can be made only with samples which have been processed in the same way. Because analyses of unfrozen samples recovered immediately after coring involves least sample manipulation, results of these analyses have been given here.

This work has shown that hydrocarbon gases are present in surface and near-surface sediments of the southern Bering shelf and slope. Concentrations of hydrocarbons are about the same in shelf and slope sediments in the interval from 0 to about 60 cm. On the shelf, acoustic anomalies at 200-300 m depth do not produce hydrocarbon gas anomalies in the near-surface sediments above them. The concentrations and distributions of hydrocarbon gases in the sediments examined here do not indicate that gas seeps are active in the areas sampled or that the gas in the sediments constitutes a geologic hazard because of high concentrations.

Discussion

The petrology of the surface sediments suggests that small amounts of material from mainland Alaska has been transported to the outer shelf relative to the volcanic material derived from

Table 14. Hydrocarbon Gases - Southern Bering Slope S6-77

Sta	Sample	Interval (cm)	Water Depth (m)	Concentrations (nL/L wet sediment)							$\frac{C_1}{C_2 + C_3}$
				C_1	C_2	$C_{2:1}$	C_3	$C_{3:1}$	i-C_4	n-C_4	
15	G-15	0-10	825	970	26	47	16	14	6	9	23
	"	100-110		925	43	62	30	26	6	9	13
16	G-18	0-10	1195	815	23	32	16	14	-	6	21
	"	50-60		2880	23	24	14	9	-	-	79
	"	100-110		4090	26	29	14	11	-	6	104
17	G-21	0-10	2224	1290	31	32	25	9	6	9	23
	"	50-60		1610	17	18	9	6	-	-	62
	"	100-110		2090	17	15	5	6	-	-	95
	"	150-160		4070	23	9	9	-	-	-	127
20	G-25	10-20	2900	1010	11	26	9	9	-	-	51
	"	70-80		4600	17	14	7	6	-	-	192
	"	110-120		5330	23	14	9	9	-	-	167
	"	160-170		7730	23	20	9	12	-	-	242
	"	200-210		6650	28	20	9	15	-	-	180
21	G-27	0-10	3158	5120	20	23	9	6	-	-	177
	"	50-60		4740	17	14	5	6	-	-	215
	"	102-112		7920	20	17	7	-	-	-	293

Table 13 (Cont.)

9	G-12	0-10	154	8330	204	75	106	19	29	32	27
	"	50-60		3160	117	6	30	5	-	-	21
	"	100-110		4820	333	6	95	16	15	9	11
10	G-13	0-10	166	1170	47	39	25	14	9	9	16
	"	50-60		3170	35	9	11	11	-	-	69
	"	100-110		3100	79	9	7	27	-	-	36
	"	150-160		3950	158	12	9	49	-	-	24

Table 13. Hydrocarbon Gases - Southern Bering Shelf S6-77

Sta.	Sample	Interval (cm)	Water Depth (m)	Concentrations (nL/L wet sediment)							$\frac{C_1}{C_2 + C_3}$
				C_1	C_2	$C_2 : 1$	C_3	$C_{3:1}$	i-C_4	n-C_4	
2	G -1	0-10	136	810	30	34	17	11	-	-	17
	"	50-60		4480	42	28	22	5	6	9	70
	"	92-102		5160	63	44	43	14	9	12	49
3	G -2	0-10	129	890	18	22	13	6	-	-	29
	"	42-52		2150	42	28	24	8	9	9	33
4	G -4	0-10	110	1040	27	34	13	17	-	9	26
	"	55-65		3230	39	31	22	11	-	9	53
5	G -6	0-10	108	1040	27	38	19	11	-	6	23
	"	50-60		3930	48	28	28	8	6	9	52
6	G -7	0-10	109	790	24	22	15	6	-	-	19
	"	27-37		2070	51	50	34	17	12	12	24
7	G-10	0-10	130	750	15	25	9	8	-	2	31
	"	34-44		2300	36	38	24	14	-	-	38
8	G-11	0-10	145	1860	47	45	26	14	6	9	25
	"	50-60		2680	29	18	17	8	6	8	58

the Aleutian Islands and Alaskan Peninsula. The present-day continental shelf of the southern Bering Sea is extremely flat and broad. Bottom gradients typically are much less than 0.25° (1:13,000) and the mouths of large rivers that feed sediment into the Bering Sea, the Yukon, Kuskokwim. Kvichak, and, to a lesser extent, the Nushagak Rivers, are over 500 km away from the outer shelf. Sediment is transported from these rivers into Bristol Bay, but has almost no opportunity to be advected to the outer shelf because of the extremely low topographic gradients and insufficient watermass movement. Structural fronts in the water-column are parallel to the 50-m isobath (Schumacher et al., in prep.). These fronts may have some effect in impeding the seaward dispersal of detritus toward the outer continental shelf.

The Aleutian Islands and the Alaskan Peninsula are obvious sediment sources for the volcanic components today but the Bering Canyon (Figure 6) provides a topographic depression that traps sediment before it can get to the outer shelf. The sluggish, semi-gyre cyclonic circulation pattern that characterizes surface flow in the southern Bering Sea (Favorite, 1974; Takenouti and Ohanti, 1974) is only on the order of 2 to 3 cm/sec (Schumacher, et al., in prep.), too slow to transport even clay-sized particles.

The Pribilof Islands and Pribilof Ridge also are potential sediment sources for some of the volcanic components but the low relief and small area of the features preclude any large contributions. Lack of a dominant circulation and very low current velocities also eliminate the Pribilof Ridge as a major source. Thus, today, the source areas are isolated from the site of deposition.

Consequently, it seems unlikely that sediments are presently being transported to and deposited on the outer continental shelf of the southern Bering Sea in significant quantities, and the uppermost deposits must be relict from a previous depositional environment. Diatom floras from the bottom of each of our cores all fall within the Denticula semina zone (J. Barron, personal communication, 1976 and 1977), which ranges from 260,000 years BP to present (Koizumi, 1973). Although we believe that the sediments are relict and not modern, about all we can say about their age from existing data is that they are late Quaternary in age.

The dominant influence on Quaternary continental shelves has been glacioeustatic lowering of sea level, and it seems probable that this influence was magnified on the broad, flat shelf of the Bering Sea. Estimates of the lowering of sea level during the Pleistocene glacial periods are all about 130 m (Curray, 1960, 1965; Bloom, 1971). We have drawn a shoreline in Fig. 30 along the present-day 130-m isobath and subtracted 130 m from each of the isobaths to yield a schematic bathymetric chart of a low sea level period. Several features of this chart are worth noting. The region landward of the shoreline is featureless and flat with gradients much less than 0.25°. Any streams that flowed across

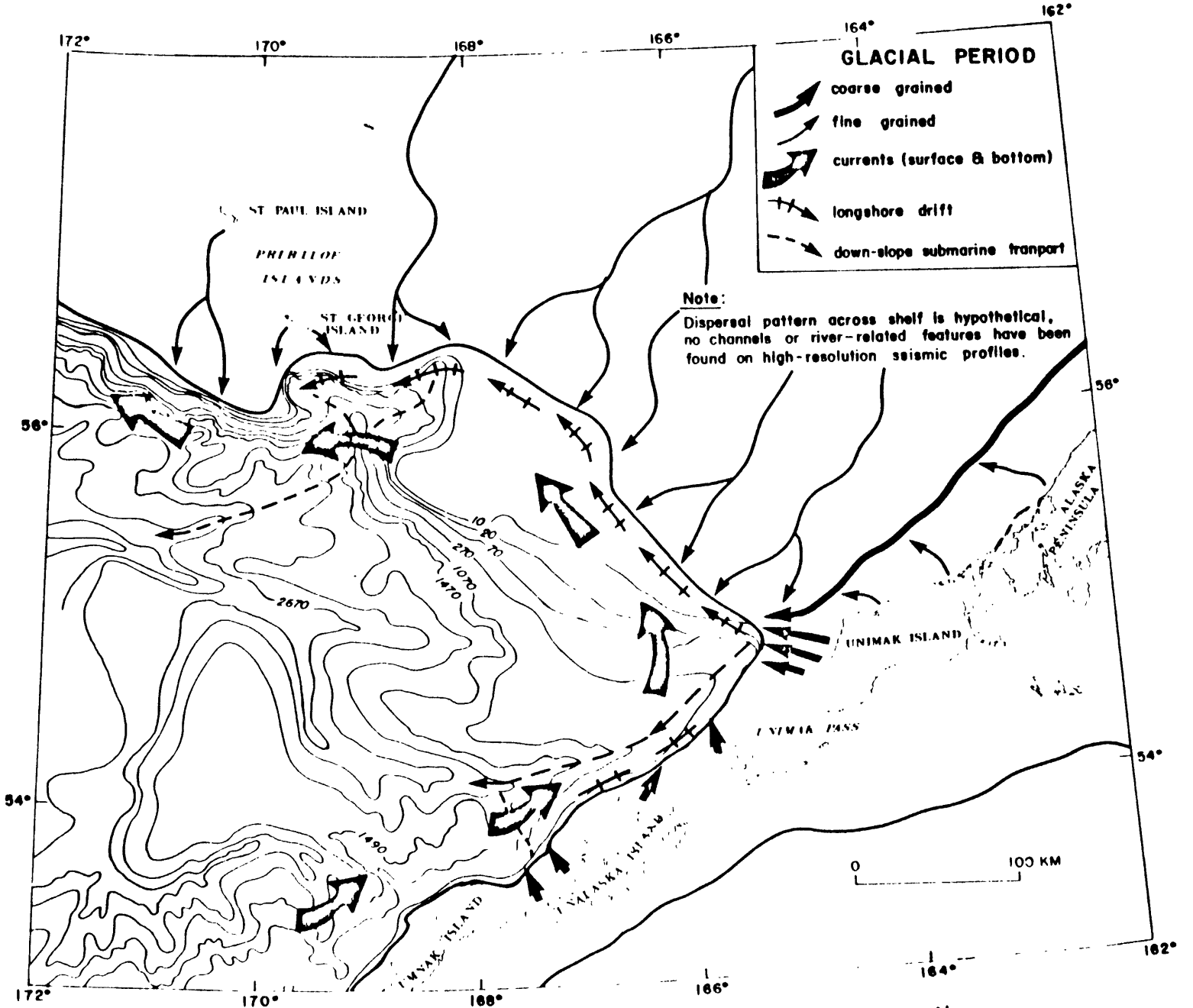

Figure 30. A paleobathymetric map of the continental margin of the southern Bering Sea during a period of worldwide glacial conditions.

this emerged shelf must have been very meandering with a large dendritic distributary system. This is especially important in light of speculations by Scholl et al. (1970) that the Yukon and (or) Kuskokwim Rivers cut the Pribilof Canyon during the Pleistocene. We see no evidence of buried or surface stream channels on more than 10,000 km of high-resolution seismic data (12 kHz, 3.5 kHz, and 1.5 kHz), and so we conclude that no rivers cut channels across this portion of the continental shelf during Pleistocene lower sea levels and that Pribilof Canyon was formed much earlier than the Pleistocene. Streams that debouched into the southern Bering Sea during glacial periods were not competent to transport much coarse-grained sediment. The mainland components (factor 2 of the Q-mode analysis) are represented by quartz, garnet, epidote, orthopyroxene, metamorphic rock fragments, Si, K, and Ba. However, all of these components are distributed as background with relatively low concentrations over the outer shelf.

Superimposed on this background of mainland materials are northwest-trending gradients of sediments that contain relatively high concentrations of andesitic components (factor 1), decreasing away from the Aleutian Islands in the vicinity of Unimak Pass. This Aleutian component is represented by clinopyroxene, volcanic glass, volcanic rock fragments, smectite + vermiculite, Na, Ca, Mg, Fe, Ti, Al, Co, Cu. Mn, V, and Zn. Volcanic debris is also distributed as an aureole of local extent around the Pribilof Islands. The northwest-trending gradients away from the Aleutian Islands reflect longshore transport of clay- to sand-size material from the Aleutians during periods of low sea levels. Much, and perhaps the vast majority, of the detritus shed off the Aleutians and Alaskan Peninsula was trapped by the Bering Canyon and funneled onto the continental rise. However, apparently material was periodically captured by longshore currents and transported onto and along the narrow shelf. Possibly the head of Bering Canyon may have periodically filled up, which allowed sediment to be transported across to the shelf. The strong gradients seen especially in the geochemical data suggest that a relatively strong, cyclonic, nearshelf circulation may have existed that was competent to transport coarse sediment along the shelf.

When sea level rose during periods of glacial to interglacial transition, the shift in the position of the shoreline must have been rapid because of the very low topographic gradients (Fig. 31). If we use the Pleistocene to Holocene transgression as a model, then the initial retreat of the shoreline was slow with a 50-m rise in sea level producing a transgression of about 70 km. Sea level curves (Curray, 1960, 1961; Morner, 1971; Bloom, 1971) indicate that the first 50-m rise in sea level took about 5,000 years. However, the next 10-m rise in sea level produced a 175-km retreat of the shoreline in only about 1,000 years. The remaining 70-m rise in sea level caused a 250-km transgression in the remaining 6,000 to 8,000 years. Therefore, when the shoreline began to retreat, it did so

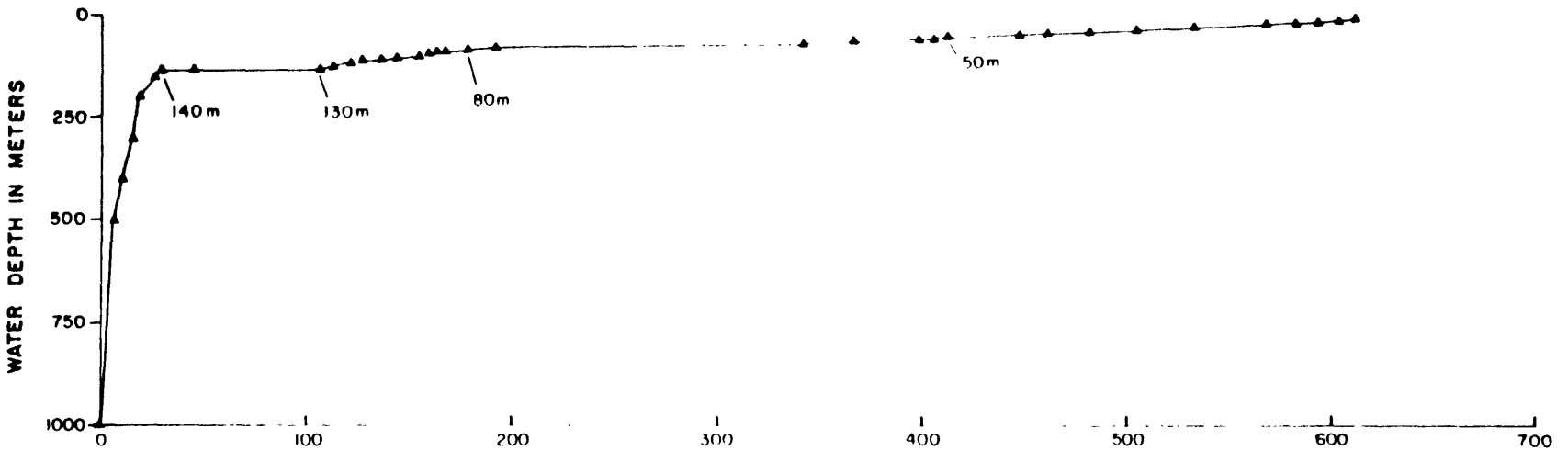

Figure 31. A profile of the continental margin of the southern Bering Sea drawn as distance from the 1000 m isobath. Each solid triangle from 140 to 0 m represents a 5-m sea level rise.

rapidly and, in effect, deserted a sediment distribution pattern with little modification. The result is a glacial-period sediment distribution pattern and an interglacial-period oceanographic circulation, as is observed today.

Present-day oceanographic conditions have modified the distribution and character of the sediments to a small degree, and in this context they are palimpsest (Swift, et al., 1971). Maps of lithofacies and sorting (Figs. 8 and 9) show that a tongue of moderately sorted, coarse sediments extends along the shelf break south of Pribilof Canyon and along the northern flank of Bering Canyon. The tongue of Pribilof Canyon seems to be restricted in extent and this restriction coincides with the steepest portion of the continental slope. Conversely, the poorest sorted and finest-grained sediments, with relatively high concentrations of absorbed organic material (Q-mode factor 3), are found in the center of St. George basin. This distribution of textures can be explained by a combination of long-period storm waves and a gravity potential, i.e. a change in bathymetry significant enough to provide the energy necessary to keep sediment in transit. Komar et al (1972) show that waves with a 15-sec period cause rippling of sandy sediments off the Oregon coast in water depths down to 149 m. Thus, high sea states that commonly occur in the southern Bering Sea during the late summer and fall can affect bottom sediments of the outer shelf. Resuspension of surface sediments by long-period storm waves would increase the density of the shelf-bottom boundary layer with the incorporation of clay and silt. The coarser sediment would probably fall out of suspension quickly. If this dense boundary layer were located in an area closely adjacent to a gravity potential (i.e. a region with a slope of perhaps 2^{o} or more), then the dense boundary layer would flow down slope and out of the area. This mechanism would tend to winnow out the fine-grain sizes and impart a better sorting to the sediment than remains behind. The patterns of textural parameters (Figs. 8 and 9) show this result. The broad continental slope north of Bering Canyon has gradients of about 1.5^{o} and apparently is too gentle to provide the critical gravity potential, thus little winnowing is occurring there. However, the slope just south of Pribilof Canyon has gradients in excess of 3^{o} and evidence of winnowing is suggested by better sorting and coarser grain sizes.

Sediments in St. George basin also are affected by these long-period storm waves but, because of lack of a gravity potential, the shelf-bottom boundary layer is restricted to the limits of the basin and the sediment is redeposited in the same general area. The fact that St. George basin is a surface graben also helps to explain the general lack of transport of sediment out of this area. Storm waves mix sediments in St. George basin, but the only apparent effect is to obscure the boundaries between the textural provinces and to concentrate finer-grained and more poorly-sorted sediment into a bull's-eye pattern.

Distribution patterns of grain size do not reflect the graded-shelf size distribution described by Sharma et al. (1972). However, their sampling stations stop along the northern boundary of the area covered by our data. When the data of Sharma et al. (1972) are joined to our data, the two complement each other very well, yet each tells a different story. Their data are concentrated in the shallow (<100m) reaches of Bristol Bay and reflect a gradual decrease in grain size with distance from shore. Our data are concentrated in depths greater than 100m, and show the overprints of the effects of topography (gravity) controls on the redistribution of sediment. Sediments in Bristol Bay are presently affected by storm waves because even the relatively short-period waves can affect the sediment surface. The outer shelf is immune to the normal sea state because of depth and only periodic large storm waves affect the sea floor in this region and only for short durations.

DISTRIBUTION OF FAULTS AND POTENTIALLY UNSTABLE SEDIMENTS

Summary

Seismic-reflection data are used to identify and map faults beneath the outer continental shelf of the southern Bering Sea. We studied more than 10,000 km of single-channel and 600 km of multichannel seismic-reflection profiles. Our seismic systems can resolve offsets that range from a fraction of a meter to several kilometers. Faults are classified as major, minor, and surface based on the type and amount of displacement. Major faults are those resolved on both multi-channel and single-channel seismic-reflection records. These faults generally penetrate from several hundred meters to several kilometers beneath the sea floor and some displace reflectors more than 60 meters. Major faults are principally distributed along or near the borders of St. George basin and they trend NW-SE parallel to the basin's long axis. Major faults often offset the seafloor and as surface faults, are most abundant along the boundaries of St. George basin. Minor faults are widely distributed throughout the outer shelf; however, to the east they are concentrated in the middle of St. George basin. Most minor faults exhibit displacements of 5 m or less and almost all approach the sea floor to within 4 or 5 m. The precise age of faulting is not known although both surface and minor faults do offset upper Pleistocene sediment. Major faults are probably related to stress fields established by Mesozoic and Cenozoic plate motions and minor faults are related to high seismicity in the nearby Aleutian subduction zone.

Classification of Faults

We classify faults in this study by their relative amount of vertical displacement. The resolutions of the seismic systems, which determine the minimum offset we can detect with each system, are shown in Table 3 and were calculated using the velocity of sound in water and by following the procedure of

Moore (1972). The following seismic-reflection data were used to map the distribution of faults: 1) 3.5 kHz; 2) 2.5 kHz; 3) single-channel seismic-reflection (60 KJ to 160 KJ sparker, and up to 1326 in^3 air-gun sources); and 4) 24-channel system using a 1326 in^3 air-gun array.

A gap may exist in the resolving range of our systems between about 0.5 m and 3 m, which suggests that offset features in that range may not be resolved. Our studies concentrate on faults cutting strata above the acoustic basement as resolved on our single-channel seismic-reflection system. However, our multichannel data also indicate that many faults occur within the acoustic basement.

Faults are classified as surface, minor, and major faults. Surface faults offset the surface of the sea floor regardless of the recording system. They offset the sea floor no more than a few meters. Minor or near-surface faults are resolved on 2.5 kHz and/or 3.5 kHz records, but not on single or multichannel seismic-reflection profiles. These faults typically displace reflectors less than 0.006 sec (5 m); most minor faults are close to but do not break the sea floor. Sediment can be seen in places to drape over near-surface faults. Major faults are defined as those resolved on multichannel and single-channel seismic-reflection profiles. These faults generally are growth structures and many offset acoustic basement. Boundary faults are major faults that mark the boundaries of St. George basin.

Fault Distributions

Distribution of faults is shown in Fig. 32 . The true orientation of most faults is unknown because of the relatively wide spacing of tracklines. Faults found on northeast-southwest tracklines, perpendicular to the long axis of St. George basin, greatly outnumber those observed on northwest-southeast tracklines which indicates that the majority of the faults have a northwest-southeast trend and parallel the trend of the basin. Faults bounding St. George basin can be confidently traced between tracklines. We believe that most faults beneath the shelf and those in St. George Basin in particular, trend northwest-southeast parallel to the basin and to the margin.

Boundary faults clearly delineate St. George basin and the north side of the Pribilof ridge. These faults are normal faults, occur in groups, and exhibit increased offset with depth, which indicates growth-type structures. These faults in many places cut nearly all of the sedimentary section, and often offset acoustic basement, but rarely offset the sea floor.

Major faults (other than boundary faults) principally occur within St. George basin, although a few occur within Amak basin (Figure 33). This class of fault decreases in abundance near the

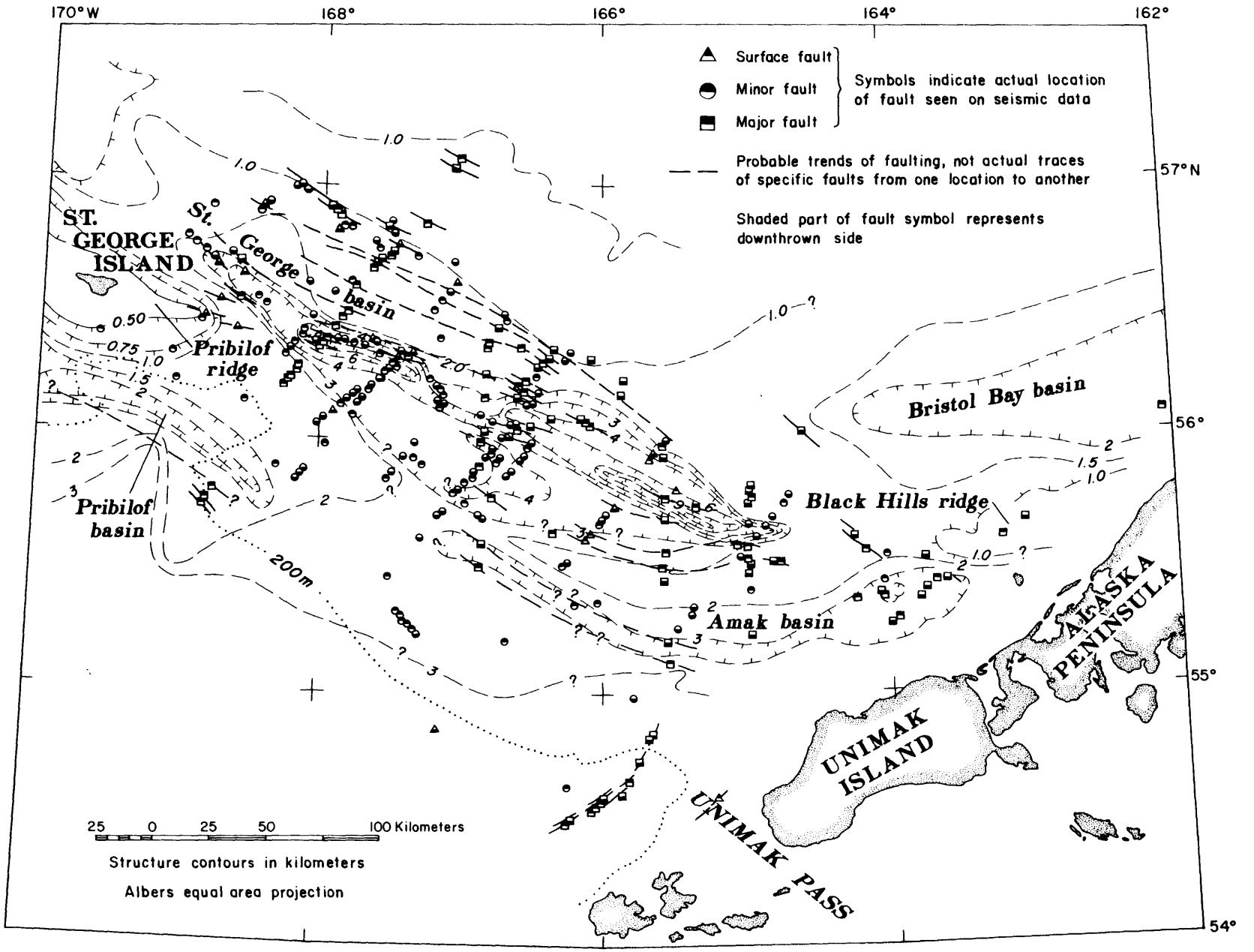

Figure 32. Map of distribution of faults in the southern Bering Sea. Lines through fault symbols are inferred trend of the fault, not any known strike. Structure contours of acoustic basement from Marlow et al. (1976, 1977a).

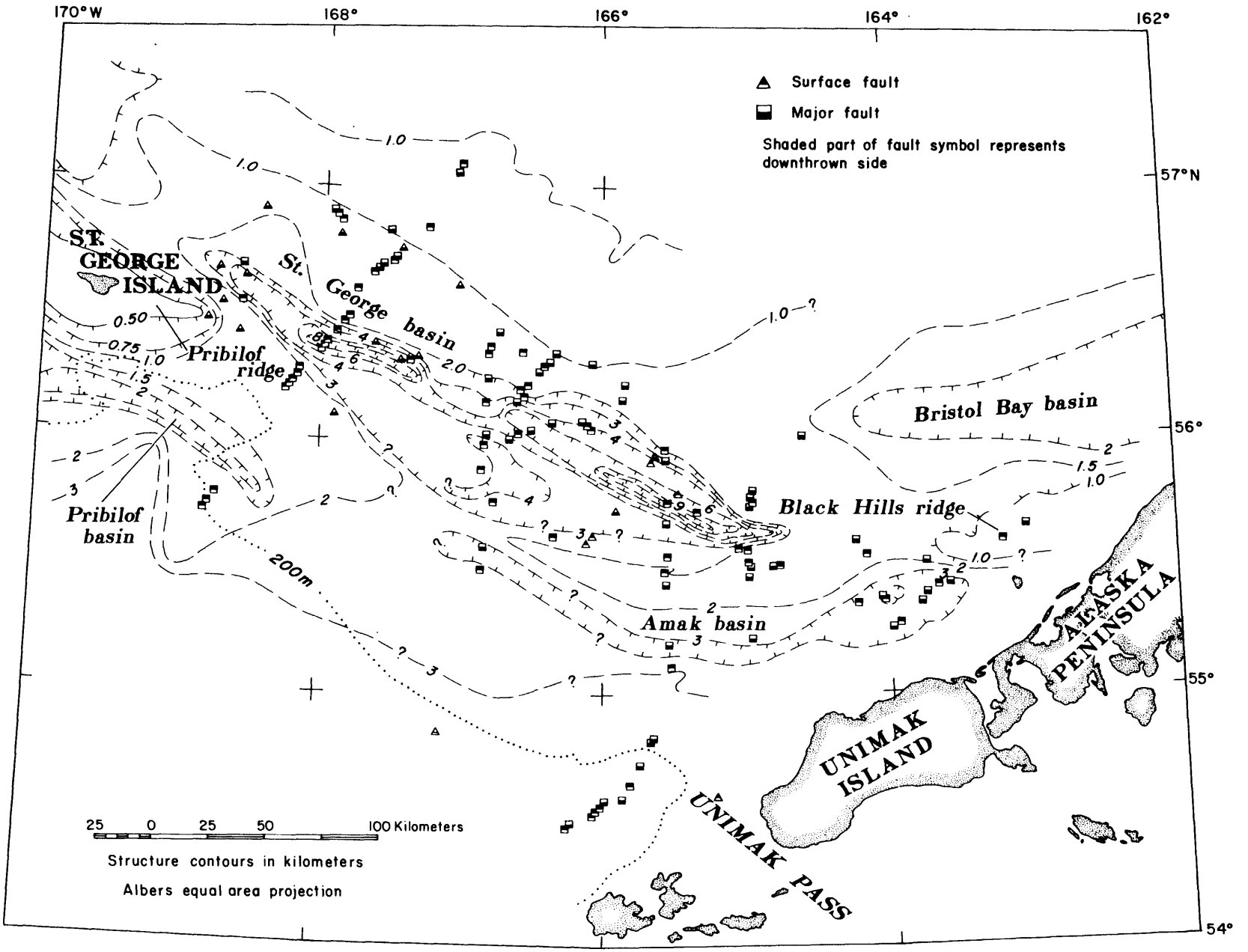

Figure 33. Distribution of surface and major faults. Structure contours on acoustic basement from Marlow et al. (1976, 1977a, 1977b).

Pribilof Islands. Major faults show displacements that generally are less than the larger boundary faults but offsets greater than 0.08 sec (60 m) occur in the central region of St. George basin. Major faults are not always offset in the same sense as adjacent boundary faults, which suggests that deformation of the outer shelf has involved more than simple subsidence.

Surface faults tend to be more abundant along the outer margin of St. George basin and along Pribilof ridge than in the center of the basin (Figure 33). Most surface faults can be traced from high-resolution to low-resolution records, which suggests that most surface faults are expressions of major faults and of boundary faults.

Minor faults (Figure 34) occur throughout the southern outer shelf, although, like other classes of faults, they are also concentrated in the middle region of St. George basin, away from the Pribilof ridge. Minor faults are more frequent south of the ridge than to the north (Figure 34). Most minor faults offset reflectors less than 0.006 sec (5 m) and almost all these faults cut the top 0.005 sec (approximately 4 m) of the sedimentary section. Diatoms recovered in sediment from gravity cores up to 2m long are younger than 260,000 years (all within the Denticula seminae Zone; John Barron, pers. commun., 1976, 1977). If we assume that a 2m core just penetrated the entire Denticula seminae Zone, then the minimum accumulation rate is 0.8 cm/10^3 yr. If we assume that this minimum accumulation rate is typical for the top 4 m of sediment (the thickness generally affected by minor faults), then the maximum age of the sediment, calculated at 0.8 cm/10^3 yr. is 520,000 YBP. Thus, minor faulting may be no older than Pleistocene in age. Accumulation rates may be much greater, for example 10 cm/10^3 yr. as suggested by C^{14} dates from areas farther north (Askren, 1972), in which case the minor faults could cut sediment as young as 40,000 YBP.

Potentially Unstable Sediments

Areas of potentially unstable sediment masses (Fig. 32) were determined from the seismic reflection records by using one or more of the following criteria: 1) surface faults with steep scarps and rotated surfaces; 2) deformed bedding and/or discontinuous reflectors; 3) hummocky topography; 4) anomalously thick accumulation of sediment; and 5) acoustically-transparent masses of sediment. Regions that show unstable sediments (e.g. gravity slides, slumps, creep, scarps, etc.) are confined to the continental slope and rise and the Pribilof and Bering canyons. Zones of creep, as shown by irregular, hummocky topography, begin near the shelf break at depths of about 170 m and continue onto the upper continental slope. Hummocky topography occurs on the continental slope on a large scale and mass movement is a common feature. We regard the entire continental slope and the walls of the major submarine canyons to be zones of potentially unstable sediment. Regimes of active

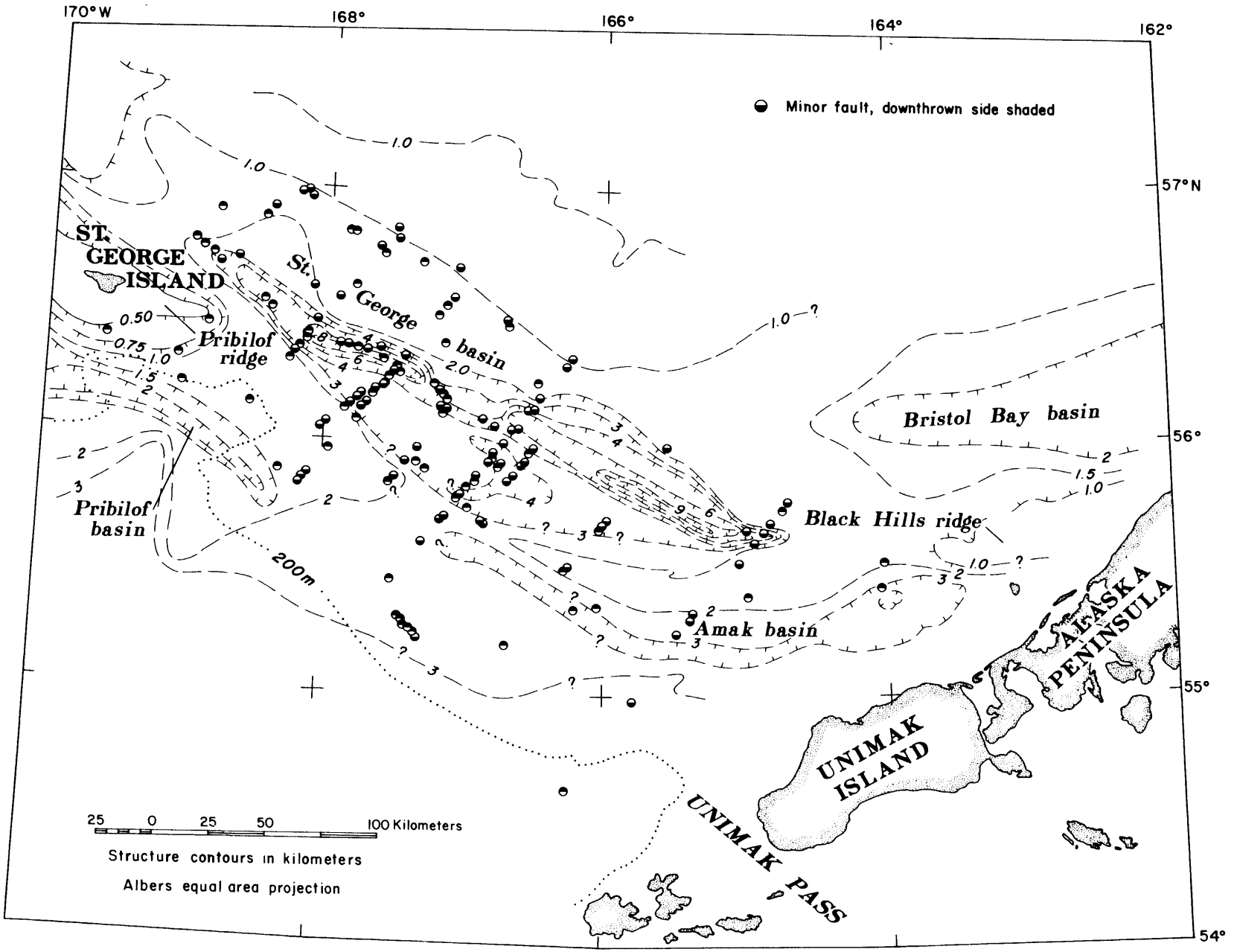

Figure 34. Distribution of minor faults. Structure contours from Marlow et al. (1976, 1977a, 1977b).

sediment movement could respond to a variety of energy sources including earthquakes, storms, internal waves, and gravity.

Discussion

Faults of the outer continental shelf of the southern Bering Sea are concentrated in St. George basin. Many faults cut upper Pleistocene sediment and some offset the sea floor, indicating that the area is tectonically active. The processes that initially formed St. George basin are presently active. Principal structural features along the outer continental shelf, e.g. St. George and Amak basins, as well as other minor basins (see Marlow et al., 1976), probably all had a common origin and tectonic history. Subduction between the Kula (?) and North American plates along the Bering Sea margin is thought to have been oblique during the Mesozoic (Marlow et al., 1976). However, reconstructions by Cooper et al. (1976), indicate that the ancient margin may have been a transform fault separating two plates. Nevertheless, structural patterns were developed parallel to the margin. The Mesozoic stress field and thermal regime changed when subduction jumped from the Siberian margin to near the present Aleutian trench. If oblique subduction did occur along the Bering Sea margin, then a southward shift of the site of compression would have isolated the margin in late Mesozoic time. A relaxation of compression would then give way to extension and thus to formation of grabens beneath the outer shelf. The complementary horst structures hypothesized by Bott (1976) for this type of model may be represented by the Pribilof ridge. If the Bering margin was instead a transform fault zone during the Mesozoic, then some complex model such as a combination of sediment loading (Watts and Ryan, 1976), mantle metamorphism (Falvey. 1974) and mantle flowage (Bott, 1976) may have lead to the collapse of the margin and formation of large grabens along the outer shelf. Whatever the tectonic stresses are that caused extension, they are presently active as evidenced by large growth faults bounding St. George basin. Second-order structures such as minor faults are probably superimposed features which resulted from subduction beneath the arc during the Cenozoic.

The southern Bering Sea margin is within 500 km of the Aleutian Trench, the present site of subduction between the Pacific and North American plates. Several intermediate - to deep-focus (71 to 300 km deep) and many shallow-focus (less than 71 km deep) earthquakes were recorded beneath the southern Bering Sea margin from 1962 to 1969 as shown in Figure 35 . The St. George basin and surrounding areas have been subject to earthquakes with intensities as high as VIII (modified Mercalli scale), which corresponds to a magnitude 5.7 earthquake (Meyers and others, 1976). Recurrence rates of earthquakes for the area bounded by latitudes 50° and 60° N and longitudes of 160° to 175° W have been as high as 6.4 earthquakes per year from 1963 to 1974 for magnitudes of 4.0 to 8.4, and 0.013 earthquakes per year of

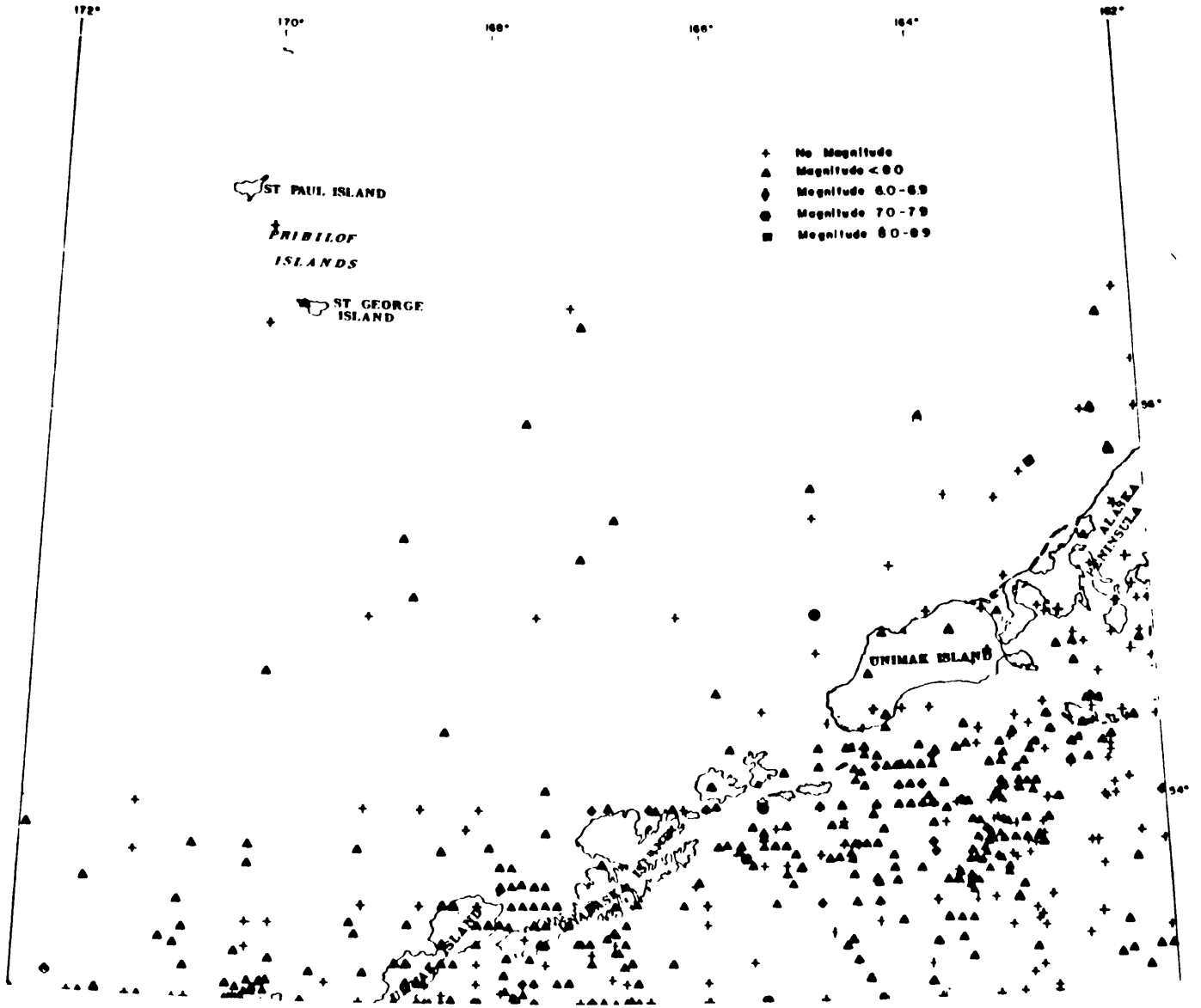

Figure 35. EPICENTERS UP THRU 1964
(DEPT. OF COMMERCE, 1970)

magnitude 8.5 to 8.9 (1 every 130 years) from 1899 to 1974 (Meyers and others, 1976).

The correlation of earthquakes to shallow faulting is not well understood (Page, 1975). We believe, however, that many of the faults in the southern Bering Sea are active and that they probably respond to earthquake-induced energies and possibly to sediment loading in St. George basin.

CONCLUSIONS

Detailed conclusions are given in the discussion sections of parts 2 and 3. Some of the major conclusions are repeated in this section.

The large number of faults, evidence for recent movement along some, and the high seismicity indicate that faulting is a major environmental concern in the outer continental shelf region of the southern Bering Sea, especially in St. George basin. All faults are potentially active, their movement probably influenced by seismic energies and the local geology, including basement structures and sediment loading. Unstable sediment masses pose potential threats to developments on the continental slope and walls of the submarine canyons.

Mineralogical and inorganic geochemical data show three major sources of sediments and one sediment sink. The Alaska mainland source forms a mineralogical and chemical background to most samples from the shelf. The dominant source is the Aleutian Islands and a third, very local source, is the Pribilof Islands. St. George basin has served as a sink for fine-grained sediment.

Sediment distributions do not appear to reflect present-day deposition. Rather, we believe that the distributions are the result of accumulation during periods of lower sea level in the Pleistocene, modified by present-day processes. Evidence for this conclusion is shown by a concentration of Aleutian sediments, between the 100 m and 200 m isobaths, which exhibit a strong gradient, or "plume", that decreases away from Unimak Pass into St. George basin. Lack of present-day currents sufficient to move even clay-size material and the presence of the Bering submarine canyon between the Aleutian Islands and the outer continental shelf and slope indicate that Holocene sediment dynamics cannot be used to explain the observed distribution of surface sediments derived from the Aleutian Islands. We believe it is logical to suggest that this distribution pattern is relict and is the result of sediment dynamics during lower sea levels.

REFERENCES

Anderson, R. L. and Bancroft, T. A., 1952, Statistical theory in research: New York. McGraw-Hill Book Co., 399 p.

Askren, D. R., 1972, Holocene stratigraphic framework-southern Bering Sea continental shelf: MS Thesis, Univ. of Washington, 104 p.

Bader, R. G., 1962, Some experimental studies with organic compounds and minerals: Univ. Rhode Island, Graduate School of Oceanography Occasional Pub. No. 1, 85 p.

Biscaye, P. E., 1965, Mineralogy and sedimentation of Recent Deep-sea clay in the Atlantic Ocean and adjacent seas and oceans: Geol. Soc. Amer. Bull., v. 76. p. 803-831.

Bloom, A. L., 1971, Glacial-eustatic and isostatic controls of sea level since the last glaciation: in Turekian, K. K. (ed.) Late Cenozoic Glacial Ages, Yale Univ. Press, New Haven, p. 355-379.

Bordovskiy, O. K., 1965, Accumulation and transformation of organic substances in marine sediment: Marine Geology, v. 3, P. 3-114.

Bott, M. H. P., 1976, Formation of sedimentary basins of graben type by extension of the continental crust: Tectonophysics, v. 36, p. 77-86.

Connor, J. J., Feder, G. L., Erdman, J. A., and Tidball, R. R., 1972, Environmental geochemistry in Missouri - a multiplinary study, in Earth science and the quality of life--Symposium 1: Internat. Geol. Cong., 24th, Proc., p. 7-14.

Cooper, A. K., Scholl, D. W., and Marlow, M. S., 1976, Plate tectonic model for the evolution of the eastern Bering Sea Basin: Geol. Soc. Amer. Bull., v. 87, p. 199-1126.

Creager, J. S., Scholl, D. W., et al., 1973, Initial Reports of the Deep Sea Drilling Project, V. 19: Washington (U. S. Government Printing Office), 913 p.

Curray J. R., 1960, Sediments and history of Holocene trans-gression, continental shelf, northwest Gulf of Mexico:- in Shepard, F. P., Phleger, F. B., and van Andel, T. H. (eds.), Recent Sediments, Northwest Gulf of Mexico, Tulsa, Oklahoma, Am. Assoc. Petroleum Geologists, p. 221-266.

_____1961, Late Quaternary sea level: a discussion: Geol. Soc. Amer. Bull., v. 72, p. 1707-1712.

1965, Late Quaternary history, continental shelves of the United States: in Wright, H. E., Jr., and Frey, D. G. (eds.), The Quaternary of the United States, Princeton, N. J., Princeton University Press, p. 723-735.

Emery, K. O., 1960, The sea off southern California. A modern habitat of petroleum: New York, John Wiley and Sons, 366 p.

Favorite, F., 1974, Flow into the Bering Sea through Aleutian passes: in Hood, D. W. and Kelley, E. J (eds.), Oceanography of the Bering Sea, Inst. of Marine Science, Univ. of Alaska, Occasional Pub. 2, p. 3-37.

Folk, R. L., and Ward, W. C., 1957, Brazos River bar: a study in the significance of grain size parameters: Jour. Sed. Petrology, v. 17, p. 3-27.

Hein, J., Scholl, D. W., and Gutmacher, C., 1975, Neogene clay minerals of the far northwest Pacific and Southern Bering Sea: Sedimentation and diagenesis, in Bailey, S. W. (ed.) AIPEA proceedings, International Clay Conf., Mexico City, p. 71-80.

Jordon, C. F., Jr., Fryer, G. E., and Hemmen, E. H., 1971, Size analysis of silt and clay by hydrophotometer: Jour. Sed. Petrology, v. 41, p. 489-496.

Kemp, A. L. W., 1971, Organic carbon and nitrogen in the surface sediments of Lake Ontario, Erie, and Huron: Jour. Sed. Petrology, v. 41, No. 2, p. 537-548.

Klovan, J. E., and Imbrie, J., 1971, An algorithm and FORTRAN IV program for large scale Q-mode factor analysis and calculation of factor scores: Jour. Internat. Assoc. Mathematical Geology, v. 3, no. 1, p. 61-77.

Koizumi, J., 1973, The Late Cenozoic diatoms of sites 183-193, Leg 19, Deep Sea Drilling Project: in Creager, J. S., Scholl, D. W., and others, Initial Reports of the Deep Sea Drilling Project, v. 19: Washington, D. C., p. 805-856.

Komar, P. D., Neudeck, R. H., and Kulm, L. D., 1972, Observations and significance of deep-water oscillatory ripple marks on the Oregon continental shelf: in Swift, D. J. P., Duane, D. B., and Pilkey, O. H., Shelf Sediment Transport Process and Patterns, Dowden, Hutchinson, and Ross, Inc., 601-619.

Marlow, M. S., Scholl, D. W., and Cooper, A. K., 1975, Structure and evolution of the Bering Sea Shelf south of St. Lawrence Island: Am. Assoc. of Petroleum Geologists Bull., v. 60, p. 161-183

Marlow, M. S., Scholl, D. W., Cooper, A. K., and Buffington, E. C., 1976, Structure and evolution of Bering Sea shelf south of St. Lawrence Island: Amer. Assoc. Petroleum Geologists Bull. v. 60, P. 161-183.

Marlow, M. S., Scholl, D. W. and Cooper, A. K., 1977a, St. George Basin, Bering Sea shelf: a collapsed Mesozoic margin: in Island Arcs, Deep Sea Trenches, and Back-Arc Basins, Maurice Ewing series, Amer. Geophysical Union, v. 1. p. 211-220.

Marlow, M. S., Cooper, A. K., and Scholl, D. W., 1977b, Mesozoic structural trends beneath the southern Bering Sea shelf: (abs.) Geol. Soc. Amer. Ann Mtg, 1977, v. 9, p. 460-461.

Meyers, H., Brazee, R. J., Coffman, L. L., and Lessig, S. R., 1976, An analysis of earthquake intensities and recurrence rates in and near Alaska: N.O.A.A. Tech. Memorandum, EDS NGSDC-3, 101p.

Miesch, A. T., 1976, Geochemical Survey of Missouri, Methods of sampling, laboratory analysis, and statistical reduction of data: U. S. Geol. Survey Prof. Paper, 954-A, 39 p. Moore, D. G., 1972, Reflection profiling studies of the California continental borderland: structure and Quarternary turbidite basins: Geol. Soc. Amer. Spec. Paper 197, 142 p.

Moore, D. G., 1972, Reflection profiling studies of the California continental Borderland: Structure and Quaternary turbidite basins. Geol. Soc. Amer. Sp. Pap. 107, 142 p.

Morner, N. 1971, Eustatic changes during the last 20,000 years and a method of separating the isostatic and eustatic factors in an uplifted area: Paleogeography, Paleoecology, v. 9, p. 153-181.

Nelson, C. H., Hopkins, D. M., and Scholl, D. W., 1974, Cenozoic sedimentary and tectonic history of the Bering Sea: in Hood, D. W., and Kelley, E. J. (eds.), Oceanography of the Bering Sea, Inst. of Marine Science, Univ. of Alaska, Occasional Publ. 2, P. 485-516.

Page, R. A., 1975, Evaluation of seismicity and earthquake shaking at offshore sites: Offshore Technology Conference Proceedings, p. 179-190.

Ratmanoff, G. E., 1937, Explorations of the seas of Russia: Publ. Hydrol. Inst. 25, p. 1-175.

Scholl, D. W., Buffington, E. C., and Hopkins, D. M.1968, Geologic history of the continental margin of North America in Bering Sea: Marine Geology, v. 6, p. 297-330.

Scholl, D. W., and Hopkins, D. M., 1969, Newly discovered Cenozoic basins, Bering shelf, Alaska Amer. Assoc. Petroleum Geologists, Bull., v. 53, p. 2067-2078.

Scholl. D. W.. Buffington, E. C., Hopkins. D. M., and Alpha, T. R., 1970, The structure and origin of the large submarine canyons of the Bering Sea: Marine Geology, v. 8, p. 187-210.

Scholl, D. W., Buffington, E. C., and Marlow, M. S., 1975, Plate tectonics and the structural evolution of the Aleutian-Bering Sea region: in Forbes, R. B., (ed.), Contributions to the Geology of the Bering Sea Basin and Adjacent Regions: Geol. Soc. America Spec. Paper 151, p. 1-32.

Schumacher, J. D., Kinder, T. H., Pashinski, D. J., and Charnell, R. L., in prep., Structural fronts over the continental shelf of the eastern Bering Sea: submitted to J. Physical Ocean.

Sharma, G. D. 1974, Contemporary depositional environment of the eastern Bering Sea: in Hood, D. W. and Kelley, E. J., (eds.), Oceanography of the Bering Sea, Inst. of Marine Science, Univ. of Alaska, Occasional Publ. 2, p. 517-540.

_____1975, Contemporary epicontinental sedimentation and shelf grading in the southeast Bering Sea: in Forbes, R. B. (ed.), Contributions to the geology of the Bering Sea Basin and adjacent Regions, Geol. Soc. Amer. Spec. Pap. 151, p. 33-48.

Sharma, G. D., Nardu, A. S., and Hood, D. W., 1972, Bristol Bay: A model contemporary graded shelf: Amer. Assoc. Petroleum Geologists, v. 56, p. 2000-2012.

Swift, D. J. P., Stanley, D. J., and Curray, J. R., 1971, Relict sediments on continental shelves: a reconsideration: J. Geol., v. 79, p. 322-346.

Takenouti, A. Y., and Ohtani, K., 1974, Currents and water massesin the Bering Sea: A review of Japanese work: in Hood, D. W. and Kelley, E. J., (eds.), Oceanography of the Bering Sea, Inst. of Marine Science, Univ. of Alaska, Occasional Publ. 2, p. 39-57.

Thiede, J., Chriss, T., Clauson, M., and Swift, S. A., 1976, Settling tube for size analysis of fine and coarse fractions of oceanic sediments: Oregon State Univ., School of Oceanography, Reference 76-8, 87 p.

Thomas, R. L., 1969, A note on relationship of grain size, clay content, quartz and organic carbon in some Lake Erie and Lake Ontario Sediments: Jour. Sed. Petrology, v. 39, p. 803-809.

Trask, P. D., 1932, Origin and environment of source beds of petroleum: Houston, Gulf Pub. Co., 323 p.

U. S. Department of Commerce, 1970, Seismicity of Alaska NEIC Map 3011: Environ. Science Adm., U. S. Coast and Geol. Survey, Washington, D. C., 1 ed.

Van Straaten, L. M. J. V., 1954, Composition of recent marine sediments in the Netherlands: Leid. Geol. Meded., v. 19, p. 1-108.

Watts, A. B. and Ryan, W. B. F., 1976, Flexture of the lithosphere and continental margin basins: Tectonophysics, v. 36, p. 25-44.

APPENDIX A. List of Publications and Major Reports

Marlow, M., McLean, H., Vallier, T., Scholl, D., Gardner, J., and Powers, R., 1976, Preliminary report on the regional geology, oil and gas potential, and environmental hazards of the Bering Sea shelf south of St. Lawrence Island, Alaska: U. S. Geological Survey Open-File Report 76-785, 60 p.

Gardner, J. V. and Vallier, T. L., 1977, Faulting, unstable sediments and surface sediments in the southern Bering Sea outer continental shelf and slope: EOS Transactions, Amer. Geophys. Union, v. 58, No. 6, p. 404.

Gardner, J. V., Vallier, T. L. and others, 1977, Distribution and carbon content of surface sediments in the outer continental shelf of the southern Bering Sea: Geol. Soc. Amer. Abs. with Programs, Annual Mtg., p. 985.

Kvenvolden, K. A., and Redden, G. D., 1977, Low molecular weight hydrocarbons in sediments of the southern Bering shelf: Geol. Soc. Amer. Abs. with Programs, Cordilleran Section Mtg., v. 9, p. 449.

Vallier, T. L., Gardner, J. V., and others, 1977, Heavy minerals and clay mineralogy of surface sediments, southern Bering Sea continental margin: Geol. Soc. Amer. Abs. with Programs, Annual Mtg. p. 1207.

Vallier, T. L. and Gardner, J. V., 1977, Maps showing types and data of faults interpreted from seismic profiles in the St. George Basin, southern Bering Sea: U. S. Geol. Survey Open-File Report 77-591, 14 p. plus maps.

Gardner, J. V. and Vallier, T. L., 1977, Underway geophysical data collected on U. S. G. S. Cruise S4-76, southern Beringian shelf: U. S. Geol. Survey Open-File Report 77-524, 4 p. plus microfilm copies of the records.

Gardner, J. V., Vallier, T. L., and Dean, W. E., 1978, Grain size, total caarbon, mineralogy, and inorganic geochemical data from surface sediments of the southern Bering Sea continental shelf: U. S. Geological Survey Open-File Report 78-923, 31 p.

Gardner, J. V., and Vallier, T. L., 1978, Underway seismic data collected on U. S. G. S. Cruise S6-77, southeastern Bering Sea: U. S. Geol. Survey Open-File Report 78-322, 5 p. plus microfilm copies of records.